Experimental and Numerical Performance Investigation of Solar Air Heater for Drying Agricultural Products and Space Heating for Brooding of chicken

By

Yisak Tola Debele

Thermal and Aerospace Engineering Department

School of Mechanical, Chemical, and Materials Engineering

Adama Science and Technology University

Adama, Ethiopia

March, 2020

Experimental and Numerical Performance Investigation of Solar Air Heater for Drying Agricultural Products and Space Heating for Brooding of Chicken

A thesis submitted to Thermal and Aerospace Engineering Department School of Mechanical, Chemical, and Material Engineering in partial fulfillment of the requirement for the degree of Master of Science in Thermal Engineering

By: Yisak Tola Debele

Advisor: Dr. Gezahegn Habtamu

Adama, Ethiopia

March, 2020

CANDIDATE’S DECLARATION

First, I hereby declare that this M.Sc. thesis entitled **“Experimental and Numerical Performance Investigation of Solar Air Heater for Drying Agricultural Products and Space Heating for Brooding of Chicken”** is my bona fide work and that all sources of materials used for this thesis have been duly acknowledged. This thesis has been submitted in partial fulfillment of the requirements for the award of M.Sc. degree in **Thermal Engineering** at Adama Science and Technology University, **School of Mechanical, Chemical and Material Engineering**. I solemnly declare that this thesis is not submitted to any other institution anywhere for the award of any academic degree, diploma, or certificate. All relevant resource information used in this thesis has been duly acknowledged.

....	....	....
Student	Signature	Date

This is to certify that the above statement made by the candidate is correct to the best of my knowledge and belief. This has been submitted for examination with my approval.

....	....	....
Advisor	Signature	Date

ADVISOR’S APPROVAL SHEET

This is to certify that the thesis entitled **“Experimental and Numerical Performance Investigation of Solar Air Heater for Drying Agricultural Products and Space Heating for Brooding of Chicken”** submitted in partial fulfillment of the requirements for the degree of **Master of Science in Thermal Engineering**, Graduate Program to the Department of **Thermal Engineering** and has been carried out by **Yisak Tola Debele, (A/PR15457),** under my supervision. Therefore, I recommend that the student has fulfilled the requirements and hence hereby he can submit the thesis to the department.

Name of Advisor	Signature	Date

APPROVAL OF BOARD OF EXAMINERS

We, the undersigned members of the Board of Examiners of the final open defense by **Yisak Tola Debele** have read and evaluated his thesis entitled **"Experimental and Numerical Performance Investigation of Solar Air Heater for Drying Agricultural Products and Space Heating for Brooding of Chicken"** and examined the candidate. Therefore, this is to certify that the thesis has been accepted in partial fulfillment of the requirement of the Degree of Masters of Science in Thermal Engineering.

____________________________	________________	______________
Internal Examiner	Signature	Date
____________________________	________________	______________
External Examiner	Signature	Date
____________________________	________________	______________
Chairperson	Signature	Date

DEDICATION

I dedicate this project to Jesus Christ Almighty my creator, my strong pillar, my source of inspiration, wisdom, knowledge, and understanding. He has been the source of my strength throughout this program and on His wings only have I soared. I also dedicate this work to my family and to those who have been affected in every way possible by this quest. Thank you. God bless you.

ACKNOWLEDGMENT

First and foremost, I would like to thank my Lord Jesus Christ for giving me the blessings, wisdom, protection and helps me throughout my life. Then, I'm grateful to express my sincere gratitude to Dr. Gezahegn Habtamu, the thesis advisor, for his unlimited support, encouragement, constructive comment and unreserved guidance on the critical issues of the study. I also would like to thank Dr. Addisu Bekele for his kind help in giving measuring instrument during my experimental work. I extend my deep gratitude to thank my families for they have been beside me all the time supported, encouraged, and motivated me. And, express Special thanks to my mother Aslefech Mersha for her help and support in all facets of my academic life. I am also grateful to express my sincere gratitude to Adama Science and Technology University for giving me the opportunity to join this master's program with a full scholarship. At last but not least, I extend my deepest and heartfelt gratitude towards my friends who have been always on my side in my academic life. This long academic life involved lots of ups and downs, hope and despair, and needed immense moral and material support. Thank you all for your persistent support all along.

ABSTRACT

Solar energy is an inexhaustible source of energy and nonpolluting. The simple and efficient form of utilizing solar energy is to convert it into thermal energy for heating application by using solar air heater. With the increased attention on this renewable energy resource, the efficiency of solar heating facilities are becoming increasingly important. In this thesis work the performance of enhanced solar air heater integrated with longitudinal fin, gypsum sensible thermal storage material, solar reflector and combination of them was separately investigated numerically as well as experimentally at Adama, Ethiopia weather condition. A 1.5 mx1 mx 0.12 m convectional SAH that integrated to crop dryer was constructed from locally available material and subsequently, modified using the three enhancement techniques. The performance of each set up was evaluated in drying 5 kg of injera, tomato and banana.

The results for conventional and finned absorber solar air heater shows that, the numerical and experimental average efficiency is found to be 40.3 and 38 % for conventional, 42 and 40.2 % for finned absorber plate, respectively while the pressure drop across the finned absorber SAH increase relative to the convectional one. Whereas, the integration of gypsum sensible thermal storage result in an increase of operational time and 6 % efficiency increment compared to the conventional one. When it comes to other enhancement technique integrating three reflectors: top, left and right side reflector result in a sharp increase outlet temperature of fluid, about 15.1 ^{o}C, due to an increasing in the radiation on the absorber by a factor of 2-3 times respect to the solar air heater without reflector. Finally the performance study of the combined effect of longitudinally finned absorber, gypsum sensible thermal storage and reflector is conducted. The study shows that the highest average efficiency is achieved by combined enhanced solar air heater which is 68 and 71.3 % for experimental and numerical one, respectively and the average drying efficiency also increased by 20 % compared to the convectional SAH.

Finally, for poultry farm, the annual heating load and ventilation rate required was estimated for brooding 1000chickns. The result show that 5units of enhanced solar air heater was demanded to satisfy the estimated heating load.

Keywords: Solar air heater, solar Reflector, Thermal storage, Solar radiation, Solar crop dryer, Space heating

TABLE OF CONTENTS

CONTENTS **PAGE**

LIST OF FIGURES

LIST OF TABLE

ABBREVIATIONS

SAH	Solar air heater
TES	Thermal energy storage
STES	Sensible thermal energy storage
LHS	Latent heat thermal storage
FPC	Flat plate collector
FDM	Finite difference Method
HTF	Heat transfer fluid

NOMENCLATURE

m	Mass(kg)
T	Temperature (^{o}C)
P	Pressure (pa)
h	Enthalpy (J/kg)
Q	Heat flow (W)
Pr	Prundtle Number
R	Heat transfer resistance/gas constant
L	Length (m)
k	Thermal Conductivity (W/m^2K)
n	Day of the year/ratio of collector width and reflector width
W	Width (m)/light wattage (W)
g	Gravity (m/s^2)
Nu	Nusselt number
U	Overall heat transfer coefficient (W/m^2K)
A	Area (m^2)
Re	Reynolds number
H	Global daily radiation
I	Global hourly radiation
Ns	Day time duration

V	Velocity (m/s)/Volume (m^3)
t	Time (s)
C	Heat capacity (J/K)

GREEK SYMBOLS

Δ	Change
ρ	Density (kg/m^3)
β	Inclination angle (^{o})
δ	Declination Angle (^{o})
ω	Hour angle (^{o})
θ_z	Zenith Angle (^{o})
μ	Dynamic Viscosity (kg/ms)
λ	Reflector inclination angle (^{o})
ε	Emissivity
σ	Steven Boltzmann constant
α	Thermal Absorptivity
η	Efficiency (%)
ν	Kinematic viscosity (m^2/s)
ϕ	Fin efficiency (%)

SUBSCRIPTS

c	Cover
p	absorber plate
b	Bottom
a	air
rPC	Radiation from absorber plate to cover
f	Fluid
t	Top
u	Useful heat gain

amb	ambient
i	node
ff	Fin
fc	Fluid to cover
F	Finned absorber
s	Sensible storage
ps	Plate to storage
sb	Storage to base
r	Radiation
g	Glass
ins	Insulation
char	Charging
dis	Discharging
sc	Solar constant
o	Extraterrestrial/Standard time
G	Global
D	Diffuse
B	Beam
max	Maximum
min	Minimum
T	Tilted surface
t	Top
L	Left
R	Right
vent	Ventilation
tr	transmission
ins	insulation

CHAPTER 1: INTRODUCTION

1.1. Background

Solar energy is one of the clean and abundant renewable energy sources available which allows flexibility of locations, modularity and scalability of the conversion system. Solar energy can be converted into different forms of energy, either to thermal energy or to electrical energy. Solar energy is converted by solar collector into thermal energy. Solar collector works by absorbing the direct solar radiation and converting it into thermal energy, which can be stored in the form of sensible heat or latent heat or a combination of sensible and latent heats. Among others solar air heater is a solar thermal conversion technology used to heat air that can be used to dry crops and heat a space. However, the use of solar energy source is seriously constrained by low efficiency of solar equipment's.

Solar air heaters have not yet been given the amount of detailed study as solar water heaters, but air heaters have a number of advantages, for instance simplicity, low cost and lack of freezing hazards; furthermore leakages which may occur will not cause damage to the extent that water can create (Eggers, 1979). The use of efficient solar energy equipment like solar air heater for applications of dryer and space heating can play a significant part in tackling the power deficit and environmental challenges. Indeed, because of the abundance of its sunny days, the solar energy represents an important alternative for convectional energy source.

As history shows, Ethiopia is a country with a history of severe famine and remains dependent on food imports to feed its population. Despite significant increases in the area of land under cultivation, food security in the country remains fragile. An estimated 40% of the population still consumes less than the minimum daily requirement of calories. In a country like Ethiopia where production and productivity is low and post-harvest loss is quite high, much effort shall be made to generate technologies that would boost production and minimizes loss (Asmaru *et al*., 2013 and Mulualem *et al*., 2015).

Because, Fresh horticultural crops are high in water content, they are subjected to desiccation and to mechanical injury. Fruits, vegetables and root crops are living plant parts containing more water, and they continue their living processes after harvest. Scientists reported total Post-harvest loss of banana as 26.5% where 56% of the loss was occurred at the retail level due to rotting before reaching consumers in Ethiopia (Mulualem *et al.,* 2015). Besides, Post-harvest loss assessment was conducted in Jimma zone and the result indicated that there were greater postharvest losses of mango (35.5%) and banana (40.0%) in Jimma town and the postharvest losses were mainly attributed to poor preservation methods and handling during transportation (Adugna *et al*., 2011).

In other perspective, the current level of poultry-farm productivity in the small holder production system is low due to factors such as lack of proper production system which include providing energy efficient and reliable space heating system for the poultry house. On the other hand, the use of convectional energy source for space heating and lack of ventilation system of the farm reduces the productivity and leads to reduce the growth of the sector though its high contribution to the country food sustainability.

The aim of this thesis is to study the experimental and numerical performance of SAH by using three enhancement techniques; finned absorber, gypsum sensible storage, reflector and combination of them. The convectional solar air heater with overall dimension of 1.5x1x0.12m that integrated into dryer box is constructed from locally available material as shown in Figure 1.1.(a) and its performance is evaluated in drying three products; injera, tomato and banana subsequently. Then after, the constructed convectional solar air heater was modified by employing three different enhancement techniques: finned absorber, gypsum sensible thermal storage and reflector separately to study the effect of each enhancement independently. After the effect of each enhancement is studied separately, the last experiment was conducted to investigate the combined effect of the three enhancement techniques. All the performance investigation of the solar air heater configuration was conducted with load simultaneously while evaluating the drying performance of the dryer in drying 5kg of injera, tomato and banana at each set up alterations.

a) Convectional b) Enhanced

Figure 1.1: Constructed experimental solar air heater set up

The numerical performance study was based on finite difference method and python program code was developed to analysis the model of convectional solar air heater and each enhanced solar air heaters. Finally, the performance of the combined enhanced SAH was predicted for space heating of local poultry farm that brood 1000chickens by estimating the annual heating load of the farm.

1.2. Problem statement

Solar air heaters are widely used for low to moderate temperature application like space heating, crop drying, timber seasoning and other industrial applications. However, the pace of development of air heating collector is slow mainly due to lower thermal efficiency. Conventional solar air heaters have poor thermal efficiency principally due to high heat losses and low convective heat transfer coefficient between the absorber plate and flowing air stream which result in low temperature output. In drying process the amount of moisture removed depends on the temperature to which it is heated in the collector, i.e. warm air can hold more moisture than cold air to maintain relative humidity. The higher drying rate gives a higher throughput of food and a smaller drying area. Similarly, in space heating application in order to meet the heating load demand of the space, using poor thermal efficiency solar air heaters result in large number of units which makes the system expensive.

In this thesis work, the convectional solar air heater was constructed and its performance was tested experimentally. Then after, the performance of enhanced solar heater with three enhancement techniques: longitudinally finned absorber, gypsum thermal storage and reflector were evaluated separately by integrating them into the constructed solar air heater and also the last enhancement was made by combining the three enhancement techniques all together and its performance was studied experimentally and numerically. the results found for each set up through dry experimental and numerical analysis was compared and finally the drying efficiency of a crop dryer integrated with the convectional and each enhanced solar air heaters were evaluated by drying crops and food. Whereas, the space heating performance of the enhanced solar air heater is predicted for locally selected poultry farm which brood 1000chiken after estimating the heating load at Adama weather condition.

1.3. Objective

1.3.1. General objective

The general objective of this thesis is to design and analysis the experimental and numerical performance of enhanced solar air heater by integrating finned absorber, sensible storage material and solar reflectors and comparing the enhanced solar air heater with the conventional one. Then after, to adopt the enhanced solar air heater for agricultural crop drying and poultry farm space heating application.

1.3.2. Specific objective

- Constructing convectional and the enhanced solar air heaters
- Conducting experiment to evaluate the performance of convectional and the enhanced solar air heaters for drying injera, tomato and banana
- Numerical modeling and performance analysis of convectional and enhanced solar air heaters.
- Estimation of enhanced solar air heater required for heating local poultry farm that broods 1000chicken.

1.4. Scope and limitation

1.4.1. Scope of the study

This study focuses on the experimental and quasi-dynamic numerical analysis of the enhanced solar air heater which is designed to extend the efficiency and working time of the solar air heater. And to use the solar air heater with the best performance to dry selected crops and space heating of poultry farm by evaluating experimentally.

1.4.2. Limitation of the study

As the thesis aim is to increase the efficiency of the conventional solar dryer using different enhancing methods, the work is entirely focused on the thermal analysis and design of each component, whereas the aero-dynamical and multi-dimensional analysis of solar air heater is not included in this study. In the experimental work the lack of enough budget for the construction of quality set ups and lack of measurement devices limits me from taking all the data needed.

1.5. Significance of the study

This study has the following significance in different aspects

- It promotes the adoption of solar air heaters technology to local farms and household use for drying products.
- It greatly reduces the postharvest loss which as a result contributes to the prosperity of the country.
- It stimulates and increases the productivity of the fading poultry farm sector due to lack of conditioned space for brooding by substituting the electric heater with enhanced solar air heater.
- It encourage the use of alternative energy to cope up the problem of energy shortage
- Specifically the effort made on the integration of reflector and its angle manipulation method contribute an alternative method of enhancement techniques for solar air heater.

CHAPTER 2: LITERATURE REVIEW

2.1. Introduction

Solar air heater is a simple device which captures the solar energy, Producing hot air by using solar air heater, is a renewable energy heating technology used to process heat generation for space heating. Such systems produce heat at zero cost and minimum maintenance like cleaning of collector only is required (Tyagi *et al*., 2012).

This chapter concerns about information on Solar Air-heater, Enhancement Technique, Solar Dryer and solar Space heating system. In addition previous research works on different solar air heaters, Reflector enhanced solar air heater and applications of solar air heaters on Solar Dryers and solar space heaters are used as input for the current work.

2.2. Classification of solar air heater

It is very complex to classify solar air heater due to the many numbers of shapes and empirical constructions **(**Ravish and Ajeet, 2017)**.** Ekechukwu and Norton (1999), conducted a detailed review on different designs, construction and principles of operation for a wide variety of solar air heaters (SAHS). SAHS can be classified based on mode into: active, hybrid and passive.

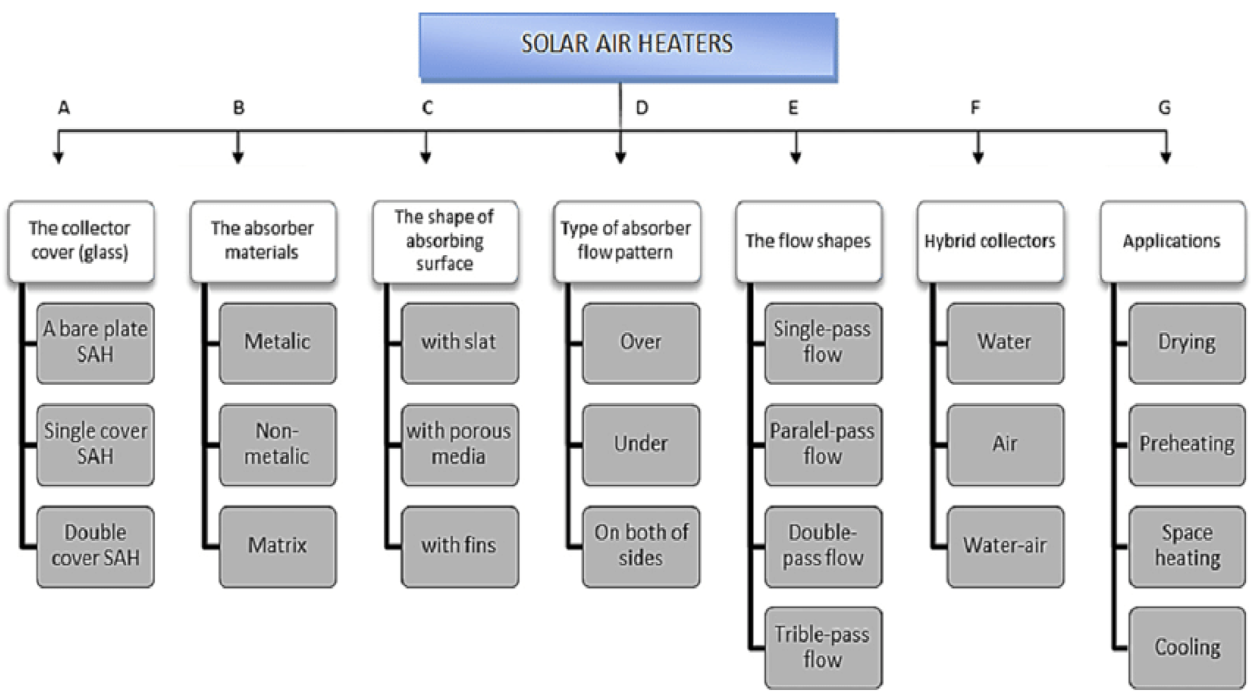

Figure 2.1: Classification of solar air heaters (Hakan F. Oztop et al., 2013)

Tyagi *et al*., (2012), classified the solar air heaters according to their tracking axis, energy storage, extended surface and numbers of covers. In passive solar air heating systems, hot air is generated at different places and directed to end use. Heat storage materials are commonly utilized in active SAHS to generate hot air during off day time. On other hand passive SAHS are generally utilized during daytime. From another perspective, SAHS may be classified according to the number of air passes into single-pass and double-pass with or without heat storage. In single-pass air solar heater, air flows in one way either above the absorber plate or below it from the air inlet to outlet. While in double-pass air solar heater, air flows in two passages, which may be either counter or parallel **(**Ravish and Ajeet, 2017**).** SAHS consist mainly of air flow duct and absorber plate. To reduce heat losses from both bottom and sidewalls, thermal insulation with low thermal conductivity is used.

Classification according to air channel design

By changing the air channel design, the efficiency of a solar air heater can be enhanced significantly. Based on the air channel design the air heater can be flat plate or conventional type and extended surface assisted solar air heater.

Conventional solar air heater

Conventional solar air heater type is the simplest form of solar air heater. This type of solar air heater includes one or more glass covers and an absorber plate. All sides of the solar air heater except the glass cover should be well insulated to prevent heat loss. Air can flow either over or under the absorber plate. Flat plate solar air heaters can be designed as single pass, double pass, double flow or recycled. The absorber plate is generally a smooth plate and it does not contain a fin, obstacle or roughness element. That is why this type of solar air heater is called a “Flat Air Channel” (Garg and Sharma, 1984).The construction of a Flat Air Channel solar air heater is simple; hence it has a low cost. Since no mechanism or method is used to enhance heat transfer in the channel, the efficiency of this kind of solar air heater is lower than other types (Pradhapraj *et al*., 2010).

Extended surface assisted solar air heater

Several designs have investigated how to increase the low thermal efficiency of flat air channel solar air heaters. Since the type of absorber plate is one of the most important parameter that affects the thermal efficiency of solar air heaters, many absorber modifications were studied

(Kabeel and Mearik, 1998).The extension of the surface area of the absorber plate can be an efficient way to improve the performance of solar air heaters. Attaching fins, ribs, obstacles or any other roughness element (any element that causes roughness on the absorber plate) on the absorber plate could extend the surface area of the solar air heater (Gizem, 2012).A solar air heater collector whose channel is assisted by an extended surface can be designed as a single pass, double pass, double flow or recycled model. Although the use of roughness elements or fins increases the surface area and heat transfer coefficient, the pressure drop through the channel will be increased at the same time. An increase in the pressure drop of the channel will result, an increase in the required power of the fan or blower that supplies the air to the heater is also required (Vivek *et al*., 2017).

2.3. Solar air heaters components

a) Cover plate

Most important part of solar air heater is a cover plate, which transmits the maximum amount of solar radiation to the absorbing plate. There are three purposes of the cover plate (Himanshu *et al*., 2018): (i) to transmit the solar radiation as much as possible to absorbing plate, (ii) to reduce heat losses to the atmosphere from the absorbing plate, and (iii) to serve as a protective shield.

b) Absorber

Plate Absorber plate is a flat-plate made of materials, which have high thermal conductivity, better tensile strength, and non-corrosive (e.g., copper). The solar collector is made of steel or galvanized iron, aluminum, and types of thermoplastics. For fabrication of absorber plate, a thin sheet of metal (Cu or Al) may be taken with insulations, i.e., to non-flow sides. Radiations from the sun get rapidly absorbed by the thin sheet of aluminum or copper, and this heat is then transferred to air to increase its temperature (Billy, 2010). Important characteristics required for employing a cover plate are durability, energy transmission, non-degradability, and strength (e.g., glass). Before selecting the glass as a cover plate, its strength must be measured in order to ensure that it should stand against the harshest environment (e.g., snow loads in the winter season).

Thermal impact on glass must be additionally considered due to day variations in the solar intensity of the sun, variation in the ambient temperature during the morning and evening time (Himanshu *et al*., 2018). Again, in the cloudy weather, glass temperature varies with a different rate. Mainly, somewhere at the center of solar collector subjected to more heat rather than the side of the collector. This results in thermal shock, which can lead to the breakage of glass (Prashant *et al*., 2018).

One of another important characteristics must consider during the selection of glass is its rigidity. The rigidity of glass is directly proportional to the cube of the thickness of the glass. For better rigidity, plastic materials can be used (Himanshu *et al*., 2018).

c) Insulation

Insulation prevents heat losses by absorbing plates either in the form of conduction or convection. The most commonly used insulations nowadays is glass wool. Glass wool filled under the absorbing plate, and sides depends on the type of solar air heater is employed. The main use of insulation is to provide the best heat resistance (Himanshu *et al*., 2018).

d) Framing

Material used to hold the components together.

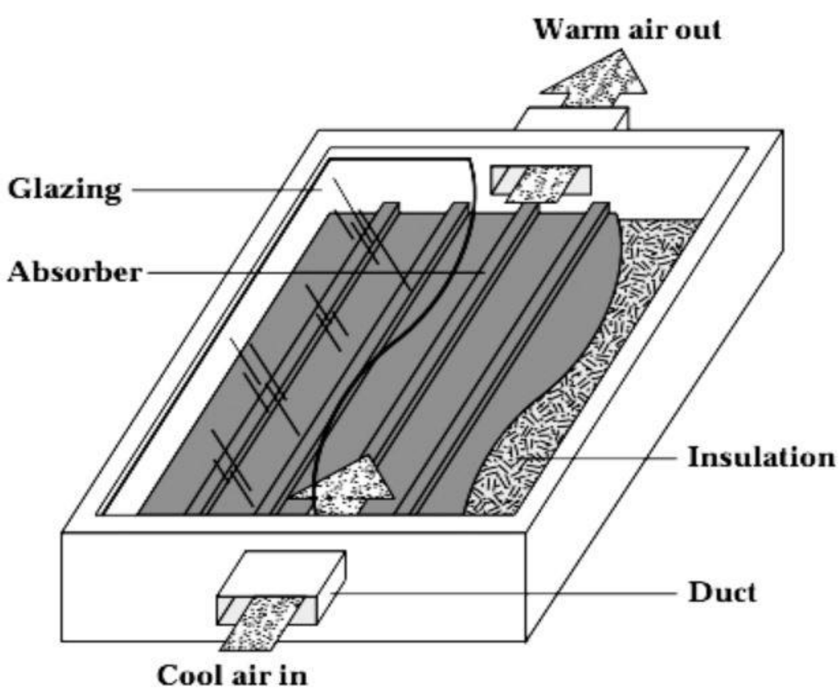

Figure 2.2: Components of conventional solar air heater (Neelkanth et al., 2010)

2.4. Solar air heater performance enhancement techniques

The way to improve heat transfer performance is referred to as heat transfer enhancement (or augmentation or intensification). Nowadays, a significant number of thermal engineering researchers are seeking for new enhancing heat transfer methods between surfaces and the surrounding fluid (Siddique *et al*., 2010). Due to this fact, (Bergles *et al*., 2008) classified the mechanisms of enhancing heat transfer as active or passive methods. Those which require external power to maintain the enhancement mechanism are named active methods. Examples of active enhancement methods are well stirring the fluid or vibrating the surface. Hagge and Junkhan, (2014), described various active mechanical enhancing methods that can be used to enhance heat transfer. On the other hand, the passive enhancement methods are those which do not require external power to sustain the enhancements' characteristics. Examples of passive enhancing methods are: treated surfaces, rough surfaces, extended surfaces, displaced enhancement devices, swirl flow devices, coiled tubes, surface tension devices, additives for fluids, and many others.

The performance of a flat plate solar air collector has been found to depend strongly on the rate of incidents solar radiations, the losses from the absorber surface and the rate of heat transfer from the absorber plate to the air (Maheshwari *et al*., 2011). The following are some of the design modifications used for the enhancement of thermal efficiency of collectors by reducing thermal losses:

2.4.1 Using selective absorber surfaces

In solar thermal collectors, a selective surface or selective absorber is one of a means of increasing its operation temperature and/or efficiency. Selective surfaces are especially important when the collector plate temperature is much higher than the ambient air temperature, and usually the largest heat losses are through emittance from the collector surface (Caouris, 2012).

(Ramadhani *et al*., 2014), studied the maximum radiation loss appears at the wave length of about 10 microns if the collector plate is close to room temperature and at about 5 microns if collector plate temperature is around 300^{o}C. If the absorbing surface of the collector is treated such that it absorbs most of the solar energy between 0.3 and 2.5 microns and it emits only a small fraction of the infrared radiation, it is possible to increase the efficiency of solar energy collector significantly.

2.4.2 Using thermal energy storage material

Energy storage not only plays an important role in conservation of the energy but also improves the performance and reliability in wide range of energy systems and becomes more important where the energy source is intermittent in nature such as solar. Energy storage process reduces the rate of mismatch between energy supply and its demand (Ioan and Calin, 2018). The thermal energy storage can be used in such places where the variation between the day and night temperature is much more.

Thermal energy can easily be stored in a rightly insulated container. There is a change in internal energy of liquids or solid materials as a sensible heat or latent heat or thermo-chemical and by combination of all of these (Sarada *et al*., 2013).

2.4.2.1 Sensible heat storage

In this type of storage, thermal energy is stored in fluid or solid by raising the temperature more than that of its nominal temperature without phase-change. The total amount of heat can be stored in fluid or solid is directly proportional to the medium change in temperature and specific heat of amount of storage materials (Getu, 2018). One of the most attractive features of sensible heat storage systems is that charging and discharging operations can be expected to be completely reversible for an unlimited number of cycles, i.e., over the life-span of the storage(Garg *et al*., 2019).

The economics of this mode of heat storage demands sensible heat storage material which is inexpensive. Solid materials such as cast steel, stone, rock, sand, concrete, gypsum and ceramic have usually been selected as sensible heat storage media depending on the required temperature range and specific application (Sarbu, 2018). The advantages of using a sensible heat storage media include the low cost of the thermal storage media, the high heat transfer rates into and out of the media, the ease of handling of the material, the availability of the material, and uncomplicated processing. Table 2.1 shows the advantage and disadvantage of using sensible thermal storage system.

Table2. 1: Advantage and disadvantage of sensible thermal energy storage (Ioan *et al*., 2018)

Advantage	Disadvantage
Abundant	High Vapor pressure
Low cost	Difficult to stratify
Nontoxic	Low surface tension
Excellent transport Properties	Non isothermal energy delivery
High specific heat	
High density	
Well known corrosion control Methodology	

2.4.2.2 Latent heat storage

It is the technique of absorbing and discharging of heat when the storage materials change its phase at a constant temperature. LHS is one of the most efficient ways of storage medium compared to the competing SHS. It provide much higher storage density with a smaller temperature difference between storing and releasing heat, and it depends on the phase change process of the material(Dakuri and Hayavadana, 2014).

Table 2. 2: Advantage and disadvantage of Latent heat thermal energy storage (Ioan *et al*., 2018)

Advantage	Disadvantage
High storage density	High Cost
Smaller volume	Density change
Smaller temperature change between storing and releasing energy	Corrosiveness
	Low thermal conductivity
	Phase separation
	Incongruent melting
	Super cooling

2.4.3 Using finned absorber surface

The low heat transfer rate from absorber plate to air in the duct results in relatively higher absorber plate temperature leading to higher thermal losses to the environment. These losses can be reduced by lowering the absorber plate temperature by increasing the heat transfer coefficient between absorber and air. Extended, corrugated and finned surfaces fall under this category. Fins used as passive elements for enhancing heat transfer rates through increasing heat transfer area (Shyam *et al*., 2016).

2.5. Applications of solar air heater

2.5.1 Agricultural product drying

The inadequate method of preserving agricultural produce which is usually produced in larger quantities during harvest has remained one of the main problems facing farmers (Deepak and Prasanta, 2017). High crop losses due to inadequate dry, fungi attacks, insects, birds, rodent encroachment and unpredictable weather effects such as dust, rain, and the wind have remained some of the inherent limitations of the traditional open sun drying method widely being practiced by rural farmers (Eze and Agbo, 2011). The open sun drying also results in physical and structural changes in the agricultural produce such as unnecessary shrinkage, case hardening and loss of volatiles and nutrient components. (Rajkumar, 2007).Therefore, a control mode of drying which preserves the color, nutrient components and unnecessary shrinkage of the agro-produce is necessary. One of these control modes involves constructing a solar crop dryer.

After agricultural products are harvested, there is the need for proper storage for future use. The products upon harvesting have high moisture content which makes it unsafe for storage as the moisture in the crops attracts microorganisms which result in deterioration of the products. Among other reasons, crops are dried to improve shelf life, retain original flavor and reduce weight for easy transport and trade. Drying ensures water evaporation from agricultural products to the drying medium- usually hot air. Drying plays a vital role in the preservation of agricultural products (Amma, 2014).

Conservatively, many cereal crops, vegetables and fruits are dried by thinly spreading them on a prepared ground, mats, and paved ground in open sunlight. Large losses are generally incurred as a result of using this method. The losses are attributed to bird’s rodents, domestic animals and the wind blowing the product beyond recovery (Bolaji, 2005). High humidity levels associated with tropical environments has been contributing immensely to crop lost to fungal and microbial degradation (Drew, 2011). The further disadvantage of this open air sun drying technique is lack of control over the drying rate which results in under drying or over drying (Bolaji, 2005). Controlled solar drying gives quality end product, rapid drying and more hygienic product.

Many dryer types have been in used in both domestic and industry sectors. The simplicity of design and economic consideration make cabinet dryer most extensively used. A cabinet dryer consists of several stacks of trays placed in an insulated chamber in which hot air is distributed by a fan or natural flow (Misha *et al.*, 2013). The major shortcoming of the cabinet dryer is uneven drying because of poor air flow distribution in the drying chamber. Good air flow distribution in the drying chamber will help in attaining uniform moisture contents of the products being dried on different a tray.

2.5.2 Space heating applications

Space heating for residential and commercial applications can be done through the use of solar air heaters. This configuration operates by drawing air from the building envelope or from the outdoor environment and passing it through the collector where the air warms via conduction from the absorber and is then supplied to the living or working space by either passive means or with the assistance of a fan (Neelkanth *et al*., 2016).

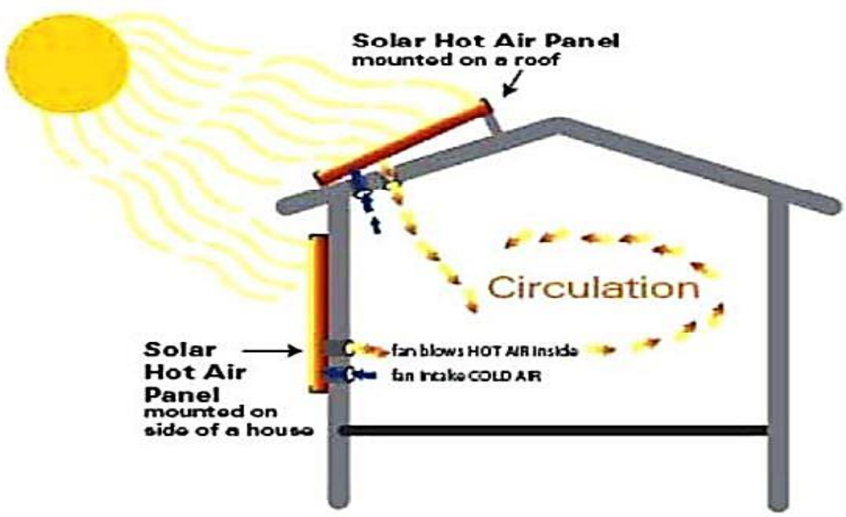

Figure 2.3: Application of solar air heater for space heating (Himanshu, T *et al*., 2018)

When sun arises and sunlight radiates on the solar air heating collector, solar absorber inside begin to absorb thermal energy from sunlight. Interior temperature reaches setting value immediately, the temperature Sensor inside collector will send signal to drive fan to work (Kalogirou, 2004). Cold air enters into collector through the air inlet, and then is heated circularly by heat absorber, and finally hot air is droved out of collector by the fan, and enters into the house through air outlet (Neelkanth *et al*., 2016).

2.6. Related previous works

2.6.1 Related works on solar air heater with longitudinal finned absorber

Foued *et al*., (2014), investigated experimentally, the thermal performance of a single pass solar air heater with five fins attached. Longitudinal fins were used inferior the absorber plate to increase the heat exchange and render the flow fluid in the channel uniform. The effect of mass flow rate of air on the outlet temperature, the heat transfer in the thickness of the solar collector, and the thermal efficiency were studied. Experiments were performed for two air mass flow rates of 0.012 and 0.016 kg s^{-1}. Moreover, the maximum efficiency values obtained for the 0.012 and 0.016 kg s^{-1} with and without fins were 40.02, & 51.50% and 34.92, & 43.94%, respectively. A comparison of the results of the mass flow rates by solar collector with and without fins shows a substantial enhancement in the thermal efficiency.

The experimental studies on two non-porous solar absorber solar air heaters with and without fins have been reported by (Indrajit *et al*., 1985). During experiments it was found that air heaters with fins are seen more efficient in comparison to the air heater without fins for air flow rates ≤0.0388 kg/s/m^2.

Naphon, (2005), developed a mathematical model to evaluate thermal performance and entropy generation of the double-pass flat plate solar air heater with longitudinal fins as shown in Figure. 2.4. This model was based on study conducted by Naphon and Kongtragool, (2003) with the assumption that the flow of air is steady, air-side convective heat transfer coefficient is constant along the length of solar air heater, tube-side convective heat transfer coefficient is constant along the length of solar air heater and, thermal conductivity of fin is constant along the length of solar air heater. The predictions were done at air mass flow rate ranging between 0.02 and 0.1

kg/s. It was found that the thermal efficiency increases with increasing the height and number of fins. The entropy generation is inversely proportional to the height and number of fins.

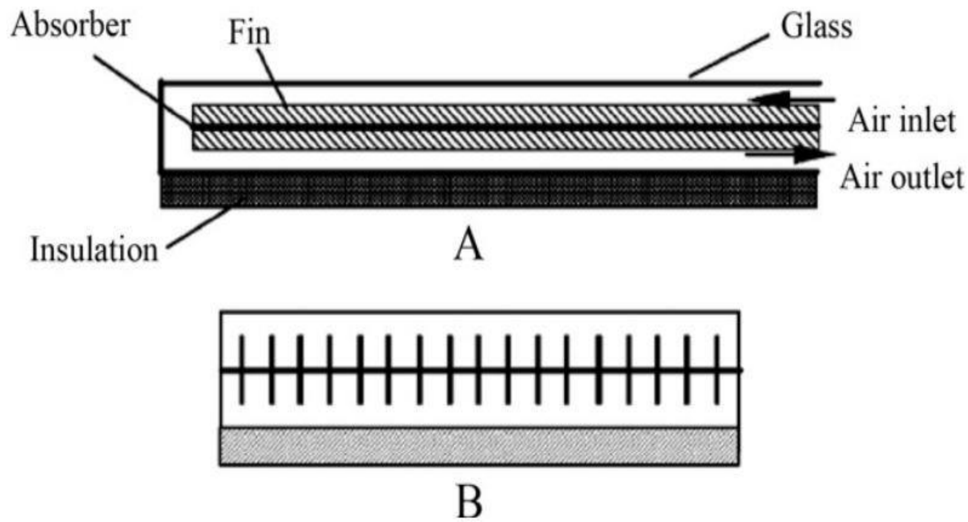

Figure 2.4: Double pass flat plat solar air heater with longitudinal fins (Naphon, 2005)

Ho *et al*.,(2012) studied the collector efficiency of upward-type double-pass flat plate SAHs with fins attached and external recycle was investigated theoretically, as shown in Figures 2.5. The double-pass device was constructed by inserting the absorbing plate into the air conduit to divide it into two channels. The double-pass device introduced here was designed for creating a solar collector with heat transfer area double as well as the extended area of fins between the absorbing plate and heated air. The double-pass type SAHs was proposed in their study. They had the extended heat transfer area and the strengthened convective heat transfer coefficient, leading to improved thermal performance on the new device. It was shown that the desirable effect of increasing the fluid velocity using the recycling operation to overcome the undesirable driving force decreased (temperature difference) for heat transfer due to remixing at the inlet.

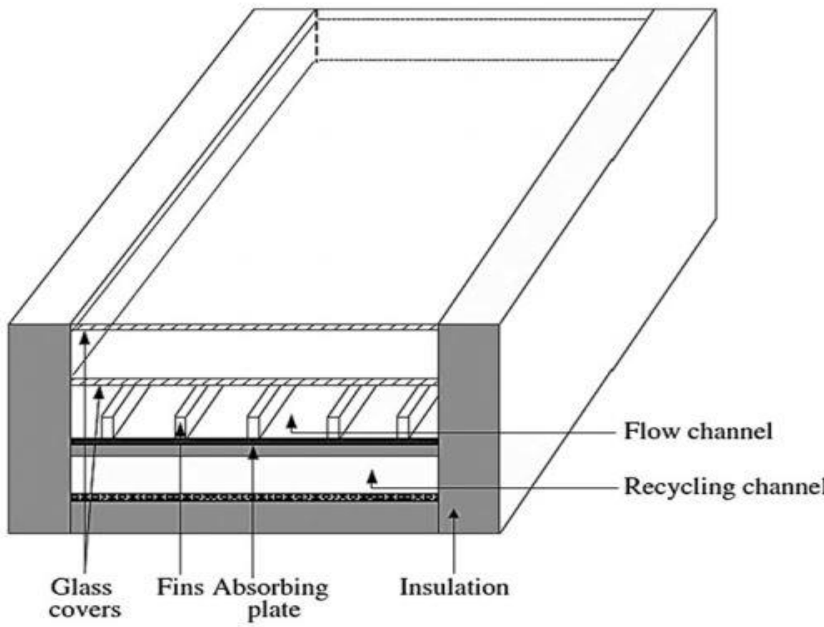

Figure 2.5: Upward-type double-pass flat plate SAHS with fins attached (Ho *et al*.,2012)

Energy and exergy analysis of three different types of designed flat plate solar air heaters, two having fins (type II and type III) and the other without fins (type I), one of the heater with a fin had single glass cover (type III) and the others had double glass covers (type I and type II) was carried out by Alta *et al*., (2010). The energy and exergy output rates of the solar air heaters were evaluated for various air flow rates per absorber area (25, 50 and 100 m^3/m^2h), tilt angle (0◦, 15◦ and 30◦) and temperature conditions versus time. Based on the energy and exergy output rates, heater with double glass covers and fins (type II) is more effective and the difference between the input and output air temperature is higher than of the others. Besides, it was found that the circulation time of air inside the heater played a role more important than of the number of transparent sheet. Lower air flow rates should be preferred in the applications, in which temperature differences are more important.

2.6.2 Related works on solar air heater integrated with sensible thermal storage system

Saravanakumar and Mayilsamy, (2010), present thermal performance of flat plate SAH with and without thermal storages. A forced convection solar collector (FCSC) integrated with different sensible heat storage materials (sand, concrete, pure cement) has been developed and tested to evaluate its performance under meteorological conditions of Baghdad, Iraq. System consists of three flat plate solar air heaters with different heat storage materials, and the fourth without storage heat material. All collectors are supplied with centrifugal blower.

Figure 2.6: Flat plate solar air heater with different sensible thermal storage material (Saravanakumar and Mayilsamy, 2010)

The experimental results indicated that the pure cement gives better thermal performance than sand and concert. The pure cement gives heat for 240 min after 6:30 PM, but the duration was 170 min and 65 min for concrete and sand respectively. The air flow rate is more effect on both outlet air temperature storage heat times, where studied the effect of three air velocities (0.8, 1.4 and 2.1m/s) on SAH performance with best thermal storage heat material (pure cement), the increase in outlet air velocity leads to decrease in both outlet air temperature and storage time of thermal energy.

Thakar and Prajapati, (2020), present experimental evaluation of solar air heater with finned vertical absorber was done at Mahesana, Gujarat. And come on the conclusion that changing the traditional concept with flat plate and eliminating insulation from it is definitely changes the performance. A double pass solar air heater was fabricated and integrated with thermal storage system and powdered cherry pits are used as a thermal storage medium.

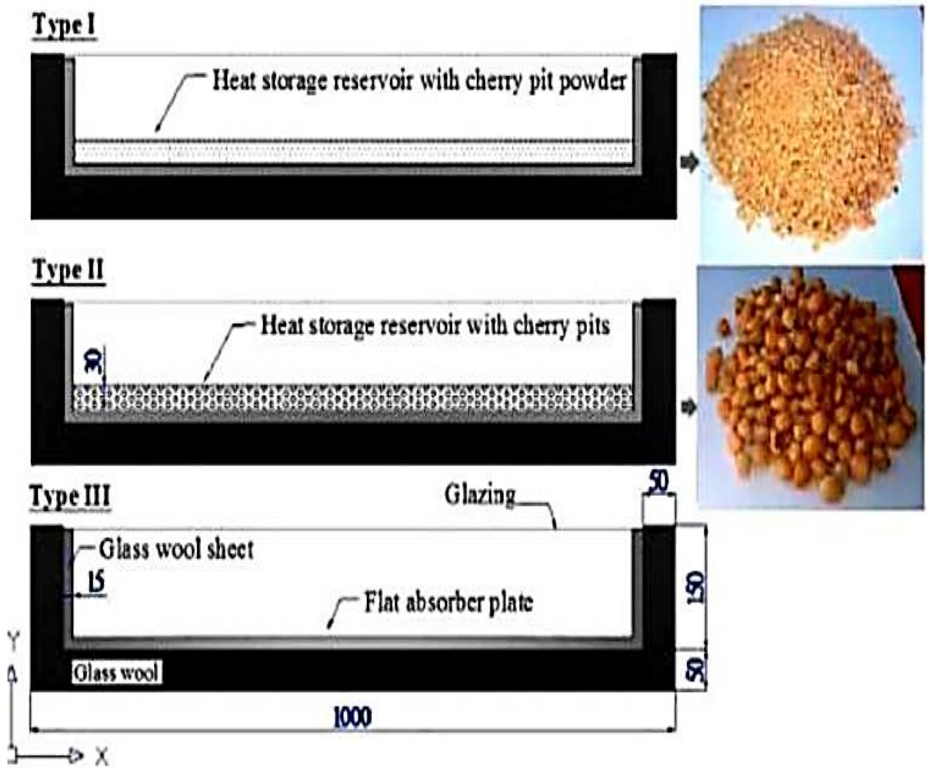

Figure 2.7: Double pass solar air heater with fabricated cherry pits thermal storage system (Thakar and Prajapati, 2020)

The performance of this heater was studied for different configurations. The solar heater integrated with thermal storage delivered comparatively high temperature. The efficiency of the air heater integrated with thermal storage was also higher than the air heater without thermal storage system. The result indicates that the highest efficiency was achieved for setup with finned and thermal storage, and that is 80.17 %, for flow rate of 0.0349 kg/s, and day average solar irradiation of 808 Wm^{-2}. And with the mass flow rate of 0.0221 kg/s and usage of 0.5 kg powdered cherry pits will lead to give time rise around 2 hours. The study concluded that the presence of the thermal storage medium at the absorber plate is the best configuration.

Aboul *et al.*, (2000), have presented a transient model for a FP-SAH with and without thermal storage. Effects of design parameters of the SAH such as length, width, gap spacing between the absorber plate and glass cover, and thickness and type of the storage material (sand, granite and water) on the outlet and average temperatures of the flowing air were studied. The flowing air was found to decrease with increasing gap spacing and of air. Improvements in the heater performance with storage were achieved at the optimum thickness of the storage material. Therefore, the SAH was used as a heat source for drying agricultural products and the drying process will continue during the night, instead of reabsorption of moisture from the surrounding air.

Alvarez *et al*., (2004), studied on the thermal performance of an air solar collector with an absorber plate made of recyclable aluminum cans. The absorber surface, which is the most important part of the solar air collector, consisted of eight circular cross sections air flow channels made of 128 Recyclable Aluminum Cans (RACs) painted in black. Their results showed that the efficiency increase of air solar collector using recyclable aluminum cans was technically and economically feasible if an adequate design was applied. From this figure, the RAC air solar collector shows an intercept increase of 26.2 %. Beyond which the increase in ZTH becomes insignificant. It was recommended to operate the system with packed bed with values of mass flow rate equal 0.05 kg/s or lower to have a lower pressure drop across the system. To validate the proposed mathematical model, based on comparisons between experimental and theoretical results, a good agreement was achieved.

2.6.3 Related works on solar air heater with Reflector

Nigussie and Teklay, (2017) worked in improving the performance of a liquid flat plate solar energy collector integrating with external reflectors. The external flat reflectors are mounted on the side of the collector. The external flat reflectors can be tilted to an angle of 15°, 30^o and 45°, on the horizontal plane due to the existence of angle adjustment. The effect of four flat plate reflectors which are mounted on bottom, top, left, and right side reflectors on the total light radiation on a collector at tilted plane angle of 45^o for each reflector was analyzed The effect of these reflectors was more evenly at solar noon since the sun is perpendicular to the collector. Based on this the effect of the reflectors on the collector were analyzed. The flat plate collector integrated with and without reflector for minimum, average and maximum solar radiation intensity under Bahirdar weather has been analyzed, constructed and tested on automotive work shop at Bahirdar Institute of Technology. Experimentations were conducted on flat plate collector with and without reflectors for particular period of various days and data was collected /for each per days. For flat plate with reflector the maximum fluid output temperature, and irradiance of 98°C, and 1,200 W/m^2, respectively, was obtained on a sunny day. Whereas, for flat plate without reflector the maximum temperature and solar insolation was 70^{o}C when the irradiance 1,200 W/m^2, respectively, was obtained on a sunny day. The total thermal energy generated by thermal collector with reflectors in optimal position is significantly higher than total thermal energy generated by thermal collector without reflectors. This solar water heating system finds useful application for cooking, pre-heater when temperature of more than 70^{o}C is needed, and for bleaching industrial process in textile factory. The theoretically and experimental results of water outlet temperature are equivalent with the results obtained by using computational fluid dynamics (CFD) and there is a good agreement in between them.

The amount of direct light gathered by a combination of reflector plus flat-plate collector has been analyzed by Daniels *et al*., (1975). The calculations were done allowing variable reflector and collector orientation angles, variables latitude, and arbitrary sun hour angle away from solar noon. The effects of reflection and transmission losses and of polarization of the incident light were included. Correction was also made for the finite size of the reflector. It was found that the optimum orientation has the collector plane almost perpendicular to the plane of the reflector. This optimum orientation is approximately independent of the sun's azimuthal dependence. The optimum reflector angle is found to be between 0° and 10° above the horizon for winter solar conditions. For typical winter operating conditions the enhancement in light gathering power for direct solar radiation is about a factor of 1.4–1.7. These results in an effective increase of 100% in the useful winter heat output from a practical reflector-collector combination with a reflector angle of 0°, over the useful heat output obtained with an optimally oriented simple flat-plate collector. An approximate calculation was also made of the overall enhancement in useful heat output for diffuse solar radiation; an increase by a factor of about 1.5 is predicted. Comparison with the preliminary analysis of the performance of the Coos Bay, Oregon solar house shows substantial agreement with the predictions of the present analysis.

Aman, (1986), investigate the use of planar reflectors which substantially improve the performance of flat-plate solar collectors. The experimental setup includes a collector panel and collector-reflector system with maximum useful heat gain. A computer simulation of the analytical and experimental recordings was made to study the comparative features of the systems. The performance study is illustrated as a function of solar altitude, azimuth angles, hour angle and the relative sizes and tilt angles of both the collector and reflector. The use of a booster mirror produces an increase of 10–15°C in water temperature. The shading effect due to the presence of the reflector has also been considered in the present analysis.

Baccoli *et al*., (2014), performed a numerical analysis of a solar collector augmented by above reflector configuration. In this paper the reflector was assumed to have identical overhangs on both sides, and the width of the collector and the reflector are the same. They have determined the optimum inclination of both the collector and reflector throughout the year at 39° N latitude for an adjustable collector and reflector system, for a stationary collector coupled with an adjustable reflector and for a stationary collector coupled with a stationary above reflector configuration. An adjustable above reflector can provide a meaningful solar flux augmentation on the absorbing plate of a solar collector, both with stationary and adjustable tilt, on a year round basis. The greatest benefit is obtained when the angles of both the collector and the reflector are oriented in the position according to which the reflector is inclined backwards in winter up to negative values, and forwards in summer; the optimum collector inclination is lower in summer and higher in winter. An above reflector configuration benefits from an off-optimum position during the winter period, when the enhancement factor reaches the maximum value in the year.

2.6.4. Related works on solar air heater application on agricultural crop drying

An indirect mode forced convection solar dryer integrated with different sensible heat storage material for crop drying had been developed by Mohanraj and Chandrasekar, (2009). The drier consists of a solar flat plate air collector provided a heat storage unit, a drying chamber and a centrifugal type blower. The experiments have done with and without the integration of heat storage materials. Sand mixed with aluminum scrap was used as a heat storage material in solar air collector. The results showed, the specific moisture extraction rate of solar dryer was estimated to be about 0.81 and 0.94 kg kW/h for cases of solar air collector with and without heat storage materials respectively. The results proved also, the time to reduce moisture content of copra from about 52% to about 8% with heat storage materials was about 80 hour, which is mean faster than without using storage materials with drying time 104 hour. The average thermal efficiency of the solar drying system with both drying modes was estimated to be about 23%. The indirect forced convection solar drier integrated with heat storage material is more suitable for producing high quality copra.

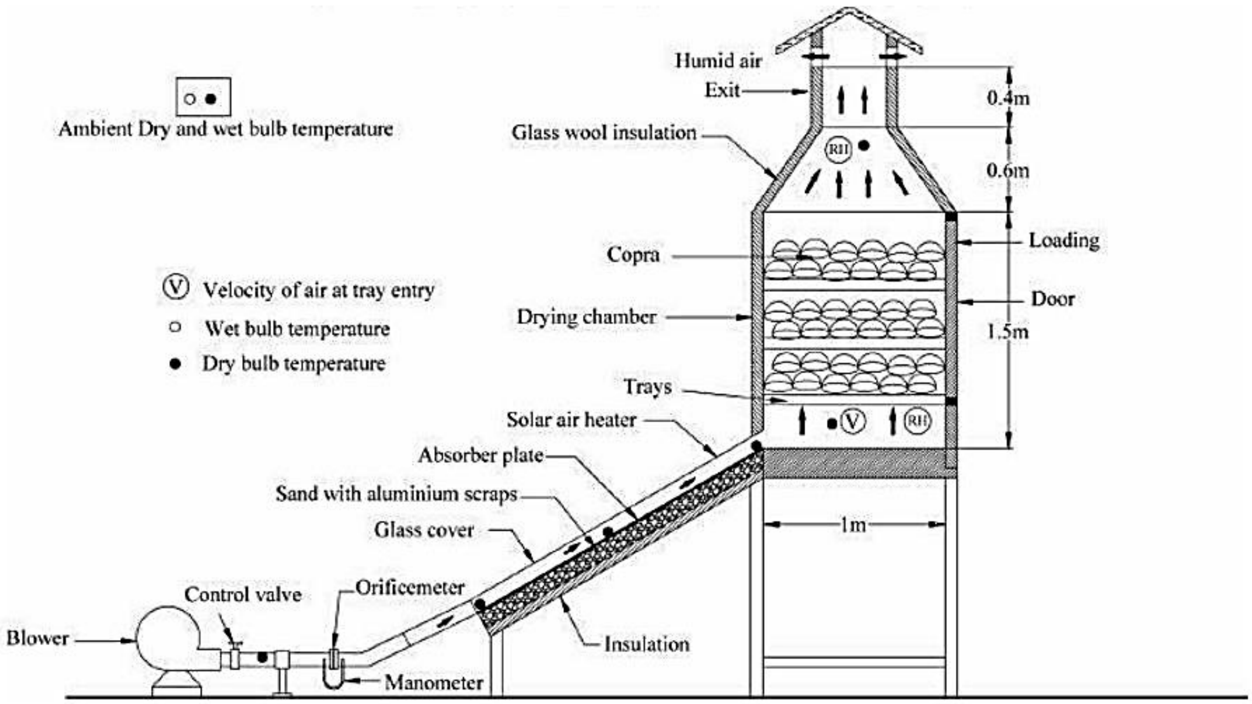

Figure 2.8: Solar dryer integrated with different sensible heat storage material for crop drying (Mohanraj and Chandrasekar, 2009)

On-farm crop drying is frequently essential to prevent mold growth and spoilage of mechanically harvested crops. Keeping this in view suspended-plate solar air heaters were installed on farms in Tennessee by Womac *et al*., (1985), to supply heat for grain and crop drying. Designs included a wrap-around heater, a portable heater and a multipurpose barn. The heaters were telemetrically monitored to determine thermal performance and to allow subsequent analyses of economic feasibility. Thermal analysis of system revealed that solar air heaters provide a suitable air temperature rise during most crop drying conditions. The heaters operated with average thermal efficiencies in the range of 50–70%. Economic analyses indicated that solar air heaters are economically feasible if they are used at least 2 months per year assuming not more than 14% annual interest and at least 4% annual fuel inflation.

An economic analysis of a roof-integrated solar air heating system, for drying fruit and vegetables was carried out by Sreekumar, (2010). The system was found efficient and economically viable and it was experimentally proved for drying pineapple. Economic analysis showed that the cumulative present worth of annual savings for drying bitter gourd over the life of the solar dryer turned out to be approximately 17 million Rs. The capital investment of the dryer was Rs. 550,000 and the payback period of the dryer was found to be 0.54 year, which is very short considering the life of the system. The cost of drying pineapple in the solar dryer was only about 20% of drying it in electric dryer. The life of the system was expected to be 20 years, because the material used in the construction is corrosion proof.

Jain and Jain, (2004), presented a transient analytical model for an inclined multi-pass solar air heater with in-built thermal storage and attached with the deep-bed dryer. This study was done for a day in the month of October for the climatic condition of Delhi (India). They studied the effect of change in the tilt angle, length and breadth of a collector and mass flow rate on the temperature. The grain temperature increases with the increase of collector length, breadth and tilt angle up to typical value of these parameters. The thermal energy storage also affects during the off sunshine hours and is very pertinent for crop drying applications. The proposed mathematical model is useful for evaluating the thermal performance of a flat plate solar air heater for the grain drying applications. It is also useful to predict the moisture content, grain temperature, humidity of drying air and drying rate in the grain bed.

2.6.5 Related works on solar air heater application on Space heating

Solar air collectors have various applications: on the one hand, they can be used for air heating in cold seasons; on the other hand they can be used in summer to evacuate the warm and polluted air from residential, offices, industrial, and commercial buildings.

Hazem and Tayler, (2011), study the application of solar air heater for transportation maintenance facilities. Solar air heating systems would benefit transportation maintenance facilities since these facilities require large volumes of outdoor air to replace air contaminated from vehicles’ exhausts, and vehicle repair and welding activities. By preheating ventilation air, SAH system reduces the consumption of conventional energy, such as natural gas or diesel fuel. As shown in Figure 2.9, the SAH system consists of two parts: (1) a solar collector and (2) a fan and air distribution system. The most common style of collector for SAH is the transpired solar collector that is usually installed on the south facing wall in the form of a rain screen. The fan pulls ventilation air through the small holes in the dark colored solar collector into an air gap where the air becomes heated between the building’s exterior wall and solar collector cover.

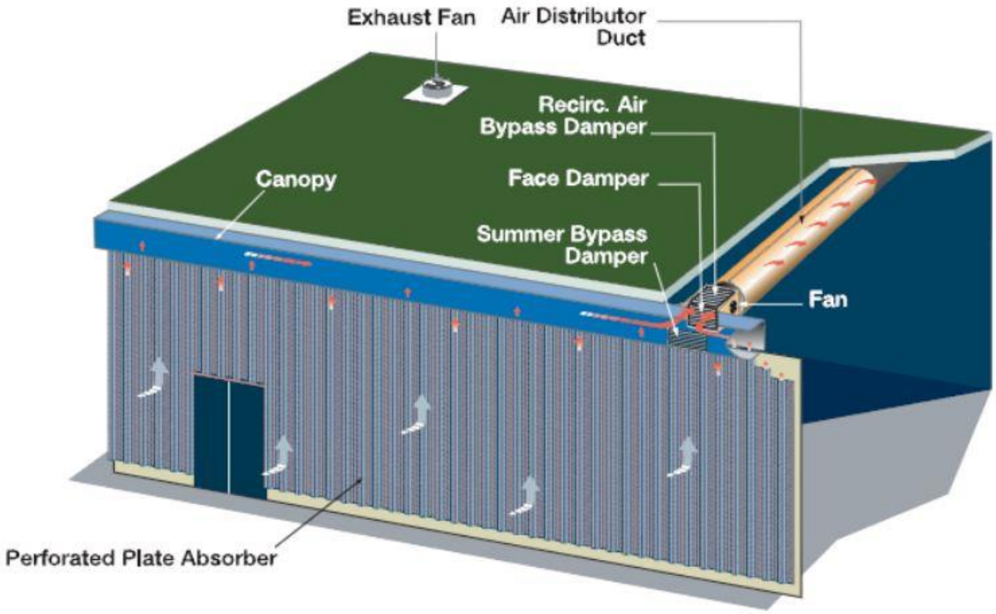

Figure 2.9: Application of solar air heater for heating transport maintenance facility (Hazem and Tayler, 2011)

Through convection, the heated air rises and is pulled into the buildings ventilation system and delivered throughout the building with the air distribution system. In the summer, a bypass damper is opened, avoiding an unnecessary load on the air-conditioning system. The bypass damper is controlled by an adjustable thermostat that senses outdoor temperature. The thermostat is typically set to open the damper when the outdoor temperature is warm enough to eliminate the need for heating

Zhao *et al*., (2011), studied on a solar air heating system for building heating season (from November to March) and hot water supply all year around in North China. Total five different working modes were designed based on different working conditions: (1) heat storage mode, (2) heating by solar collector, (3) heating by storage bed, (4) heating at night and (5) heating by an auxiliary source. These modes can be operated through the on/off control of fan and auxiliary heater and through the operation of air dampers manually. They used solar fraction of the system as the optimization parameter. They used TRNSYS program to analyze the solar collector area, installation angle of solar collector, mass flow rate through the system, volume of pebble bed, heat transfer coefficient of the insulation layer of the pebble bed and water storage tank, height and volume of the water storage tank. The results of system showed that the designed solar system can meet 32.8% of the thermal energy demand in the heating season and 84.6% of the energy consumption in non-heating season, with a yearly average solar fraction of 53.04%.

2.7. Conclusion from literatures and research gap

A literature review about the existing conventional solar air heater and some modified dryer has been studied briefly so far. From the works of literatures, it can be concluded that solar air heater can be used in a number of field of area. But contrary, the incorporation of solar energy in the air heater may affect the process stability, which results from the daily fluctuate and unpredictable nature of solar energy. Thermal energy storage is a key issue to be addressed toward the intermittency of solar energy. And on the other perspective it can be conclude that the efficiency and heat gain for most solar dryer is low. To tackle this problem a number of researchers have been dedicated to study the enhancement technics i.e., integrating storage material and usage of some modified materials that increase the efficiency of the system.

Numerical and experimental study on solar SAH has been conducted by some researchers (Mohanraj and Chandrasekar 2009; Zhao *et al*., 2011; Aboul *et al*., 2000; Thakar and Prajapati, 2020 … etc) on the base of a specific geographical location. But, there is a little study on the comprehensive effect of the whole enhancement technics for the solar air heater is developed with both experimental and open platform program aided numerical analysis.

To cope up the mentioned problems, this thesis work presents experimental and numerical evaluation of solar air heater by integrating finned absorber, sensible storage material and reflectors in the convectional solar air heaters. The python program is developed for numerical performance analysis of each enhancement techniques which helps to adopt the solar dryer for different application areas. Lastly, the enhanced solar air heater is implemented for the application of selected agricultural crops and space heating of locally selected poultry farm.

CHAPTER 3: METHODOLOGY

3.1. Introduction

In this Chapter, the methods used to meet the objectives stated in the Chapter 1 are discussed. The weather data of Adama city was collected from National Metrological Agency, Adama branch of Ethiopia and analyzed by using empirical formulas. For the experimental performance analysis the setup of the experiment was constructed for convectional SAH integrated with dryer box. After the first experiment, the convectional SAH is modified with three enhancement methods; longitudinal finned absorber, gypsum storage, reflector and lastly by the combination of them. For the case of numerical analysis, each SAH configuration was modeled and python program code was developed to perform the analysis.

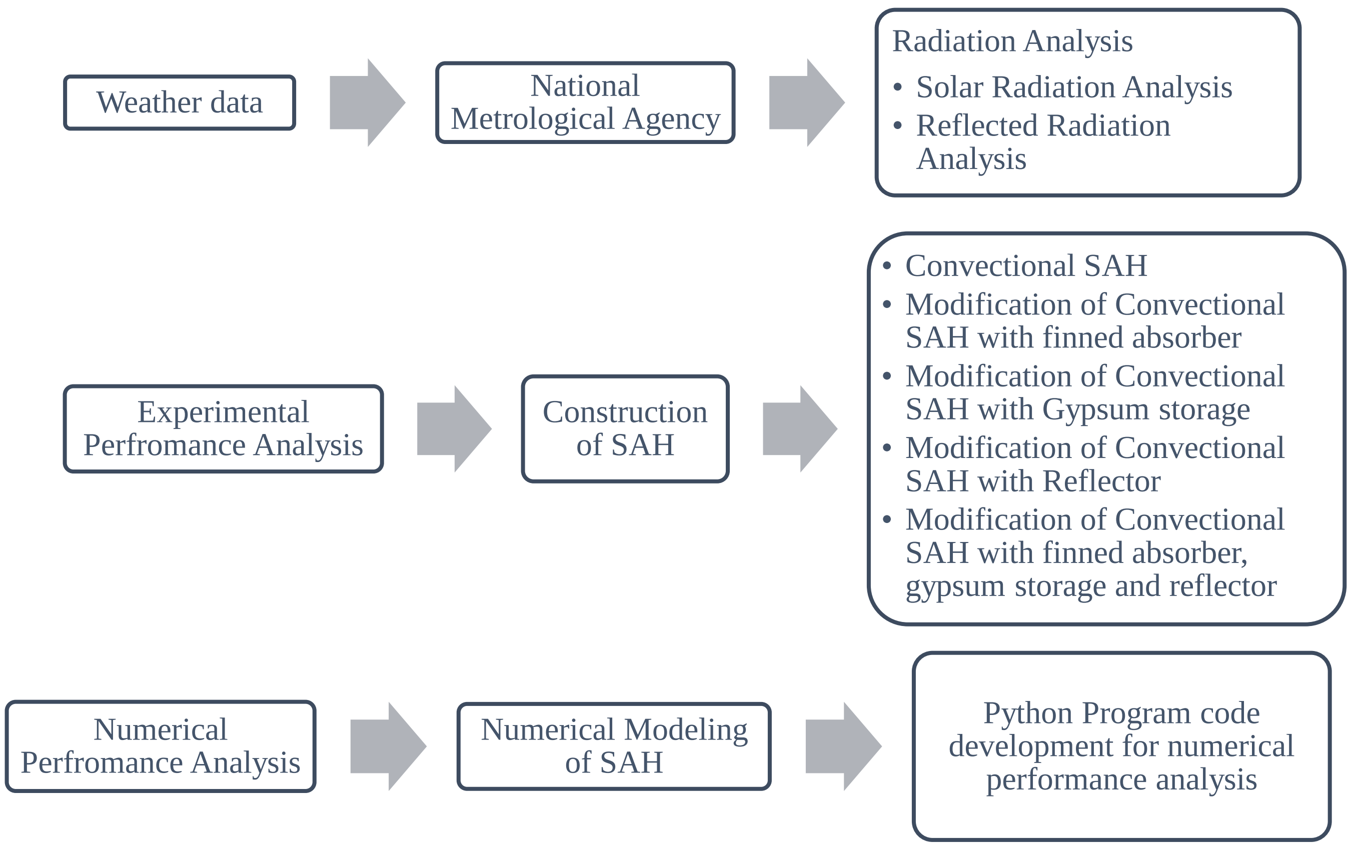

Figure 3.1: Methodology of the thesis work

3.2. Solar radiation data

Solar radiation data is important for modeling and performance prediction of solar energy conversion devices such as solar air heaters. The National Meteorological Agency collects the average sunshine hour, wind speed and temperature as solar radiation data for some cities. As a result, it is necessary to use some models and correlations to determine the hourly temperature and the global daily and hourly radiation received by the solar air heater. Five years data from 2012 up to 2017 at altitude of 1648m above sea level for Adama city was collected from National Meteorological Agency Adama branch. Figure 3.2 shows the average maximum and minimum temperature and wind speed for an annual climatic condition of Adama.

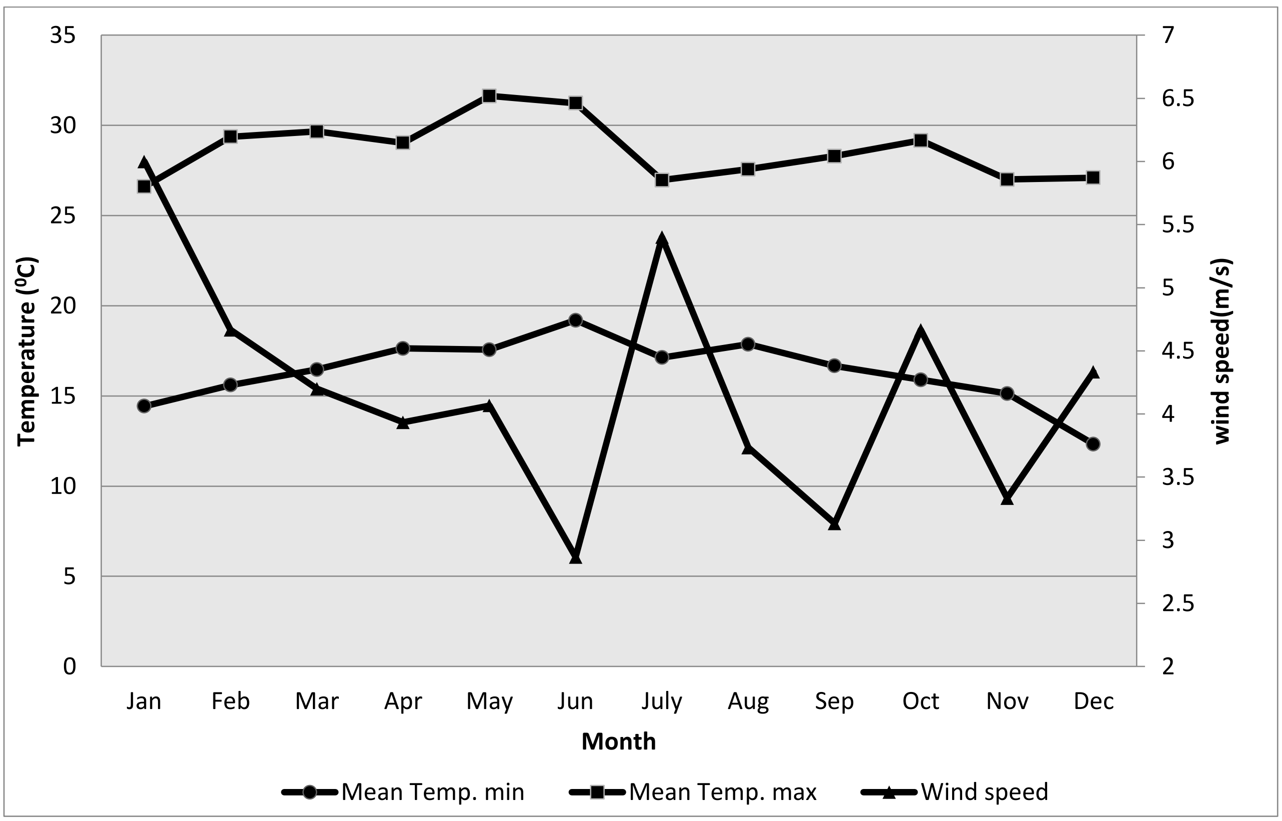

Figure 3.2: Monthly average annual climatic condition of Adama (Ethiopia national meteorological agency)

3.3. Solar geometry

The first step for modeling the incident solar irradiation is to determine the sun's position and path in the sky, as seen from the solar air heater geographic position, as a function of the day of the year and hour of the day.

Solar time: is a time based on the apparent angular motion of the sun across the sky with solar noon the time the sun crosses the meridian of the observer and it is given by Duffie and Beckman, (2013):

$solar\ time$ = $standard\ time$ + 4(L_{st} - L_{loc}) + E…………………………………………..…(3.1)

Where, L_{st} is the standard meridian for the local time zone, L_{loc} is the longitude of the location in question, and longitudes are in degrees west, that is, $0^o < L < 360^o$.The parameter E is the equation of time (in minutes), and is given by (Duffie and Beckman, 2013):

E=229.2(0.000075+0.001868$cosB$-0.032077$sinB$-0.014615$cos2B$-0.04089$sin\ 2B$).... (3.2)

$B = (n - 1)\frac{360}{365}$……………………………………………...…………………………….….... (3.3)

Where, n is the day of the year, thus $1 \le n \le 365$.

Declination angle (δ): the angular position of the sun at solar noon (i.e, when the sun is on the local meridian) to the plane of the equator, north positive, $-23.45^o \le \delta \le 23.45^o$:

$\delta = 23.45 \sin(\frac{360(284 + n)}{365})$ ………………………………………………………………….. (3.4)

Solar hour angle (ω): the angular displacement of the sun east or west of the local meridian due to rotation of the earth on its axis at 15^o per hour; morning negative, afternoon positive. And it is given by (Duffie and Beckman, 2013):

ω = 15($solartime$ - 12)…………………….....……...…………………………………… (3.5)

Latitude (φ): the angular location north or south of the equator, north positive, $-90^o \le \varphi \le 90^o$. Adama is located on 8.54^o due north of the equator.

Slop (β): the angle between the plane of the surface and the horizontal. ,$-180^o \le B \le 180^o$. $\beta < 90^0$ means that the surface has a downward-facing component

Angle of incidence (θ): the angle between the beam radiation on a surface and the normal to that surface.

$cos\theta = \cos\delta\cos\omega(\cos\varphi\cos\beta + \sin\varphi\sin\beta) + \sin\delta(\sin\varphi\cos\beta - \cos\varphi\sin\beta)$ ………..……. (3.6)

Zenith angle (θ_z): the angle between the vertical and the line to the sun or the angle of incidence of beam radiation on a horizontal surface:

$\theta z = cos\varphi cos\delta cos\omega + sin\varphi sin\delta$ ………………...………………………………………. (3.7)

3.4. Solar radiation analysis

3.4.1. Extraterrestrial and ground level radiation on a horizontal surface

The global daily solar irradiance (G_o) received by a horizontal surface at the upper limit of earth atmosphere, is calculated as follows (expressed in $J/m^2 day$) (Duffie and Beckman, 2013):

$$G_o = \frac{24*3600}{\pi} G_{sc} \left(1 + 0.033 \cos\left(\frac{360n}{365}\right)\right) * \left(\cos\varphi \cos\delta \sin\omega_{sr} + \pi\frac{\omega_{sr}}{180}\sin\varphi \sin\delta\right) \quad (3.8)$$

Where, G_{sc} is the solar constant, is 1367 W/m^2 and, ω_{sr} is the sunset hour angle, which is given by

$$(\omega_{sr}) = \cos^{-1}(-\tan(\varphi)\tan(\delta)) \quad (3.9)$$

3.4.2. Global daily solar radiation on a surface at ground level

Surface solar radiation on a ground level was suggested by Angstrom, who relates estimated, based on the daily sunshine duration experimental data, using some empirical constant obtained by regression analysis (Tiwari *et al.*, 2016):

$$\frac{G}{G_O} = a + b\left(\frac{ns}{Ns}\right) \quad (3.10)$$

Where, G is the global daily surface radiation on the ground level, and the regression constant a and b can be determined form:

$$a = -0.110 + 0.235\cos\varphi + 0.323\left(\frac{ns}{Ns}\right) \quad (3.11)$$

$$b = 1.449 - 0.533\cos\varphi - 0.694\left(\frac{ns}{Ns}\right) \quad (3.12)$$

Where, n_s is the bright sunshine hour of Adama for the successive four years and N_s is the maximum possible daily hours of bright sunshine. The average bright sunshine hour of Adama for the successive years is given in Figure 3.3.

Solar radiation reaching the air heater cover consists of: (1) Beam–or direct–radiation coming on a straight path from the sun, i.e. its trajectory is not deviated during its passage through the atmosphere. (2) Diffuse radiation, which is the fraction of solar radiation that reaches the earth after being scattered by the atmosphere (Rayleigh and aerosols scattering, reflections and scattering by the cloud cover, multiple-reflections between the ground and the atmosphere, etc.). This radiation component has no preferential path, i.e. is isotropic. (3) Albedo radiation, which is the fraction of solar radiation reaching the cover after diffuse reflection on the ground (Alexander *et al*, 2002).

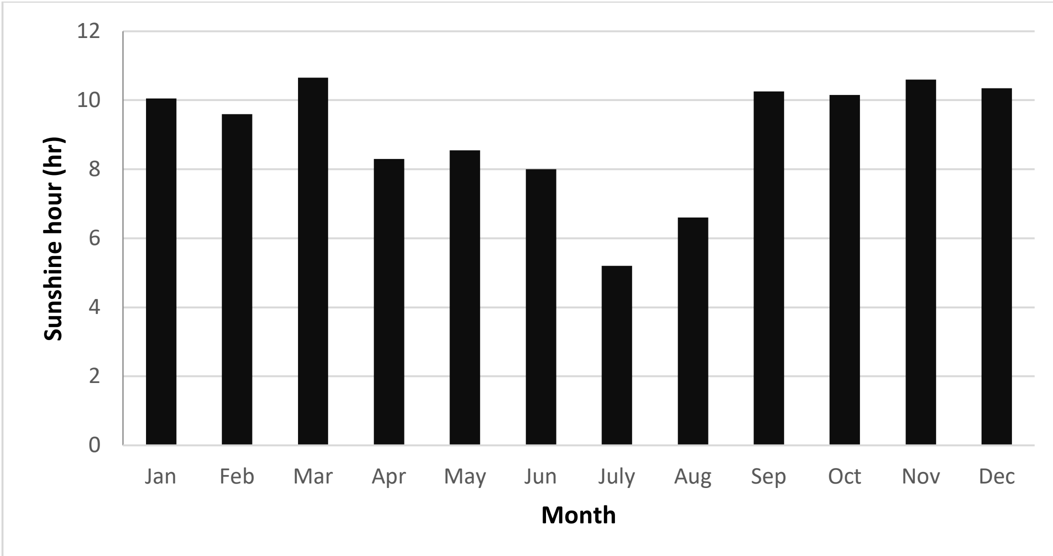

Figure 3.3: Bright sunshine hours for the representative days of each month of Adama(Ethiopia national meteorological Agency)

3.4.3. Beam and diffuse daily solar radiation on a horizontal surface at ground level

The average daily diffuse radiation on a horizontal surface, D (J/m^2day), can be determined from the average daily global radiation on a horizontal surface and the number of bright sunshine hours (Tiwari *et al.*, 2016):

$\frac{D}{G}$ = 0.931 - 0.814($\frac{ns}{Ns}$) …………………………..…………………………………..……….. (3.13)

The daily beam solar radiation hitting a horizontal surface at ground level, (J/m^2day), is simple deduced using:

B= G- D…………………………………...……………………….…………...……………..... (3.14)

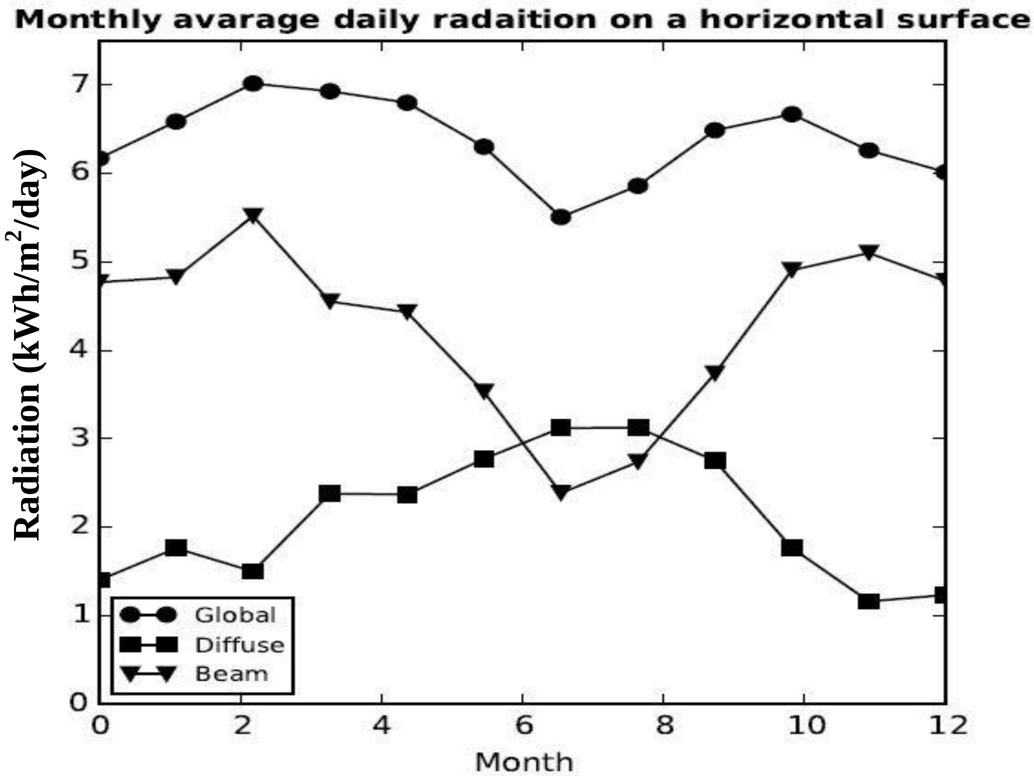

Figure 3.4: Monthly average daily global, beam and diffused radiation on a horizontal surface

3.4.4. Global, beam and diffuse hourly solar radiation on a horizontal surface at ground level

The monthly average hourly global and diffuse radiation on a horizontal surface can be calculated from the knowledge of the monthly average daily global and diffuse radiation on a ground level. The hourly global, diffuse and beam radiation on a horizontal surface at the ground level is given by Tiwari *et al.*, (2016), respectively by equation (3.15), (3.16), and (3.17)

$$\frac{I_G}{\boldsymbol{G}} = \frac{\pi}{24*3600}\left[a_1 + b_1 \cos\omega\right] * \left(\frac{\cos\omega - \cos\omega_{sr}}{\cos\omega_{sr} - \frac{\pi\omega_{sr}}{180*\cos\omega_{sr}}}\right) \quad \text{(3.15)}$$

$$\frac{I_D}{D} = \frac{\pi}{24*3600} * \left(\frac{\cos\omega - \cos\omega_{sr}}{\cos\omega_{sr} - \frac{\pi\omega_{sr}}{180*\cos\omega_{sr}}}\right) \quad \text{(3.16)}$$

$$I_B = I_G - I_D \quad \text{(3.17)}$$

Where a_1 and b_1 are regression constant given by:

$$a_1 = 0.409 + 0.502\sin(\omega_{sr} - 60) \quad \text{(3.18)}$$

$$b_1 = 0.661 + 0.477\sin(\omega_{sr} - 60) \quad \text{(3.19)}$$

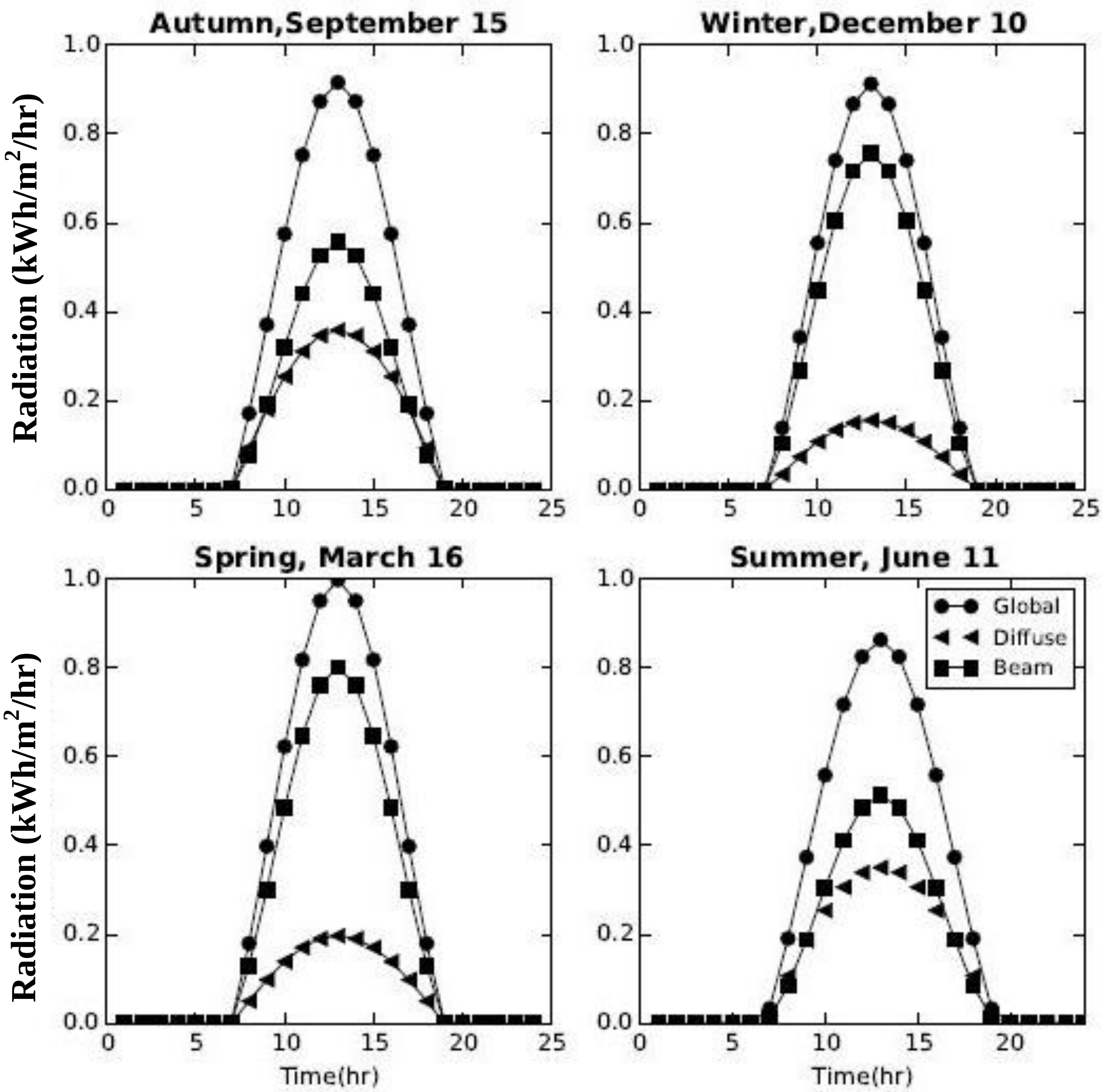

Figure 3.5: Hourly global, beam and diffused radiation on a horizontal surface for the representative day of each season of the first month

3.4.5. Incident solar radiation

Investigation of solar air heater system requires precise knowledge regarding the availability of global solar radiation and its components at the location of interests. Since the solar radiation reaching the earth's surface depends upon climatic conditions of the place, a study of solar radiation under local climatic conditions is essential. The solar radiation energy incident on the collector surface which is inclined at an angle of (β = 23^{o}) to the horizontal surface is defined in terms of global, diffuse, beam and reflected radiation. Total solar radiation incident on a surface consists of beam, diffuse and reflected solar radiation from the ground and surrounding.

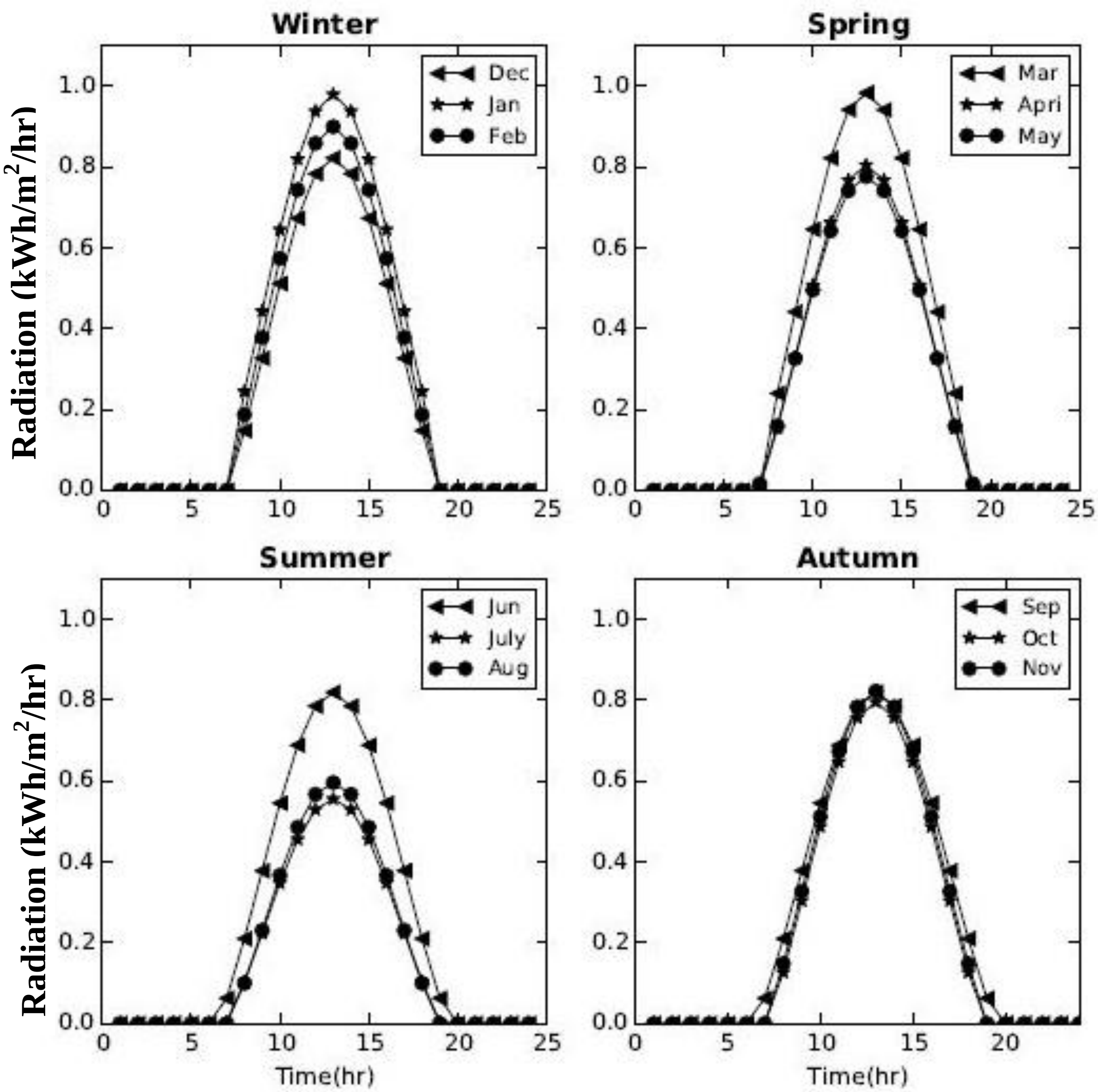

Figure 3.6: Monthly average hourly incidence solar radiation on a tilted surface for the representative day of each season of the first month

Total radiation on a surface can be evaluated by arbitrary orientation from knowledge of beam, diffuse and global radiation on horizontal surface (Duffie and Beckman, 2013). The total incident radiation on the surface can be written as:

$$I_T = B \times R_b + D \times \left(\frac{1+\cos\beta}{2}\right) + G \times \rho_g \left(\frac{1-\cos\beta}{2}\right) \qquad (3.20)$$

Where, R_b is the beam radiation factor and ρ_g ground reflectivity, the value of the reflection coefficient is 0.2 for ordinary ground. Beam radiation factor (R_b) is defined as the ratio of beam radiation incident on an inclined surface to that on a horizontal surface defined by:

$$R_b = \frac{\cos\theta}{\cos\theta_z} \qquad (3.21)$$

Where, θ is the angle of incidence and θ_z is the zenith angle. The radiation on the collector for the representative day of each month is shown in Figure 3.6.

3.5. Reflector geometry and reflected radiation analysis

3.5.1. Reflector geometrical analysis

Based on the incident angle of the sun and the seasonal variation, the inclination angel of reflectors has to be manipulated. To get efficient enhancement though the integrated of reflectors the angel tracking have to be done with a great accuracy. That is to avoid the shading effect of the right and left side reflector. Figure 3.7 shows the solar air heater orientation relative to sun position. The figure clearly shows the longitude and latitude of the earth and sun position relative to the air heater.

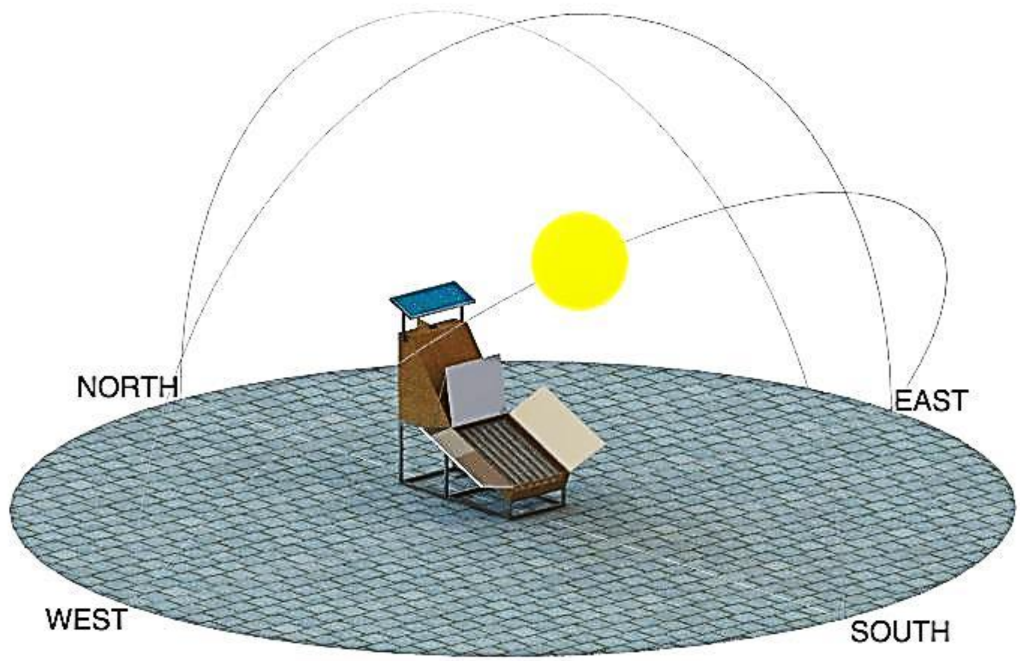

Figure 3.7: Orientation of the solar dryer with respect to solar position

3.5.1.1. Top reflector

Optimum position of top booster mirror is computed for all months and given latitude for maximizing the reflected radiation component onto the inclined absorber plate by angle β with the horizontal.

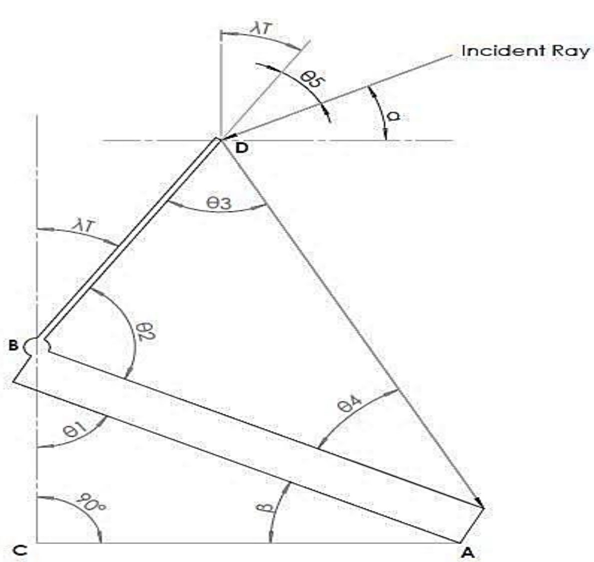

Figure 3.8: Geometrical analysis of top reflector

Top reflector the solar angles for the collector also calculated as follows (Nigussie and Teklay, 2017);

$\theta_1 + \theta_2 + \lambda_T = 180^o$……………………………………………………………….…..(3.22)

Let's take the triangle ABC

$\theta_1 + \beta + 90 = 180$……………………………………..………………...……..(3.23)

$\theta_1 = 90 - \beta$……………………………………………………………………...……..(3.24)

From equation (3.22) and (3.24) θ_2 becomes

$\theta_2 = 90 + \beta - \lambda_T$…………………………………………………………………....(3.25)

The reflected solar radiation from the top reflector falls on the collector under the angle θ_3 can be determined as follows,

From the sum of angle in triangle DBF

$\theta_2 + \theta_3 + \theta_4 = 180^o$……………………………………………………………..….(3.26)

Also

$\theta_5 = 90 - (\alpha + \lambda_T)$……………………………………………………………………….(3.27)

According to Snell's law that states the angle of incidence beam is equal to angle of reflected beam

$\theta_3 = \theta_5$…………………………………………………………………………………….(3.28)

By combining equation (3.26), (3.27) and (3.28)

$\theta_4 = 2\lambda_T + \alpha - \beta$………………………………………………………….………..(3.29)

Where, θ_1 is the angle between the line perpendicular to the ground and collector<ABC, θ_2 is the angle of the triangle DBA which is constructed between the reflector and collector, λ_T is angle between upper reflector and vertical plane, $\theta_3$is the angle between the reflector and the reflected sun ray from the reflector which reaches the collector

If ray I strikes the top of the vertical reflector mirror at an angle α, then the line DA formed by reflected ray reaching the edge of the upper glass cover and then from triangle BCD;

$\angle \mathrm{ABD} = \theta_2 \quad \angle \mathrm{BDA} = \theta_3 \quad \angle \mathrm{DAB} = \theta_4$……………………………………………...……..(3.30)

Also mathematically we know that

$\frac{AD}{\sin(\theta_2)} = \frac{AB}{\sin(\theta_3)} = \frac{BD}{\sin(\theta_4)}$…………………………………………………………..….……..(3.21)

Since, AB=W (width of the Collector), BD=W_T(Width of top reflector)

$\frac{W}{\sin(\theta_3)} = \frac{W_T}{\sin(\theta_4)}$……………………………………………………………………...………..(3.32)

Where, $n_T = \frac{W}{W_T}$, equation (3.32) can be simplified as

$\sin(\theta_4) = \mathrm{n}_T \sin(\theta_3)$………………………………………………………….……………..….(3.33)

For the case were n_T=1 equation (3.33) becomes,

$\theta_4 = \theta_3$…………………………………………………..…………………………..…..(3.34)

From equation 3.27, 3.28 and 3.29

$\lambda_T = \frac{90^o - 2\alpha + \beta}{3}$…………………………………………………….…………….………(3.35)

Equation 3.35 gives the optimum angle of top reflector (λ_T) with vertical line for each month for n_T=1. For 0<n_T<2 the optimum angle of top reflector (λ_T) is computed from implicit equation 3.33. For this work n_T=0.5 λ_T is computed and listed on APPENDEX F.

3.5.1.2. Left side reflector

Where, $\alpha + \beta$ is the solar altitude angle, $\theta_8$is the angle between collector and reflector $\theta_6$is the angle between sun ray and reflector that is the angle of incidence of the reflector, θ_{10} is the angle at which the Reflected radiation from the left side reflector falls on collector surface, $\theta_7$the angle between reflector and direct sun light to the reference plane which is perpendicular to the ground.

For the angle between sun ray and reflector that is the angle of incidence of the reflector

$\theta_6 = 180 - (\alpha + \beta) - \lambda_L$…………………………………………………………...…..(3.36)

For the angle between reflector and direct sun light to the reference plane

From opposite interior angles and equation 3.36

$$\theta_6 = \theta_7 = 180 - (\alpha + \beta) - \lambda_L \quad (3.37)$$

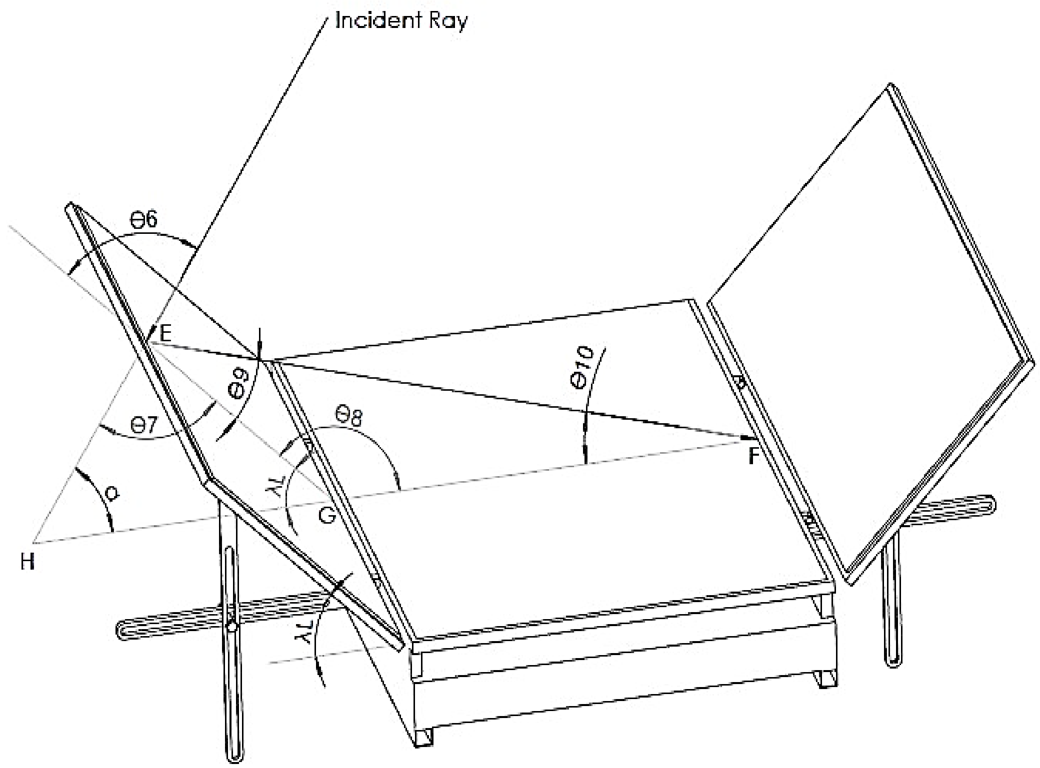

Figure 3.9: Geometrical analysis of left reflector

For the angle between collector and reflector

$$\theta_8 = 180 - \lambda_L \quad (3.38)$$

Using Snell's law and equation 3.37

$$\theta_6 = \theta_9 = 180 - (\alpha + \beta) - \lambda_L \quad (3.39)$$

The angle at which the reflected radiation from the left side reflector falls on collector surface can be determined as

$$\theta_8 + \theta_9 + \theta_{10} = 180^o \quad (3.40)$$

By combining equation (3.38), (3.39) and (3.40)

$$\theta_{10} = 2\lambda_L + \alpha + \beta - 180^o \quad (3.41)$$

If ray I strikes the edge of the left side reflector mirror at an angle θ_6, then the line EF formed by reflected ray reaching the edge of the upper glass cover and then from triangle EFG;

$$\angle EGF = \theta_8 \quad \angle GEF = \theta_9 \quad \angle EFG = \theta_{10} \quad (3.42)$$

Also mathematically, from sin law

$$\frac{EF}{\sin(\theta_8)} = \frac{FG}{\sin(\theta_9)} = \frac{GE}{\sin(\theta_{10})} \quad (3.43)$$

Since, GF=W (width of the Collector), GE=W_{lr} (Width of the left side reflector)

$$\frac{W}{\sin(\theta_9)} = \frac{W_{lr}}{\sin(\theta_{10})} \quad (3.44)$$

Where, $n_L = \frac{W}{W_{lr}}$, equation 3.44 can be simplified as

$$\sin(\theta_{10}) = n_L \sin(\theta_9) \quad (3.45)$$

For the case were n_L=1 equation 3.45 becomes,

$$\theta_{10} = \theta_9 \quad (3.46)$$

From equation 3.39 and 3.41

$$\lambda_L = 120 - \frac{2}{3}(\alpha + \beta) \quad (3.47)$$

Equation 3.47 gives the hourly variation of angle of left side reflector (λ_L) with collector plane for each month for n_L=1. For 0<n_L<2 the angle of left side reflector (λ_L) is computed from implicit equation 3.45. For this work n_L=0.5 λ_L is computed and listed on APPENDEX E.

3.5.1.3. Right side reflector

θ_{11} is the angle of incidence for the reflector that is equal to $\alpha + \beta - \lambda_R$ and θ_{12} is the angle between the reflected sun ray and the reflector and equal with the angle of incidence for the reflector.

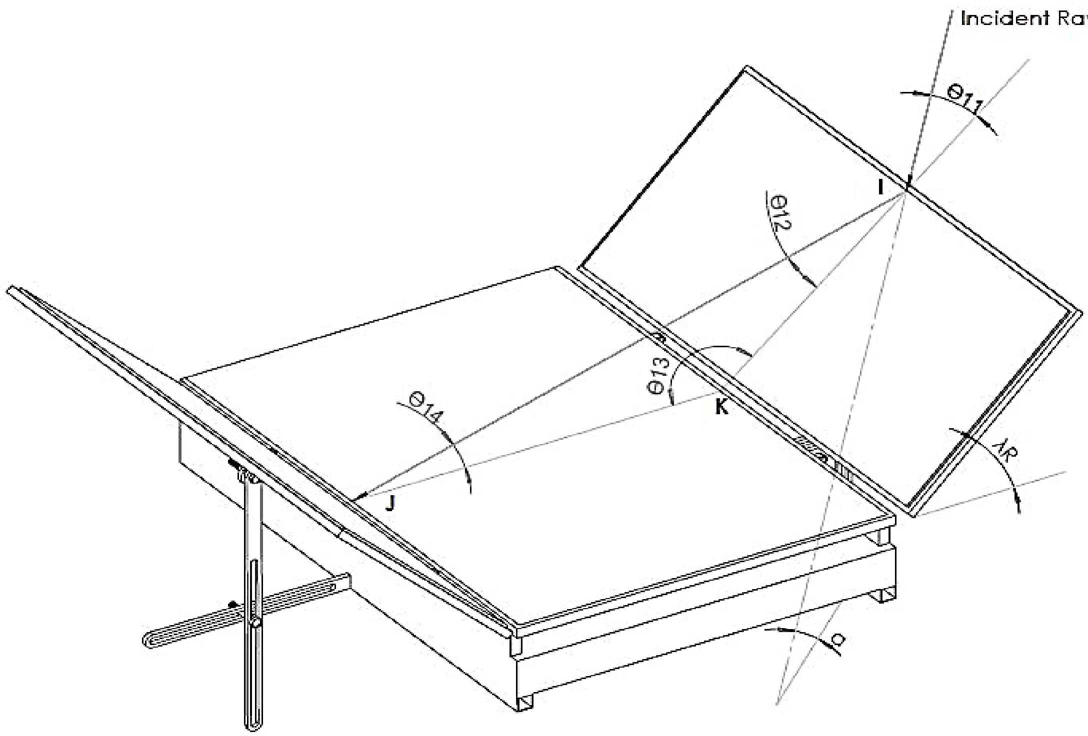

Figure 3.10: Geometrical analysis of right reflector

According to Snell's law that states the angle of incidence beam is equal to angle of reflected beam.

Therefore,

$\theta_{11} = \theta_{12} = \alpha + \beta - \lambda_R$……………………………………………………………..(3.48)

θ_{13} is the angle between the reflector edge and the collector

$\theta_{13} + \lambda_R = 180^o$………………………………………………………………….….(3.49)

$\theta_{13} = 180^o - \lambda_R$…………………………………………………………………......(3.50)

λ_R is the tilted plane angle of the right side reflector to the horizontal plane,

The angle at which the Reflected radiation from the left side reflector falls on collector surface can be determined from equation 3.48 and 3.49

$\theta_{14} = 2\lambda_R - (\alpha + \beta)$…………………………………………………………..…….(3.51)

If ray I strikes the right side reflector mirror at an angle θ_{11}, then the line IJ formed by reflected ray reaching the edge of the upper glass cover and then from triangle ΔIJK;

$$\angle \mathrm{JIK} = \theta_{12} \quad \angle \mathrm{JKI} = \theta_{13} \quad \angle \mathrm{KJI} = \theta_{14} \quad (3.52)$$

Also mathematically, from sine law

$$\frac{JK}{\sin(\theta_{12})} = \frac{JI}{\sin(\theta_{13})} = \frac{IK}{\sin(\theta_{14})} \quad (3.53)$$

Since, JK=W (width of the Collector), BD=Wrr (Width of the right reflector)

$$\frac{W}{\sin(\theta_{12})} = \frac{W_{rr}}{\sin(\theta_{14})} \quad (3.54)$$

Where, $n_r = \frac{W}{W_{rr}}$, equation 3.54 can be simplified as

$$\sin(\theta_{14}) = n_r \sin(\theta_{12}) \quad (3.55)$$

For the case were n_r =1 equation 3.55 becomes,

$$\theta_{14} = \theta_{12} \quad (3.56)$$

From equation 3.46 and 3.49

$$\lambda_R = \frac{2}{3}(\alpha + \beta) \quad (3.57)$$

Equation 3.57 gives the hourly variation of angle of Right reflector (λ_R) with collector plane for each month for n_r =1. For 0< n_r <2 the angle of right side reflector (λ_R) is computed from implicit equation 3.53. For this work n_r=0.5 λ_R is computed and listed on APPENDEX E.

3.5.2. Radiation analysis of reflector

The collector collects direct solar radiation, the reflected solar radiation from top, bottom, left and right side reflectors and the total diffuse radiation in collectors with reflectors adjacent to the absorber for increasing efficiency effect.

Therefore the total solar radiation $I_{tot.col}$ on the collector surface is:

- The sum of the direct solar radiation on collector surface which is represented by $I_{dir\text{-}c}$,
- The reflected solar radiation from top reflector which reached the collector surface which is represented by $I_{ref\text{-}r1}$ with tilted plane angle λ_T.

- The reflected solar radiation from the left side reflector which reached the collector surface which is represented by I_{ref-r4} with tilted plane angle λ_L
- The reflected solar radiation from the right side reflector which reached the collector surface which is represented by I_{ref-r3} with tilted plane angle λ_R, and the total diffuse radiation $I_{dif-col}$.

In order to analyze the flat plate solar collector integrated with reflector some reasonable assumptions are needed. Hence, the analysis is based on the following assumptions:

- The global solar radiation is considered in the present analysis.
- The flat reflector (aluminum foil) is specular with a constant reflectivity (ρ_{Al}=0.88), irrespective of the radiation incidence angle.
- Shading of the reflector on the collector is not taken into consideration (As a result of manual tracking system is available)
- The collector does not reflect radiation back to the reflectors;
- There are no mutual reflections between the reflectors;
- Only diffuse component of the solar radiation (the sky-diffuse radiation and the reflected radiation from the reflectors) falls directly on the collector.

Therefore, the total solar radiation I_{tot-c}on the collector surface is

$$I_{total-c} = I_{dir-c} + I_{dif-c} + \sum_{i=1}^{3} I_{ref-ri} \quad (3.58)$$

$$\sum_{i=1}^{3} I_{ref-ri} = I_{ref-r1} + I_{ref-r2} + I_{ref-r3} \quad (3.59)$$

Where,

I_{ref-r1} is reflected solar radiation from top

I_{ref-r2} is reflected solar radiation from right side

I_{ref-r3} is reflected solar radiation from left side

3.5.2.1. Reflected radiation from top reflector

Incident radiation on the top reflector I_{in-r1}

$$I_{in-r1} = I_{in}\cos(\lambda_T + \alpha) \quad (3.60)$$

Referring from equation 3.29 and 3.60, reflected radiations from the top reflector with the tilted plane angle λ_T are defined as:

$I_{ref-r1} = \rho I_{in} \sin\theta_4 \cos(\lambda_T + \alpha)$……………………………………………...………(3.61)

Where, I_{in} is incident radiation from the light source, α is the solar altitude angle of radiation from the light source, β is the tilted plane angle of the collector, ρ is reflectance of the reflector material.

3.5.2.2. Reflected radiation from left and right side reflector

The incident radiations on the right and left reflector can be calculated as follows, respectively. Incident radiation on the right side reflector

$I_{in-r2} = I_{in} \sin(\theta_{11})$………………………………………………………….……...(3.62)

Incident radiation on the left side reflector

$I_{in-r3} = I_{in} \sin(\theta_6)$…………………………………………………………………..…(3.63)

The reflected radiation from the left and right side reflector with the tilted plane angle λ_L and λ_R, respectively are defined as:

$I_{ref-r3} = \rho I_{in} \sin(\theta_6) \sin(\theta_{10})$……………………………………………………..…….(3.64)

$I_{ref-r2} = \rho I_{in} \sin(\theta_{11}) \sin(\theta_{10})$………………………………………………………..(3.65)

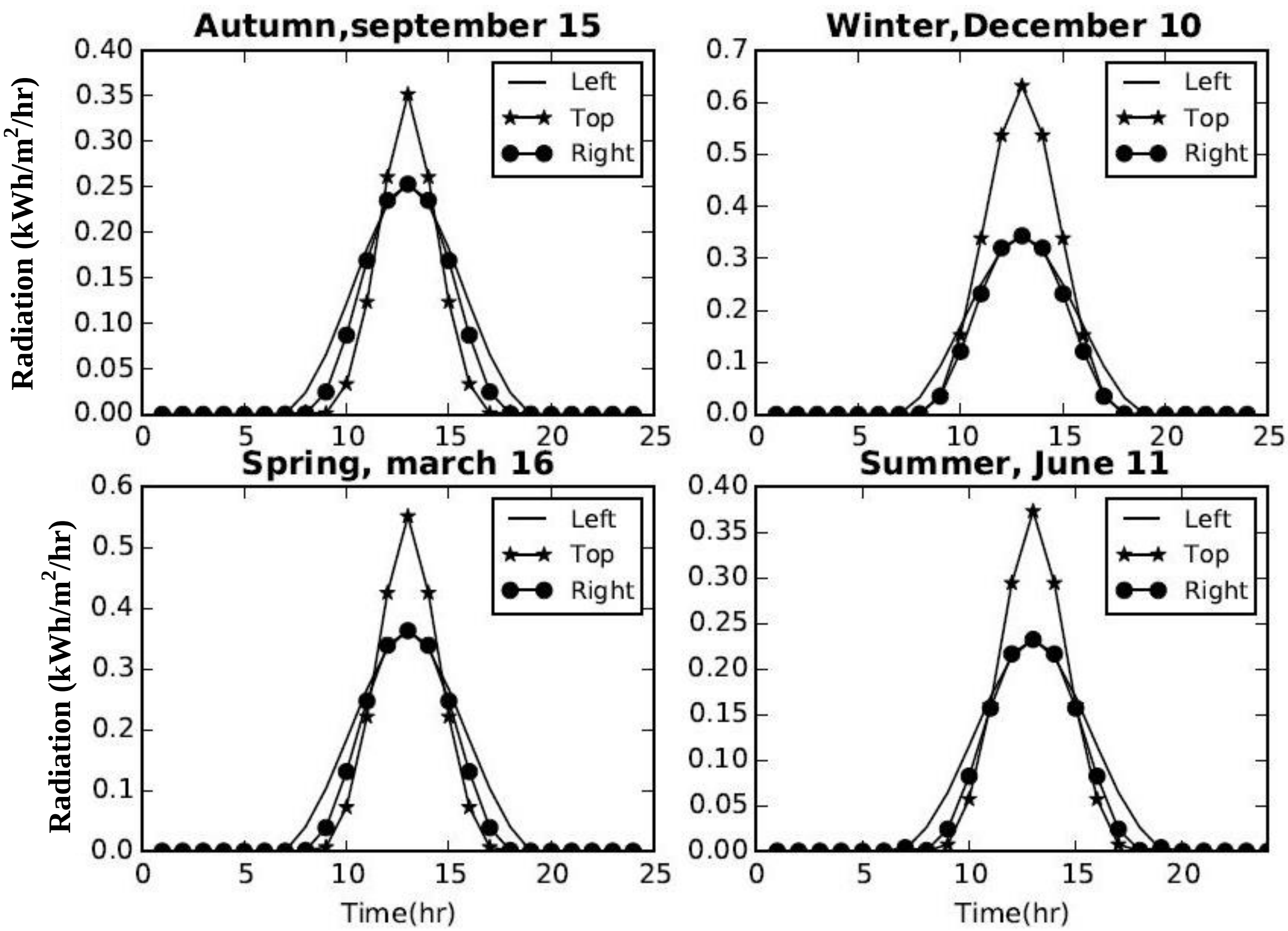

Figure 3.11: Monthly average hourly incidence solar radiation on the left, top and right reflecting surface for the representative day of each season of the first months

Figure 3.11 above, shows the incident solar radiation at each reflector on the solar heater surface for the representative day of each season of the first month. While Figure 3.12 shows the comparison between the ground solar radiation incident with and without reflector on a surface for the representative day of January 17.

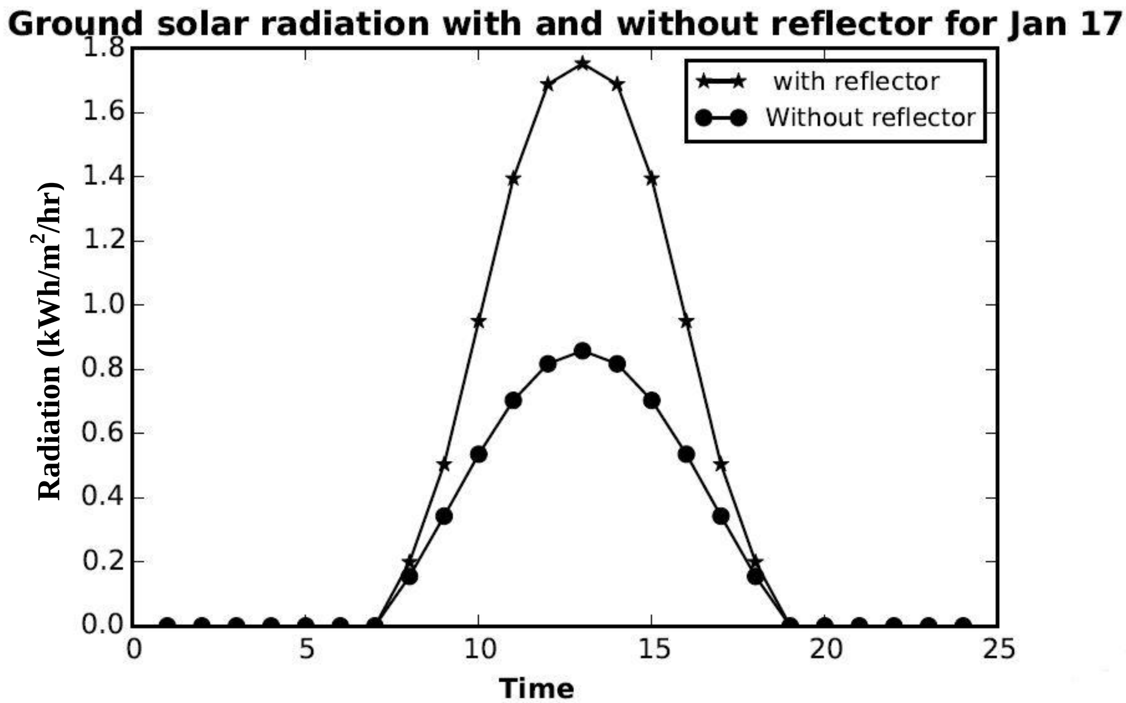

Figure 3.12: Ground solar radiation falling on solar heater with and without reflector for January 17

3.6. Sizing of crop dryer box

3.6.1. Material selection

Strength, cost effectiveness, availability, hygiene and non-reactivity of the materials with the crop slices were considered in the design.

Solar collector and drying chamber: The insulated box with a transparent glazing was constructed using a wood. One of the series problems of using wood is rotting. To prevent wood rot, the wood has to be kept dry. Wood rot is simply different fungi that consuming the wood. The fungi need water to live. Painting, sealing, allowing air to flow over and keeping the above wet surface like soil and concrete are the simple solution of avoiding wood rot. However using wood is preferable because of it is ease of availability and cheap. The collector is made up of absorber, transparent covering (glazing), and heat storage material in one of the collectors. Different materials are available for absorbers among which the dark materials are preferred due to their high absorbance. Treated black material with high absorbance and low long wave emittance are the most preferred absorber material (Sean, 2013).

Glazing: Glazing is the top cover of a solar collector. Usually the common materials used for glazing materials are glass and polythene material. It performs three major functions in particular: To minimize convective and radiant heat loss from absorber, to transmit the incident solar radiation to the absorber plate with minimum loss, and to shield the absorber plate from outside environment. Therefore, factors for consideration in selecting glazing materials in this work include strength of material, durability, non degradability when exposed to the UV ultra violet light. Polythene materials are transparent to long wavelength radiation and are therefore less effective in reducing radiated heat losses from the absorber plate. In addition, polythene cannot withstand high temperature encountered in collector especially when the collector is idle (Ramadhani *et al., 2014).* Hence, glass is selected as the glazing material in this design work as glazing.

Insulation: a wide range of insulation materials are available such as polyurethane form, expanded polystyrene, fiber glass, cork and plywood which are used to minimize heat loss from the collector. Selection of insulating material should be based on initial cost, effectiveness and durability. From an economic point of view, it may be better to choose an insulating material with a low thermal conductivity like fiber glass.

Reflector: Aluminum foil is used to reflect the radiation coming to the collector.

3.6.2. Design considerations

The following parameters were considered during the design of the solar dryers:

Properties and the quantity of the material to be dried: Solar drying system must be properly designed in order to meet particular drying requirement of specific products and to give optimal designed (Forson *et al.*, 2007). The initial and final moisture content of common crops is obtained from literatures as given in APPENDIX A.

Inclination of the solar collector: The flat plate solar collector is always tilted and oriented in such a way that it receives maximum solar radiation during the desired season of used. The best stationary orientation is due south in the northern hemisphere. The solar radiation energy incident on the collector surface which is inclined at an angle of (β=φ+15^{o}) to the horizontal surface is defined in terms of global, diffuse, beam and reflected radiation. The inclination also allows easy runoff water and enhances air circulation (Bukola and Ayoola, 2008).

Average meteorological data for Adama used for the design of the system: Investigation of solar air heater requires precise knowledge regarding the availability of global solar radiation and its components at the location of interests. Since the solar radiation reaching the earth's surface depends upon climatic conditions of the place, a study of solar radiation under local climatic conditions is essential.

Table 3.1: Design Specifications and Assumptions

Parameter	**Optimum values and assumptions**
Location and Latitude	Adama, Ethiopia ϕ=8.5265N
Crop/food	Tomato, Injera, Banana
Design Capacity	10kg
Max. allowable temperature for the chosen	$70^{o}C$ (Appendix A)
Average Slice Thickness	5mm(Tomato)
Drying time per day	5hr/day
Vertical Distance between adjacent trays	300mm (Design)

3.6.3. Drying chamber design

Energy balance for drying process

The total energy required for drying a given quantity of food items can be estimated using the basic energy balance equation for the evaporation of water (Bolaji, 2005).

$m_w L_v = \dot{m}_w C_p (T_d - T_a)$……………………………………………………………….(3.66)

Where, L_v= Latent heat of vaporization of water from the yam slices surfaces (kJ/kg). m_w = mass of water evaporated from the slices (kg), T_d = temperature of outgoing air from the drying chamber (°C), T_i = ambient air temperature (°C)

Drying heat load

The heat load is determined by the amount of crop to be dried, it's initial and final moisture contents and the time required completing the drying.

$Q_{load} = m_w L_v$……………………………………………………….………………..(3.67)

Where, m_w= amount of moisture to be removed (kg), L_v= latent heat of vaporization of water from the yam slices, 2320 kJ/kg (Sengar *et al.*, 2012)

Mass of water to be evaporated from the Slices

The mass of water M_w to be evaporated is estimated from the initial moisture content M_i and the final desired moisture content M_f (Bolaji, 2005). The total mass flow of air required for drying is determined from the amount of moisture loss from the crop (Forson *et al.*, 2007). The quantity of moisture to be removed is given by the following relationship:

$$M_w = M_{we}\left[\frac{M_i - M_f}{1 - M_f}\right] \qquad (3.68)$$

Where, M_{we} = mass of the wet slices (kg), M_i,= initial moisture content on wet basis (% wb), M_f = final moisture content on wet basis (% wb)

Volume of air required for removing the moisture

The total volume of air required for removing the moisture from Crop slices is evaluated from the equation given by Forson *et al*., (2007) as:

$$V_a = \frac{M_w h_{fg} R_a T_a}{C_p P_a (T_o - T_f)} \qquad (3.69)$$

Where, T_f= temperature of air leaving the drying bed obtained from the following relationship.

$$T_f = T_a + 0.25(T_o - T_a) \qquad (3.70)$$

Where, Ra = gas constant (kJ/kgK), T_o = temperature of air at the collector outlet (°C), P_a = partial pressure of dry air in the atmosphere, (N/m^2), Cp = specific heat capacity of air, (kJ/kgK)

Mass flow rate of air needed to effect the drying

The mass flow rate is given by (Tonui *et al.*, 2014)

$$\dot{m}_a = \dot{V}_a \rho_a \qquad (3.71)$$

Where,

$$\dot{V}_a = \frac{V_a}{t_a} \qquad (3.72)$$

t_a = Drying time per day (hrs), V_a = total volume of air required for removing the moisture (m^3), $\dot{V}_a$ = volume flow rate of the drying air (m^3/s).

Drying chamber capacity and other dimensions

The width of the collector (W) was considered equal to the width of the drying chamber (B).The volume of yam slices per tray can be obtained from equations given by Adzimah and Seckley (2009) as:

$V_y = W_T L_T Y_l$……………………………….……………………………………..(3.73)

Total volume of the slices on the trays in the drying chamber can be obtained as;

$V_T = \sum_{i=1}^{n} V_y$…………………………………….…………………………………(3.74)

Also, according to Balcomb (1992), the total volume can be related to the bulk density as:

$W_{we} = \rho_b V_T$…………………………………………………………...………..…(3.75)

Where, Y_l= Thickness of the slices in the drying chamber, (m), W_T= width of the tray which is equal to the width of the drying chamber, (m), L_T= Length of tray, (m), W_{we}= Total mass of yam slices, (kg) , ρ_b= Bulk density of crop

Fan power consumption

To determine the amount of electric consumption of the fan pressure drop through the drying bed has to be calculating first. The resistance of air flow through the packed bed of agricultural produce is expressed in the form giving by Forson *et al.*,(2007).

$U = a\left(\frac{\Delta P_B}{h_L}\right)$…………………………………………………………………………(3.76)

Where, u= Superficial air velocity (m/s), which is the volumetric flow rate divided by the cross-sectional area, h_L=Drying bed thickness, (m), a= Constant whose value is determined experimentally. For forced convection of air through a thin layer of crop ($h_L \leq 0.2m$), the value of the constant is 0.465 m^3s/kg.

Total pressure drop through the system is approximately twice the pressure drop of the drying bed that is

ΔP_T=2×ΔP_B ………………………………………………………………………………(3.77)

However, when all pressure drops are accounted for, experience shows that the gross pressure drop is about six times the value of ΔP_T (Forson *et al*., 2007) and is given by the equation.

$\Delta P_T = 6 \times (2 \times \Delta P_B)$……………………………………………………………...…………(3.78)

The ideal power consumption for a fan (without losses) can be expressed as

$P_i = \Delta P_T \times q$……………………………………………………….………………(3.79)

Where, P_i ideal power consumption (W), ΔP_T gross pressure drop, q air volume flow delivered by the fan (m^3/s).To meet the power consumption of the fan, solar panel is selected according to the rating after the power required is calculated by Equation 3.79.

3.7. Construction of experimental set-up

The aim of the experiment is to investigate the performance of the solar collector by implementing different enhancement techniques alongside drying agricultural crop dryer. In this section the components of the whole system specification and construction is discussed.

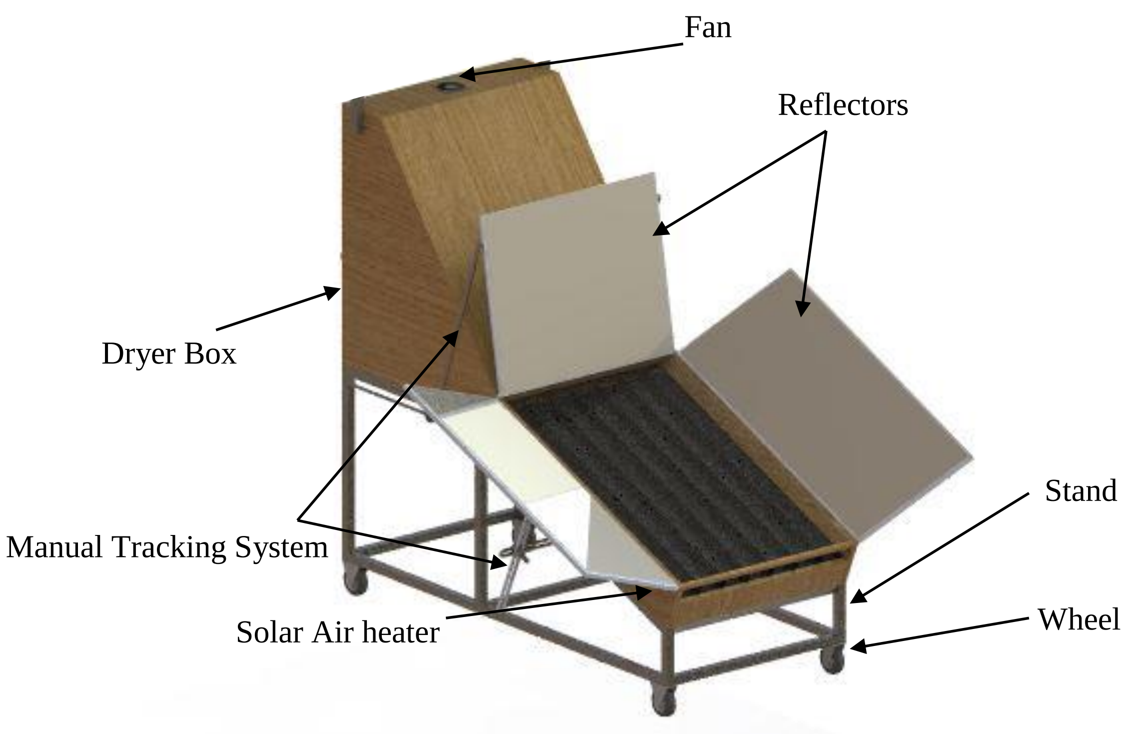

Figure 3.13: Components of experimental setup

Since the aim of this research work is to design and test efficient solar collector, most of the materials used to construct the collector is manufactured from materials that easily found and durable. In regard of this, the solar collator materials are selected and prepared as shown in the table 3.2.

Table 3.2: Components of solar collector and Materials

Component	Material	Specification
Top Cover	Glass	5 mm
Absorber	Steel Sheet	0.8 mm
Stand	RHS	40 mmx40 mmx3 mm
Thermal Insulation	Fiber glass	$K=0.02\ Wm^{-1}K^{-1}$
Side and bottom cover	Wood	$K=0.13\ Wm^{-1}K^{-1}$

3.7.1. Construction of collector box

For the construction of solar collector box wood plate with thickness of 25mm is used. The plates are nailed to form box and sealed using wood sealer. On the top side of the collector frames are prepared for positioning glass cover.

Figure 3.14: Collector box construction

3.7.2. Construction of absorber plates

Thin steel sheets are used as absorber material and painted black to increase the absorption performance of the absorber plate. The first plate is prepared for the convectional collector without any extended surface. The second type collector is prepared for the enhanced solar collector in which sheet metal strips are welded longitudinal along the length of the absorber plate.

Figure 3.15: Collector absorber plate construction

3.7.3. Insulation (convectional type)

For the case of the convectional type solar air heater performance analysis thermal insulation is used between bottom cover and absorber plate as shown on Figure 3.16.

Figure 3.16: Collector fiber glass insulation insertion

3.7.4. Sensible thermal storage preparation

Gypsum is selected as sensible thermal storage system because its light weight, easily available and cheap. The easily available gypsum powder is bought and mixed with water according to the specification. The prepared gypsum is poured in to the bottom of the absorber plate as shown in Figure 3.17.

Figure 3.17: Preparation of gypsum into bottom of absorber

3.7.5. Reflector construction

As discussed earlier chapter's three reflectors: top reflectors, right side reflector and left side reflectors are used in this work to enhance the solar air heaters. The materials are selected and constructed as described in Table 3.3 and shown in the Figure 3.18. The new thing in this work is the integration of the manual tracking system to get efficient enhancement of the reflector. The manual tracking system is provided for both side and top reflectors that allow easily manipulation of the reflector to the desired angle as shown on the Figure 3.18.

Table 3.3: Reflector Material and Specification

Component	Material	Specification
Top Reflector	MDF and Aluminum foil	1000 mmx600 mm
Left side Reflector	MDF and Aluminum foil	1500 mmx600 mm
Right Side Reflector	MDF and Aluminum foil	1500 mmx600 mm
Side reflector Manual tracking	Steel strip	8 mm
Top reflector Manual tracking	Steel strip	8mm

Figure 3.18: Construction of Reflectors

3.7.6. Manual tracking system construction

As shown on the figure 3.19, manual tracking system is constructed for both top and side reflector. The side manual tracking allows to the side reflector to be manipulated between 0^o and 90^o of reflector angle. The top reflector also provided with the manual adjustable linkage system to track the sun monthly wise. This can be done thought linkage and slot provided as shown on the Figure 3.19.

Figure 3.19: Manual tracking system

3.7.7. Construction of dryer box

The constructions of the box begin with preparing the wood plates according to the AutoCAD design. The prepared wood plates are nailed together and the box is formed. To avoid openings the wood sealer is used and all the internal part of the box and laminated. Using the stainless steel wire mesh and wood frame the trays are prepared.

Table 3.4: Dryer box components Materials and specification

Component	Material	Specification
Mesh Tray	Stainless steel Mesh	15 mmx15 mm
Box	Dry Wood	

Figure 3.20: Dryer box Construction

Trays are prepared from the stainless steel mesh and wood frame. The dimensions of the trays are increased from the bottom to top tray to accommodate the temperature variation. The mesh with 10 mmx10 mm opening is used to lower pressure drop.

Figure 3.21: Tray Preparation

3.7.8. Construction of stand

The stand is made using RHS for firm support of the collector and dryer box. The required metal is sliced and welded according to the design. To avoid rusting it’s painted with anti-rust.

Figure 3.22: Stand construction

Finally, after each component is constructed separately and the whole system is assembled in Bekas Chemicals P.L.C workshop, it’s placed where the experiment is performed at Adama Science and Technology University as shown in Figure 3.23.

Figure 3.23: Assembled solar dryer

3.8. Measuring instrument

Temperature Sensors / Thermocouples: The temperature during the experiments were measured by the thermocouples which are located along the length of the collector. K type thermocouples are used in the setup. The K-type thermocouples are composed of a positive portion, which is approximately 90% nickel and 10 chromium and a negative portion, which is approximately 95% nickel, 2% aluminum, 2% manganese and 1% silicon. The negative portion is colored red and the positive portion is colored yellow. The thermocouples can read values between -200 to 1350 °C with an error of ±2.

Data reader: Data reader is used to read the temperature sensed by thermocouples and the values are recorded manually.

Digital Weight Balance: Digital weight balance is used to measure the weight of the samples.

Manometer: To measure the pressure drop both across the collector and the dryer box is measured using U tube manometer.

a) Digital balance b) Digital thermometer

Figure 3.24: Measuring instrument

3.9. Experimental procedure

The first experiment is done on convectional solar collector fixed to dryer box. In this experiment the performance of the convectional solar collector is evaluated while meantime drying samples. Three types of samples are tested in the drying box: Injera, Tomato, and Banana. First experiment was done by using convectional SAH for drying injera, tomato and banana. In this experiment 5 kg each of wet injera, tomato and banana were inserted in the drying box and were tested on the January 25^{th}, 26^{th} and 29^{th}, respectively. The second experiment is conducted to investigate the effect of longitudinal fin on the performance of solar collector while 5 kg of injera, Tomato and Banana is loaded to dry. In this experiment longitudinal fins are fixed on the absorber plate to increase the surface area. The third experiment is to investigate the effect of reflector on the performance of the solar collector. The top and side reflectors are fixed using hinge. During experiment the top reflector is fixed to the optimum angle of inclination of the month. Using the manual tracking system the side reflectors are adjusted with respect to time hour variation since it depends on the hour angle. The final experiment is conducted to investigate the effect of using sensible thermal storage on the performance of the solar air collector. 80 mm thick gypsum sensible thermal storage was used as thermal storage in drying injera, tomato and banana.

The experiment is conducted for 5 hrs per day. In each experiment, the inlet and outlet temperature of the solar air heater, the outlet temperature of the dryer box and the weight of the sample was recorded every 1 hour interval. The pressure drop of the system was measured using manometer.

3.10. Error analysis and validation of simulation model in comparison with the experimental results

The Root Means Square Errors (RMSE) and Nash-Sutcliffe Coefficient of Efficiency (NSE) are the two statistical tools mostly used for comparing the experimental hourly collector temperatures with the predicted result from the model to determine the level of agreement between the two results. The Root Means Square Error was used to determine the level of deviation of the predicted result from the actual result. The Root Means Square Error measures the quality of fit between the actual data and the predicted model (Julien *et al.*, 2013). The Root

Means Square Error of a model prediction with respect to the estimated variable X_{model} is defined as the square root of the mean squared error (Neil, 2010).

$$S^2 = \sqrt{\frac{\sum_{i=1}^{n}\left(X_{obs,i}-X_{model,i}\right)^2}{n}} \text{...}(3.80)$$

Where X_{obs} is observed values X_{model} is modeled values. The lower the Mean Absolute Error or the Bias Percentage value, the better the performance of the model (Neil, 2010). Furthermore, the Nash-Sutcliffe Coefficient of Efficiency (NSE) defined as:

$$\text{NSE} = 1 - \frac{\sum_{i=1}^{n}\left(X_{obs,i}-X_{model,i}\right)^2}{\sum_{i=1}^{n}\left(X_{obs,i}-\overline{X_{obs,i}}\right)^2} \text{..}(3.81)$$

Where X_{obs} is observed values X_{model} is modeled values. NSE is generally used to quantitatively describe the accuracy of model outputs. Nash- Sutcliffe efficiencies can range from -∞ to 1. An efficiency of 1 (NSE = 1) corresponds to a perfect match between model and observations. An efficiency of 0 indicates that the model predictions are as accurate as the mean of the observed data, whereas an efficiency less than zero (-∞< E < 0) occurs when the observed mean is a better predictor than the model (Julien *et al.*, 2013)

CHAPTER 4: EXPERIMENTAL PERFORMANCE ANALYSIS OF SAH

4.1. Introduction

Solar air heaters have different application starting from residential space heating to industrial process heating. In this Chapter the experimental performance of the convectional solar air heater and each enhanced solar air heater performance were investigated separately in drying tomato, Injera and banana.

4.2. Agricultural crop drying

As described in literatures the use of solar crop dryer for drying crops is a crucial solution for the reduction of post-harvest losses in Ethiopia. Substituting the traditional method of drying and adopting this new technology is one of the aims of this research work. More than adopting using efficient and low cost solar dryer is also the main concern of the work. In this section the constructed of low cost and enhanced solar air heater was used for drying crops up to their safe storage moisture content. Dryer box that cope up uneven drying of the crops due to decrease of the temperature from inlet to outlet of the dryer box is designed according to the specification. The capacity of the dryer is determined from the collector performance analysis and it’s found that its designed capacity of 10 kg of tomato crops by taking 5 hr/day during time.

4.2.1. Air drying concept

The drier the surrounding air, the greater the rate of evaporation from a crop that lowers the wet bulb temperature. The specific humidity of unsaturated air increases due to water evaporation from a crop as energy transferred from air to water. A thermal equilibrium prevails when the energy transferred from warm air to the crop becomes equal to energy needed for water vaporization. At temperatures below this equilibrium thermodynamic wet bulb temperature or adiabatic saturation temperature, air will rapidly become saturated and if cooled further, will lose water in the form of dew above 0 ^{o}C. Water vapour moves from air with a higher humidity ratio (i.e. ratio of water vapour weight to dry air weight) to air with a lower humidity ratio. For appropriate combination of humidity and temperatures, air taken directly into a drying chamber will be heated sufficiently to enable drying. When the temperature and humidity of directly-introduced ambient air would provide an insufficient drying rate, an air heating solar energy collector produces higher temperature air for introduction to the drying chamber.

4.2.2. Solar crop dryer

A solar crop drier is a device used to dry crops using solar energy as a heat source either by heating air indirectly or direct. Drying through heated air is common method of for quality crop drying. The components and their description discussed as follow:

4.2.2.1. Description of the solar dryers

The solar dryers consist of the following components:

Solar collector: The collector which is essentially the air heater is an insulated box with a transparent glass cover. During sunlight exposure, the absorber heats both the air and the thermal storage material. The storage material emits the stored energy during low sunshine hour and cloud cover.

Absorber: This was made up of black painted sheet metal, which absorbs the solar radiation. The black paint enhances the absorptivity of the sheet. A good absorber is needed to raise the temperature of the collector. Sean (2013) describes a good absorber as one that absorbs almost all the incoming radiation, lose a small portion to the surroundings and efficiently transfer the absorbed solar energy to the passing air within the collector.

Reflector: Reflector is used to enhance the collector performance by increasing the about of radiation by reflecting the radiation to the collector in addition to the direct incident ray falling on the collector absorber.

Thermal storage materials: The storage material collects heat during sunlight exposure (high insolation) and dissipates during low sunshine, cloud cover and rains. A thermal storage was integrated with one of the collectors and the other has only a plain absorber.

Drying chamber: it houses the wire mesh trays in which the slice were spread on. Access door to the drying chamber was also provided. The interior of the drying cabinet was painted black to enhance elevated temperature with in the dryer.

Tray: The trays were constructed from strong wire mesh that can be easily slotted and removed for maintenance purpose as shown in Figure 4.1. The trays were designed for easier cleaning, loading and offloading of slices.

Support: The supporting structure bears the load of the drying cabinet and the air heater. It was constructed from mild steel material.

Fan: Since the dryer forced type, the fan draws air through the collector and dryer box

Solar panel: is used to power the fan where electricity does not reach.

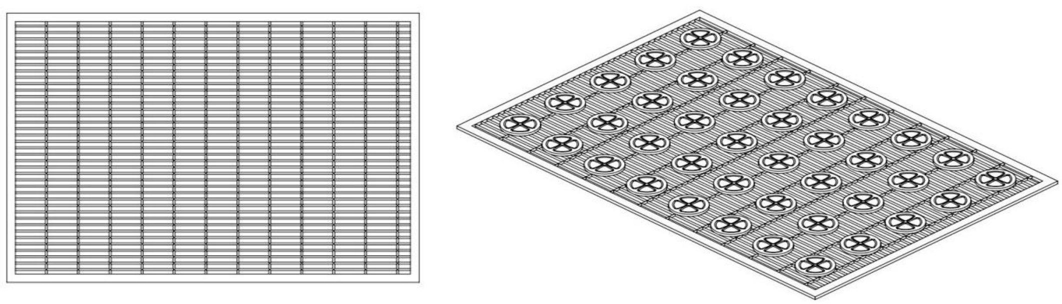

a) Wire mesh tray b) Distribution of crops

Figure 4.1: Tray

4.2.2.2. Working principle

The dryer is a passive type, sun's rays entering through the transparent top cover are being trapped, and trapping of the rays is enhanced by the black painted absorber. The Crop slices are put on trays inside the drying chamber. Air enters through the open bottom end of the collector and it is heated while it passes over the absorber with thermal storage. The heated air is allowed to flow over the wet crop slices and provided the heat for moisture evaporation by convective heat transfer between the hot air and the wet crop slices. Drying takes place due to the difference in moisture concentration between the drying air and the air in the vicinity of the crop slices surfaces.

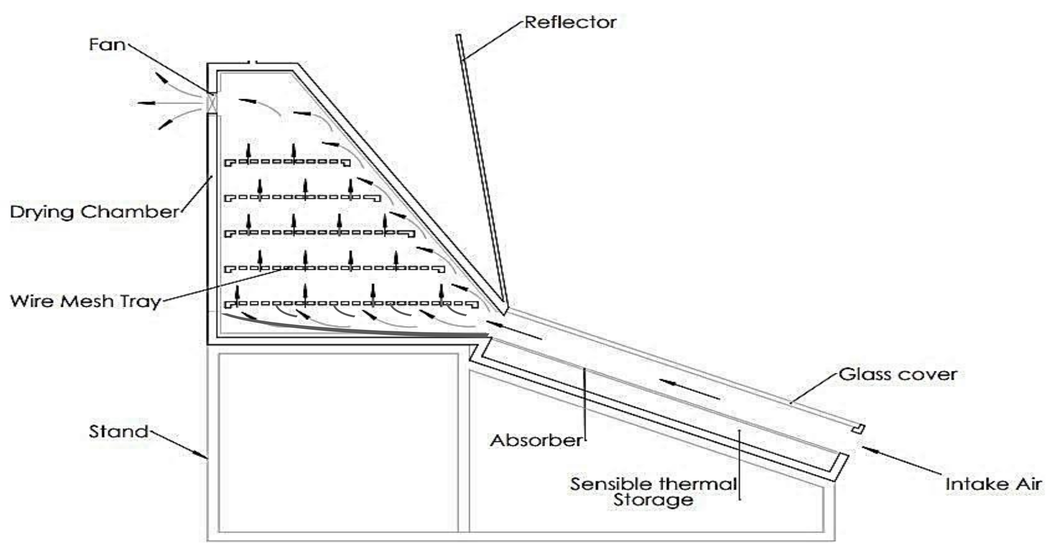

Figure 4.2: Flow of air in the crop dryer

4.2.3. Experimental performance parameters

The performance of the crop dryer integrated with convectional and enhanced solar air heater was evaluated using the drying rate, moisture loss, dryer efficiency of the dryer and solar air heater efficiency.

Solar air heater efficiency

The performance of the solar air heater can be expressed by the evaluation of efficiency of solar air heater which is the ratio of heat gain by the fluid to energy absorbed by the solar air heater. The instantaneous thermal efficiency solar air heater η_{SAH} is given as:

$$\eta_{SAH} = \frac{Q_U}{I(t)A_c} \qquad (4.1)$$

Dryer efficiency

For solar dryer, the system efficiency can be expressed as given by Forson *et al.*,(2007) and Drew (2011)as:

$$\eta_{dryer} = \frac{M_w L_v}{I_T A_c t} \qquad (4.2)$$

Where;   = mass of water evaporated, (kg) , Lv= latent heat of vaporization of water, 2320 kJ/kg (Sengar *et al.*, 2012) t = Drying time, (hr) , Ac= Collector area, (m^2)

Percentage moisture loss

The quantity of moisture in percentage of the initial mass of a material can be represented on wet and dry basis and expressed as percentage given by Mohanraj and Chandrasekar (2009) as:

$$M_C = \left(\frac{M_1 - M_2}{M_1}\right) \times 100\% \qquad (4.3)$$

Where, M_1= Initial mass of the crop slices, (kg), M_2= Final mass of the crop slices, (kg)

Average drying rate:

The quantity of moisture removed from the food item over the drying time is given by Tonui *et al.* (2014) as:

$$m_{dr} = \frac{M_w}{t_d} \qquad (4.4)$$

Where, M_w= mass of water evaporated from the crop slices, (kg) t_d= drying time per day, (hr)

4.3. Experimental performance result of SAH

On the experiment, the three experiments inlet and out let temperature of each SAH set up was recorded and since there is lack of instrument for recording weather data, Ethiopia metrological agency data was used to calculate the efficiency of the system at respected date of experiment. The thermal efficiency is presented as follow in Figure 4.3 for convectional SAH and each modified SAHs.

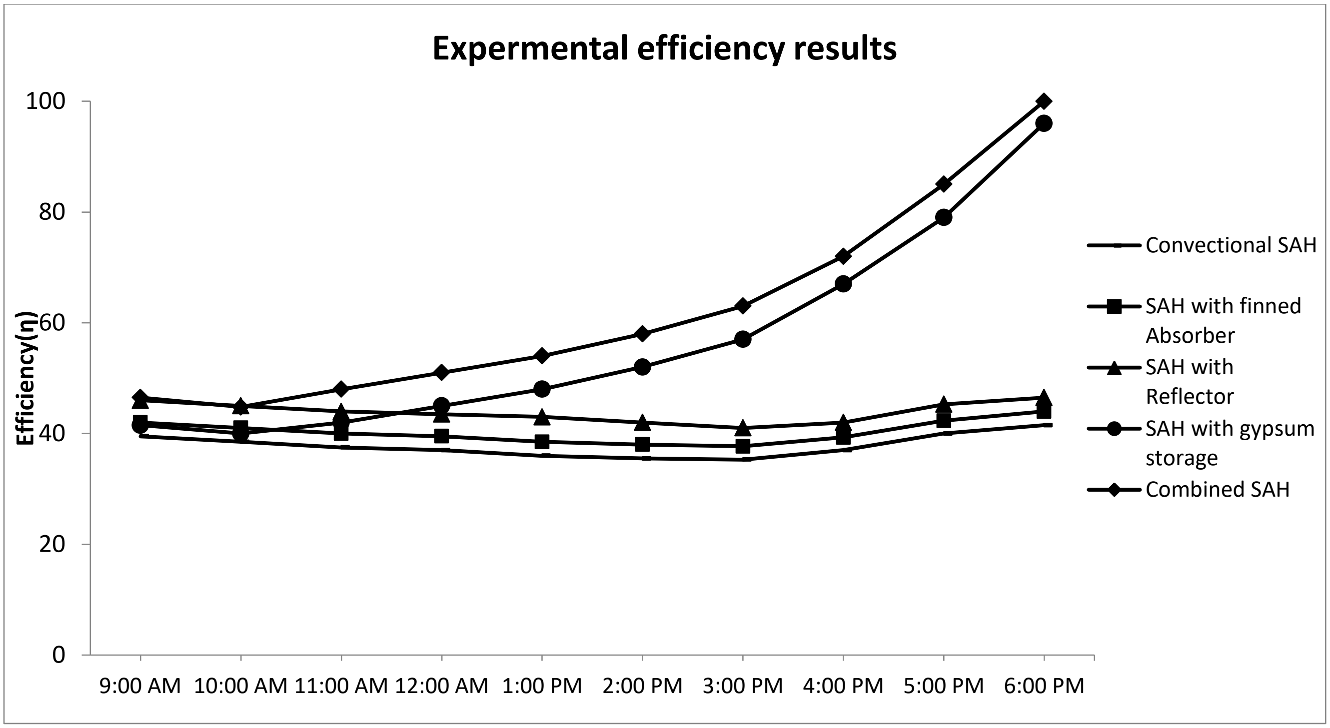

Figure 4.3: Experimental Efficiency result

4.4. Experimental result of crop dryer for drying tomato, injera and banana

Using the convectional and enhanced solar air heater integrated with the designed dryer chamber was loaded with 5 kg of tomato, Banana and Injera slices and allowed to dry. The slices are prepared with 5 mm thickness and placed on mesh tray in dryer box.

a) Wet and Dried tomato

b) Wet and Dried banana

c) Wet and Dried injera

Figure 4.4: Wet and Dried product

As shown on the Figure 4.5(a) using the convectional solar air for drying tomato gives lower drying performance. The enhanced solar air heater gives higher drying performance since the fluid temperature is higher relative to the convectional. This is due to increase in heat gain of the working fluid due to enhancement of the solar heater.

Wet basis Weight loss (%), versus drying time in hours for convectional, finned absorber, finned absorber with storage and finned absorber integrated with storage and reflectors is shown in Figure 4.6. Averages for the different samples represented for different shelves were averaged and showed in the figure. The dryer that integrated with the combined enhancement techniques shows fast drying whereas the convectional gives slowest drying.

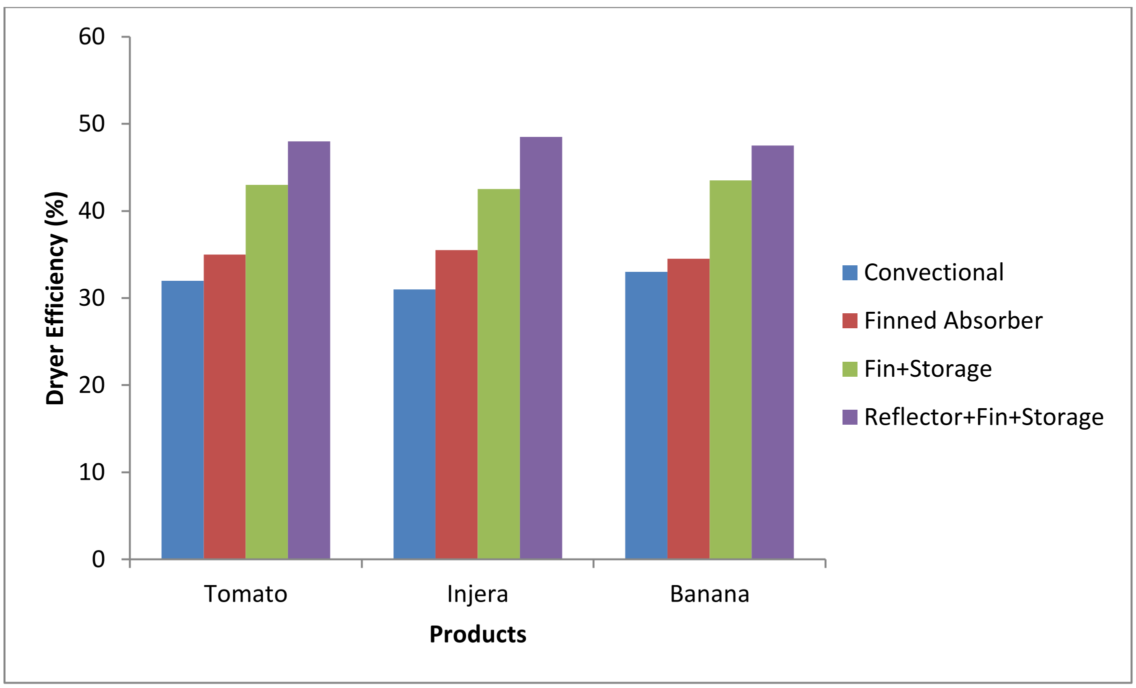

a) Drying efficiency of crop dryer

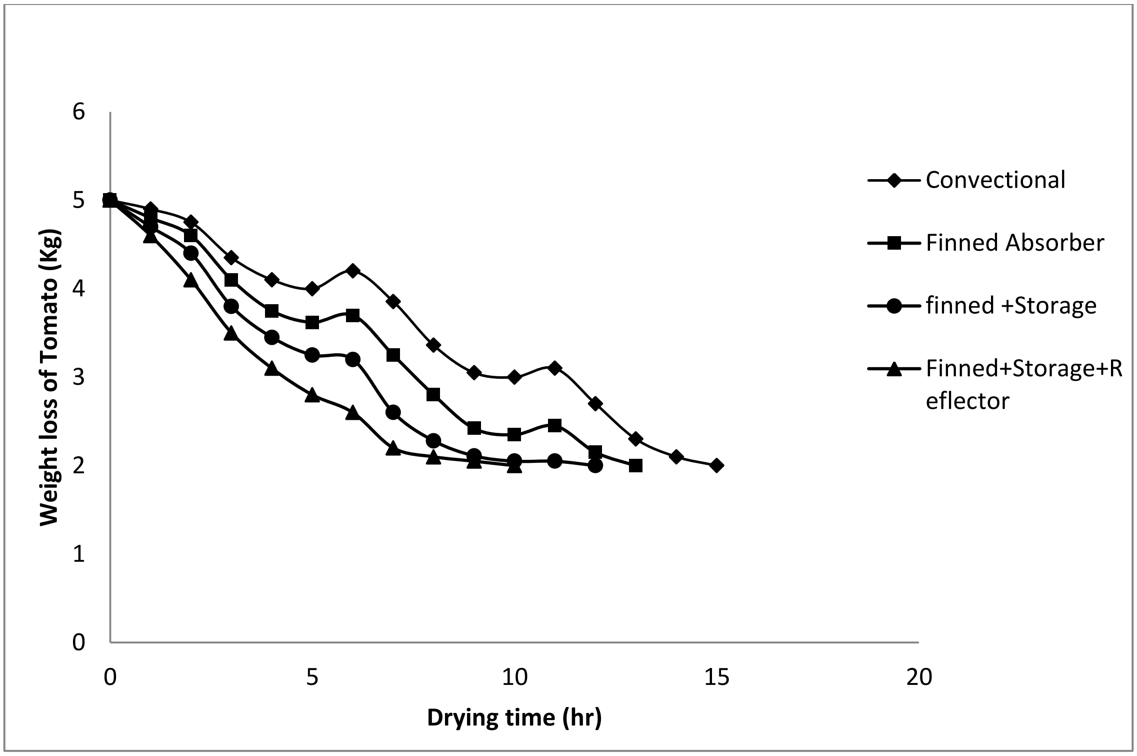

b) Tomato weight loss

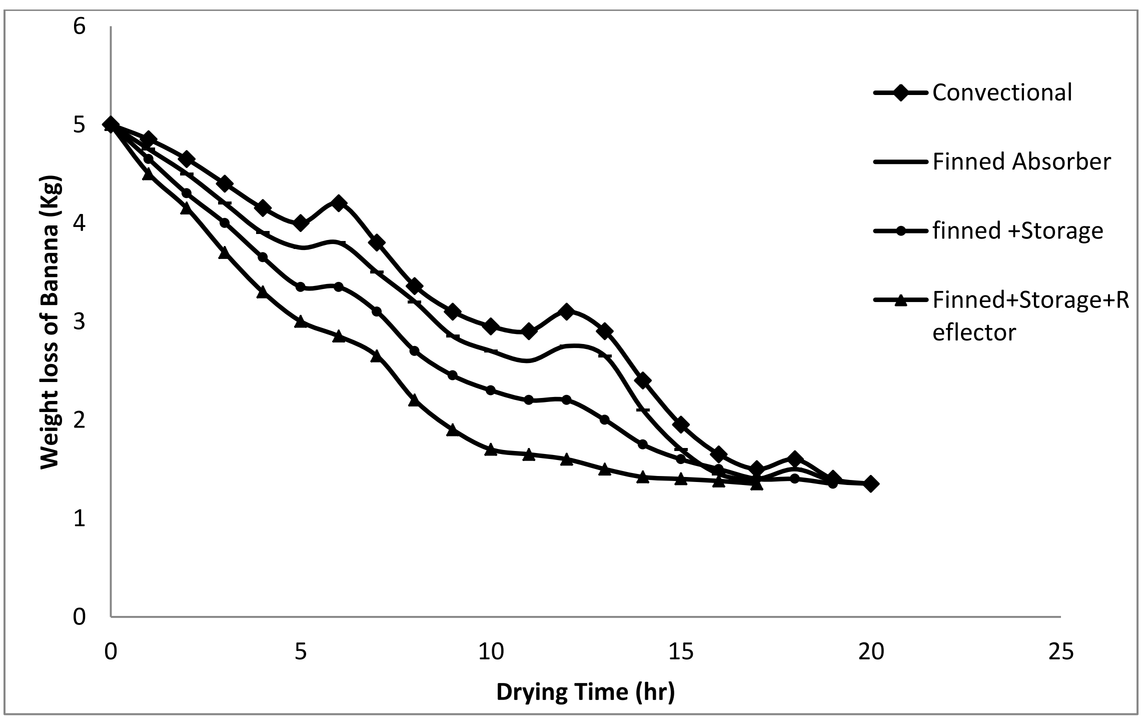

c) Banana Weight loss

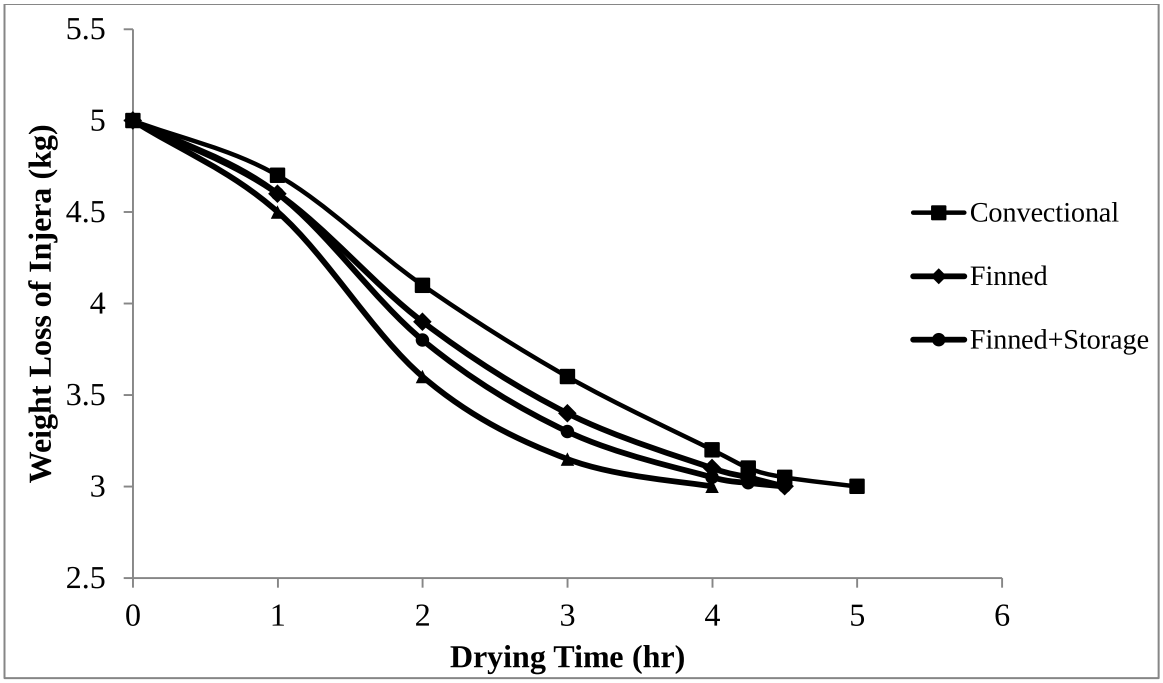

d) Injera weight loss

Figure 4.5: Dryer performance

CHAPTER 5: NUMERICAL PERFORMANCE ANALYSIS OF SAH

In this Chapter, the mathematical modeling of convectional solar air heater and each modified SAH was numerically modeled and their numerical performance results were discussed. Finally, the heating load of locally selected poultry farm was estimated theoretically and the required enhanced SAH that satisfy the spaces heating load of the poultry farm was predicted. Table 5.1 shows the specification of convectional solar air heater used.

Table 5.1: Specification of solar air heater

Component	Specification
Collector length	1500 m
Collector width	1000 mm
Thermal storage thickness	80 mm
Glass thickness	5 mm
Cover-absorber gap	70 mm
Insulation thickness	25 mm
Absorber material	Steel sheet metal
Absorber thickness	0.8 mm
Fin height	10 mm

5.1. Modeling solar air heaters

The energy-balance equations in this chapter are written under quasi-steady state conditions with the assumptions given as follows:

- There is no temperature gradient along the thickness of the glass cover and the absorber plate.
- The heat-transfer coefficients for the operating temperature range are assumed to be constant.
- The mass-flow is stream-line flow and constant.
- The side-heat losses are neglected.

- The temperature gradient along the depth of the duct is negligible; average air temperature changes along the direction of flow.
- The thermal/heat loss from the absorber plate through the bottom insulation is considered under steady-state conditions.
- Absorptive of solar radiation in a glass cover is negligible.

5.2. Modeling of convectional solar air heater

Steady-state thermal analysis can be used to determine temperatures, thermal gradients, heat flow rates, and heat fluxes in an object that are caused by thermal loads that do not vary over time. A steady-state thermal analysis calculates the effects of steady thermal loads on a system or component. As shown on the Figure 5.1, the convectional solar air heater has single glass cover at the top, air gab between glass cover and absorber plate, selective material coated absorber, insulation material between absorber plate and bottom cover and side and bottom wood covers. In this section, the steady state modeling of the convectional solar air heaters are dealt and the finite element discretization of the governing equations is derived.

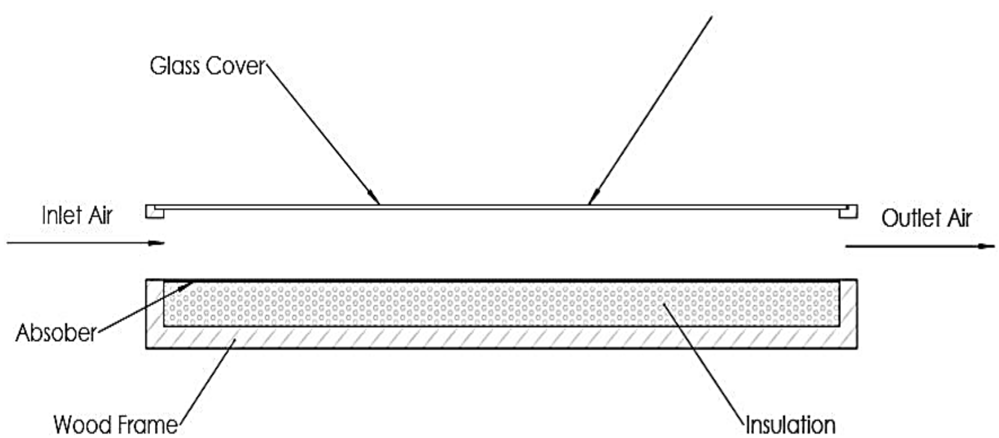

Figure 5.1: Analysis of solar collector

5.2.1 Estimation of heat transfer coefficients

Collector overall coefficient

As the collector absorbs heat its temperature is getting higher than that of the surrounding and heat is lost to the atmosphere by convection and radiation. The rate of heat loss depends on the collector overall heat loss coefficient (U_L). The heat lost from the collector is the sum of the heat lost from the top, the bottom and the sides. Each of these loses is also expressed in terms of coefficients called the top loss coefficient, the bottom loss coefficient and the side loss coefficient and defined by the equations (Duffie and Beckman, 2013):

$$Q_{top} = U_t A_c (T_p - T_a) \quad (5.1)$$

$$Q_{side} = U_s A_c (T_p - T_a) \quad (5.2)$$

$$Q_{bottom} = U_b A_c (T_p - T_a) \quad (5.3)$$

Where, Q_t , $Q_b$and Q_s are the top, bottom and side heat loss of the collector, respectively, and U_t, U_b, and U_s are the top, bottom and top heat loss coefficient of the collector, respectively.

i. Top loss coefficient

The top loss coefficient U_t is evaluated by considering convection and re-radiation losses from the absorber plate in the upward direction.

a) Convective heat transfer coefficient

Convection coefficient from the glass to the ambient air (h_{c1}): The convective heat transfer coefficient (**h_{c1}**) at the glass cover is calculated from the following empirical correlation.

$$h_{c1} = 5.7 + 3.8V_{wind} \quad (5.4)$$

Where, h_{c2} is in W/m^{2}K, and V_{wind} is the wind speed in m/s.

Convection coefficient from the absorber plate to working fluid (h_{c2}): Sieder and Tate give the following correlation to account for entrance effects in laminar flow in tubes. (Sieder *et al*,. 2007)

$$Nu_D = 1.86 \times (Re \times Pr)^{1/3} \left(\frac{D}{L}\right)^{1/3} \left(\frac{\mu_b}{\mu_w}\right)^{0.14} \quad (5.5)$$

Where, D is the diameter, μ_b is the fluid viscosity at the bulk mean temperature, μ_w is the viscosity at the tube wall surface temperature

b) Radiation heat transfer coefficient

Radiation Heat Transfer Coefficient from the Plate to the Cover (h_{r1}): The radiate heat transfer coefficient from the plate to the glass cover is expressed as (Duffie and Beckman, 2013):

$$h_{r1} = \frac{\sigma(T_p^2+T_g^2)(T_p+T_g)}{\frac{1}{\varepsilon_p}+\frac{1}{\varepsilon_g}-1} \quad (5.6)$$

Where, T_p is the plate temperature (^oK), T_g is the glass temperature (K), σ is a Boltzmann constant, ε_p and ε_g are the emissivity of plate and glass cover, respectively. Radiation Heat Transfer Coefficient from the Cover to Ambient (h_{r1}): The radiate heat transfer coefficient from the glass cover to the ambient is expressed as (Duffie and Beckman, 2013):

$$h_{r2} = \varepsilon_g \sigma \left\{\frac{T_g^4 - T_{sky}^4}{T_g - T_a}\right\} \quad (5.7)$$

Where, T_{sky} the equivalent sky temperature is evaluated according to (Swinbank, 1963) correlation (cited by Hreiz et al., 2017):

$$T_{sky} = 0.0552 T_a^{1.5} \quad (5.8)$$

Note that temperatures values should be expressed in K. The total heat transfer coefficient from collector plate to cover h_1 is expressed as (Duffie and Beckman, 2013):

$$h_1 = h_{r1} + h_{c1} \quad (5.9)$$

The total heat transfer coefficient from the cover to ambient h^2 is expressed as (Duffie and Beckman, 2013):

$$h_2 = h_{r2} + h_{c2} \quad (5.10)$$

The effective heat transfer coefficient from plate to ambient (i.e. the top loss coefficient) is given by (Duffie and Beckman, 2013):

$$U_t = \left(\frac{1}{h_1} + \frac{1}{h_2}\right)^{-1} \quad (5.11)$$

ii. Bottom loss coefficient

The bottom loss coefficient (U_b) is evaluated by considering conduction and convection losses from the absorber plate in the downward direction through the bottom of the collector. In most cases, the thickness of insulation provided is such that the thermal resistance associated with conduction dominates. Thus, neglecting the convective resistance at the bottom surface of the collector casing, we have (Duffie and Beckman, 2013):

$$U_b = \frac{K_{ins}}{\delta_b} \quad (5.12)$$

Where: k_{ins} is the thermal conductivity of the insulation, and δ_b is the back insulation thickness.

iii. Side loss coefficient

As in the case of the bottom loss coefficient, it will be assumed that the conduction resistance dominates and that the flow of heat is one-dimensional and steady. The one dimensional approximation can be justified on the grounds that the side loss coefficient is always much smaller than the top loss coefficient.

$$U_s = \frac{A_e}{A_c}\frac{k_{ins}}{\delta_e} \quad (5.13)$$

Where: $Ae = P{*}de$, P is the perimeter of the absorber plate, de is the height of the edge, and δe is the edge insulation thickness. The overall heat loss coefficient UL is the sum of the top, bottom and edge loss coefficient. That is (Duffie and Beckman, 2013):

$$U_L = U_t + U_s + U_b \quad (5.14)$$

5.2.2. Governing equations

The absorber plate:

$$I\tau_c\alpha_p = \mathrm{U}_b\left(T_p - T_a\right) + h_{rPC}\left(T_p - T_c\right) + h_1\left(T_p - T_f\right) \quad (5.15)$$

$$T_p = \frac{I\tau_c\alpha_p}{\mathrm{U}_b+h_{rPC}+h_1} + \frac{\mathrm{U}_bT_a}{\mathrm{U}_b+h_{rPC}+h_1} + \frac{h_{rPC}T_c}{\mathrm{U}_b+h_{rPC}+h_1} + \frac{h_1T_f}{\mathrm{U}_b+h_{rPC}+h_1} \quad (5.16)$$

Equation 5.16 can be simplified as:

$$T_p = a_1I\tau_c\alpha_p + a_2T_a + a_3T_c + a_4T_f \quad (5.17)$$

The cover:

$$\mathrm{U}_t(T_c - T_a) + h_{rPC}\left(T_c - T_p\right) + h_2\left(T_c - T_f\right) = I\alpha_c \quad (5.18)$$

$$T_c = \frac{I\alpha_c}{\mathrm{U}_t+h_{rPC}+h_2} + \frac{\mathrm{U}_tT_a}{\mathrm{U}_t+h_{rPC}+h_2} + \frac{h_{rPC}T_p}{\mathrm{U}_t+h_{rPC}+h_2} + \frac{h_2T_f}{\mathrm{U}_t+h_{rPC}+h_2} \quad (5.19)$$

Equation 5.19 can be simplified as:

$$T_c = a_5I\alpha_c + a_6T_a + a_7T_p + a_8T_f \quad (5.20)$$

The fluid:

$$q_u = \mathrm{h}_2\left(T_c - T_f\right) + h_1\left(T_p - T_f\right) \quad (5.21)$$

$q_u = \dot{m}C_f \frac{dT_f}{dx}$…………………………………………………………………………...(5.22)

Using the forward Finite difference method equation 5.22 can be resolved as:

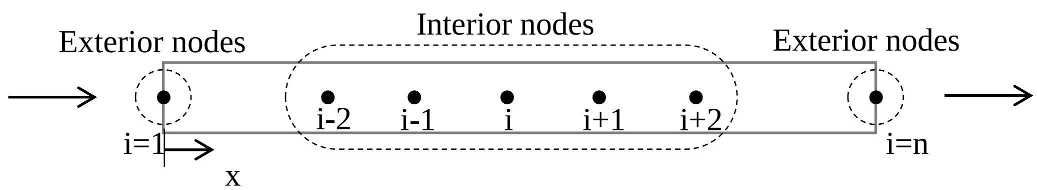

Figure 5.2: Finite difference analysis of flowing fluid

For interior nodes:

$\dot{m}C_f\left(\frac{T_{f_{i+1}} - T_{f_i}}{\Delta x}\right) = h_2\left(T_c - T_{f_i}\right) + h_1\left(T_p - T_{f_i}\right)$……………………………………...…(5.23)

$T_{f_{i+1}} = \frac{\Delta x h_2}{\dot{m}C_f}T_c + \frac{\Delta x h_1}{\dot{m}C_f}T_p + (\frac{\Delta x h_1}{\dot{m}C_f} + \frac{\Delta x h_1}{\dot{m}C_f} + 1)T_{f_i}$ ……………………………………….…..(5.24)

$T_{f_{i+1}} = a_9 T_c + a_{10} T_p + a_{11} T_{f_i}$……………………………………………………...…(5.25)

For exterior node:

$T_{f_{i+1}} = a_9 T_c + a_{10} T_p + a_{11} T_{amb}$…………………………………………….…………(5.26)

Boundary conditions

T_{fi}=T_{amb} at i=1

T_{fi}= T_{fout} at i=n

Where, $\alpha_p$absorption of solar radiation in cover, α_p absorption of solar radiatrion in the absorber plate, τ_c transmission of solar radiation through the cover, I total solar incident which is the sum of direct solar ray and reflected ray from the reflector $(I_T + I_R)$, T_p plate temperature, T_f fluid temperature, T_c cover temperature, Δx working fluid element, m mass flow rate, C_f air specific heat capacity and h is enthalpy. Each coefficient from equation 5.15 to 5.26 is given as:

$a_1 = \frac{1}{U_b + h_{rPC} + h_1}$………………………………………………………………………(5.27)

$$a_2 = \frac{U_b}{U_b + h_{rPC} + h_1} \qquad (5.28)$$

$$a_3 = \frac{h_{rPC}}{U_b + h_{rPC} + h_1} \qquad (5.29)$$

$$a_4 = \frac{h_1}{U_b + h_{rPC} + h_1} \qquad (5.30)$$

$$a_5 = \frac{1}{U_t + h_{rPC} + h_2} \qquad (5.31)$$

$$a_6 = \frac{U_t}{U_t + h_{rPC} + h_2} \qquad (5.32)$$

$$a_7 = \frac{h_{rPC}}{U_t + h_{rPC} + h_2} \qquad (5.33)$$

$$a_8 = \frac{h_2}{U_t + h_{rPC} + h_2} \qquad (5.34)$$

$$a_9 = \frac{\Delta x h_2}{\dot{m} C_p} \qquad (5.35)$$

$$a_{10} = \frac{\Delta x h_1}{\dot{m} C_p} \qquad (5.36)$$

$$a_{11} = \left(\frac{\Delta x h_2}{\dot{m} C_p} + \frac{\Delta x h_1}{\dot{m} C_p} + 1\right) \qquad (5.37)$$

The mass flow rate of the fluid is computed verses temperature of the fluid and the optimum mass flow rate is selected. Figure 5.3 shows the variation of fluid outlet temperature relative to change in mass flow rate of the fluid for convectional solar air heater. As shown from the Figure 5.3 optimum mass flow rate is selected as 0.003kg/s.

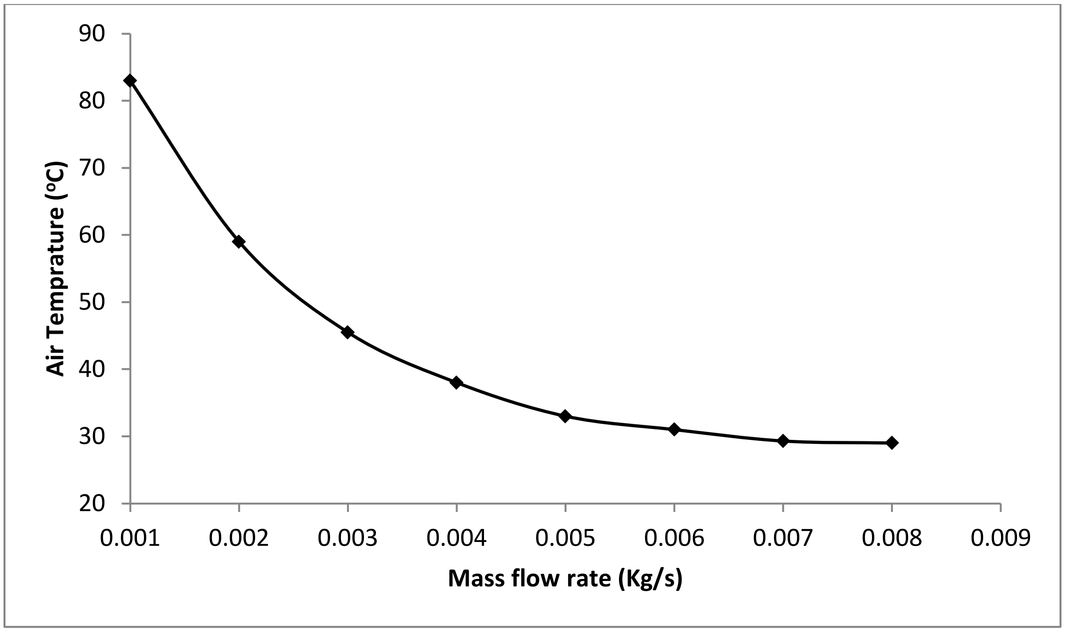

Figure 5.3: Fluid temperature versus mass flow rate

Estimation of hourly variation of atmospheric temperature is a critical data to study the thermal performance analysis of solar air heater. However, in Ethiopia it is difficult to get hourly data for most cities. Hence estimation of hourly dry-bulb temperature from the daily mean maximum and daily mean minimum temperatures will give as an approximate value. A sinusoidal variation of the dry-bulb temperature through the day and maximum temperature occurs at 15:00 hr sun time is assumed. T(t) represent the temperature variation at any time t, as given by (Jones., 1994).

$$T(t) = T_{max} - \frac{(\mathrm{Tmax} - \mathrm{Tmin})}{2}\left[1 - \sin\frac{(\pi t - 9\pi)}{2}\right] \quad (5.38)$$

Where, T_{max} = mean daily maximum temperature at 15:00 hr sun time

T_{min} = mean daily minimum temperature

t = Time of the day

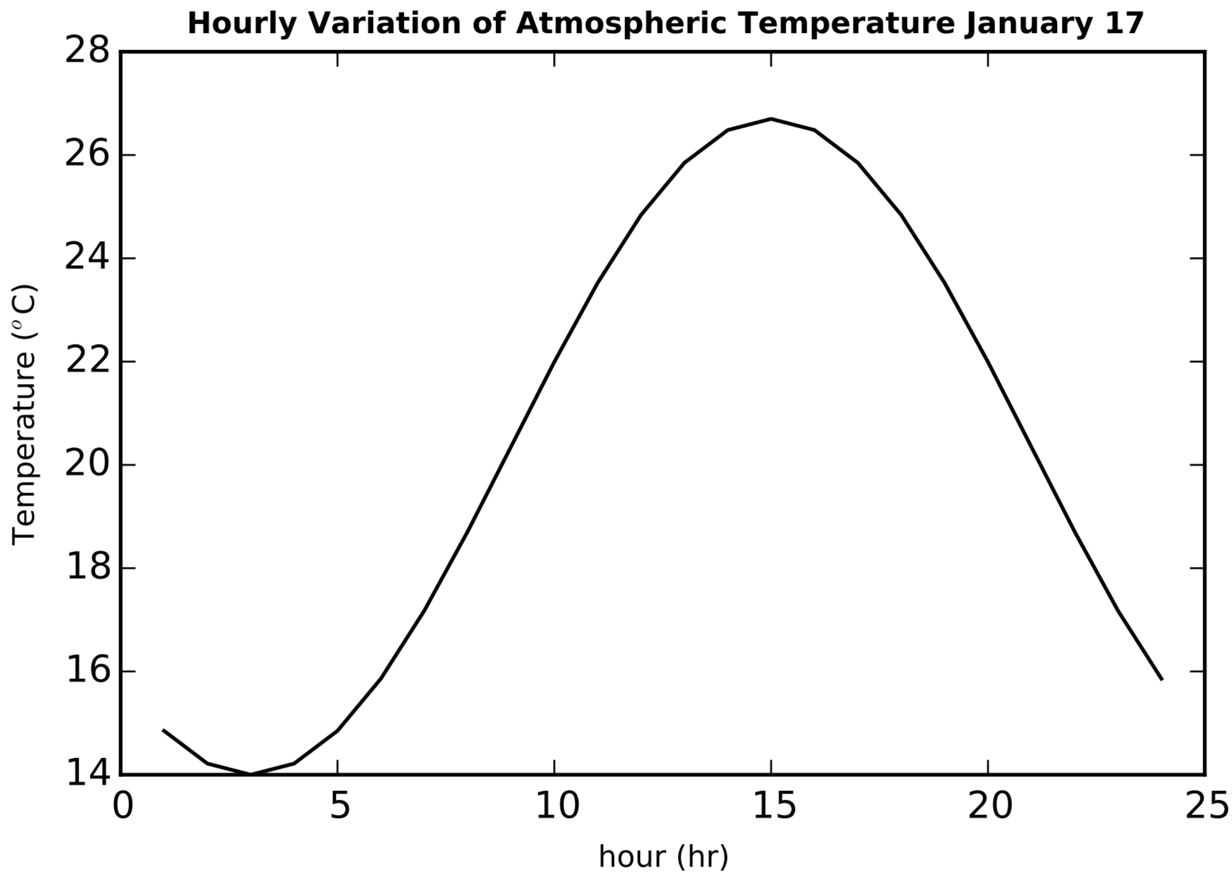

Figure 5.4: Atmospheric temperature variation of Adama on January 17

5.3. Modeling of solar air heater with finned absorber

For the case of finned absorber integrated solar air heater the absorber modeling and working fluid is modified because of the increase in heat transfer area. While the governing equation for the others are the same as the conventional one. This gives a better heat transfer coefficient to absorber plate. And give a better performance to the system.

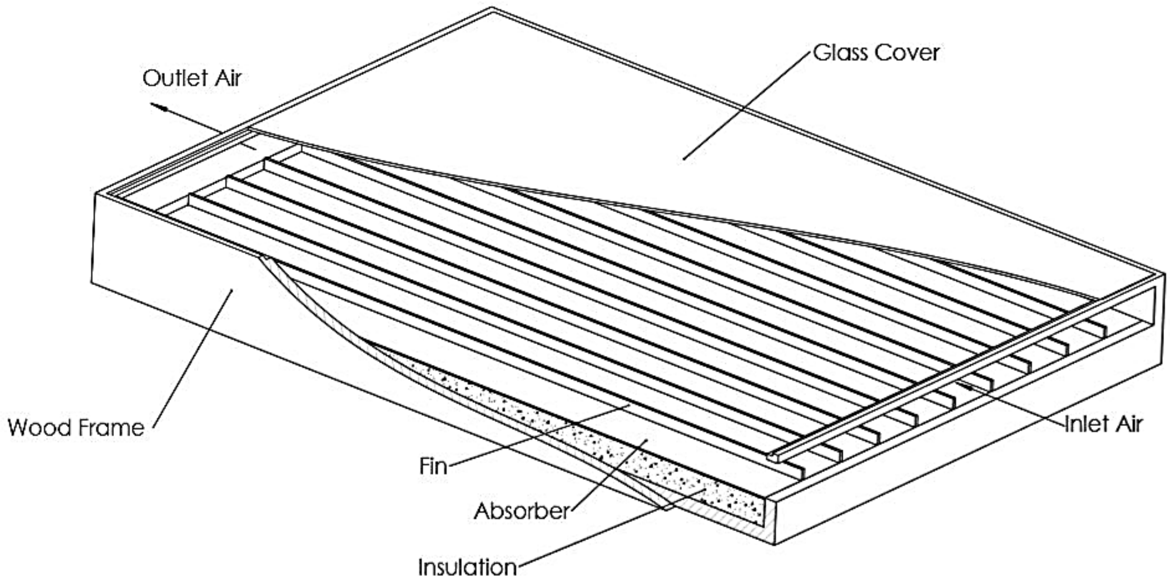

Figure 5.5: Analysis of solar collector with finned absorber

The modified absorber plate equation

$$I\tau_c\alpha_p = U_b(T_p - T_a) + h_{rPC}(T_p - T_c) + h_{11}\phi(T_p - T_f) \quad (5.39)$$

$$T_p = \frac{I\tau_c\alpha_p}{U_b + h_{rPC} + h_{11}\phi} + \frac{U_b T_a}{U_b + h_{rPC} + h_{11}\phi} + \frac{h_{rPC} T_c}{U_b + h_{rPC} + h_{11}\phi} + \frac{h_{11} T_f}{U_b + h_{rPC} + h_{11}\phi} \quad (5.40)$$

$$T_p = a_1 I\tau_c\alpha_p + a_2 T_a + a_3 T_c + a_4 T_f \quad (5.41)$$

Where, ϕ is the fin efficiency given by:

$$\phi = 1 + ({A_f}/{A_c})\eta_f \quad (5.42)$$

In which, $A_f = 2nw_fL$ and $A_c = WL$ are the surface areas of n fins and absorbing plate, respectively, while η_f denotes the fin efficiency given by:

$$\eta_f = (\tan M\, w_f)/Mw_f \quad (5.43)$$

And,

$$\mathrm{M} = \sqrt{2\mathrm{h_f}/\mathrm{kt}} \quad (5.44)$$

$$a_{1F} = \frac{1}{\mathrm{U}_b + h_{rPC} + h_{11}\phi} \quad (5.45)$$

$$a_{2F} = \frac{\mathrm{U}_b}{\mathrm{U}_b + h_{rPC} + h_{11}\phi} \quad (5.46)$$

$$a_{3F} = \frac{h_{rPC}}{\mathrm{U}_b + h_{rPC} + h_{11}\phi} \quad (5.47)$$

$$a_{4F} = \frac{h_1}{\mathrm{U}_b + h_{rPC} + h_{11}\phi} \quad (5.48)$$

The fluid

$$q_u = \left[\mathrm{h}_{fc}\left(T_c - T_f\right) + h_{11}\phi\left(T_p - T_f\right)\right] \quad (5.49)$$

$$q_u = \left(\dot{m}C_f \frac{dT_f}{dx}\right) \quad (5.50)$$

Using the forward Finite difference method equation 5.50 can be resolved as:

For interior nodes

$$\dot{m}C_p\left(\frac{T_{f_{i+1}} - T_{f_i}}{\Delta x}\right) = U_1\left(T_c - T_{f_i}\right) + h_{11}\phi\left(T_p - T_{f_i}\right) \quad (5.51)$$

$$T_{f_{i+1}} = \frac{\Delta x U_1}{\dot{m}C_p}T_c + \frac{\Delta x h_{11}\phi}{\dot{m}C_p}T_p + \left(\frac{\Delta x U_1}{\dot{m}C_p} + \frac{\Delta x h_{11}\phi}{\dot{m}C_p} + 1\right)T_{f_i} \quad (5.52)$$

$$T_{f_{i+1}} = a_9 T_c + a_{10} T_p + a_{11} T_{f_i} \quad (5.53)$$

For exterior node

$$T_{f_{i+1}} = a_9 T_c + a_{10} T_p + a_{11} T_{amb} \quad (5.54)$$

Where,

$$a_{9F} = \frac{\Delta x U_1}{\dot{m}C_p} \quad (5.55)$$

$$a_{10F} = \frac{\Delta x h_{11}\phi}{\dot{m}C_p} \quad (5.56)$$

$$a_{11F} = \left(\frac{\Delta x U_1}{\dot{m}C_p} + \frac{\Delta x h_{11}\phi}{\dot{m}C_p} + 1\right) \quad (5.57)$$

5.4. Modeling of solar air heater integrated with sensible thermal storage

Thermal energy may be stored as sensible heat or latent heat. Sensible heat storage systems utilize the heat capacity and the change in temperature of the material during the process of charging or discharging - temperature of the storage material rises when energy is absorbed and drops when energy is withdrawn. One of the most attractive features of sensible heat storage systems is that charging and discharging operations can be expected to be completely reversible for an unlimited number of cycles, i.e., over the life-span of the storage.

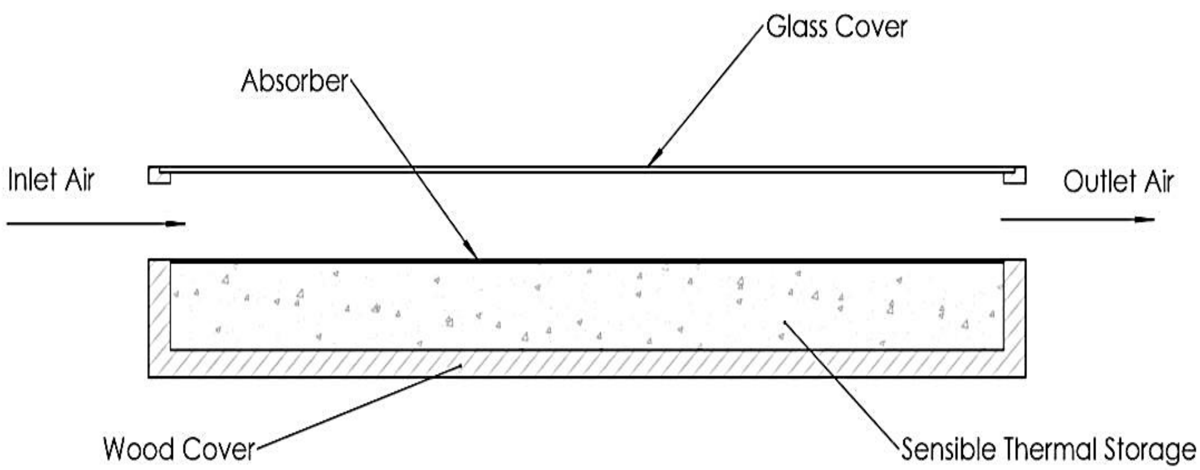

Figure 5.6: Analysis of solar collector with sensible thermal storage

5.4.1. Sensible thermal storage system

Sensible thermal energy storage stores thermal energy by raising material temperature, so stored sensible heat amount is dependent on material density, its specific heat capacity and temperature difference.

$$Q_{sensible} = m \int_{T_l}^{T_h} C_p(T)\, dT \qquad (5.58)$$

Where m is the mass of storage material, T_L and T_H are low temperature and high temperature in the same phase, respectively, Cp(T) is the specific heat capacity at different temperature. So many sensible storage materials have been studied in different countries. Out of those frequently used low cost and easily available sensible thermal storage materials are stone, sand, clay, concrete and gypsum are listed as shown in Appendix D. For this thesis work gypsum material is selected as a sensible storage material due to its light weight and lower thermal conductivity.

5.4.2. Performance parameter of thermal storage

i) Charging and discharging time

Charging time is the time taken to absorb and store energy to the amount of stored energy is dependent on the capacity and volume of the material and charging rate is depends on thermal distribution of the storage volume. Charging rate of low conductivity material is slow, due to small thermal diffusivity. Discharging time is time taken to release complete stored energy from storage medium. That is by achieving a volume average temperature of T_{inlet}. But after a certain time, the decrease in storage medium, temperature is not significant particularly when its temperature becoming near to T_{inlet}. In this way, effective discharging time of storage material is taken as the time till the temperature drop is significant.

ii) Thermal distribution

Thermal diffusivity is the rate of thermal conductivity to the thermal storing capacity of the storing material. Thermal distribution is highly dependent on the material thermal diffusivity. The large value of the thermal diffusivity represents the faster the propagation of heat into the medium. A small value of thermal diffusivity means that most of heat is absorbed by the storage material and a small amount of heat will be conducted further (Cengel, 2003).

$$\alpha = \frac{heat\ conducted}{heat\ stored} = \frac{k}{\rho.C_p} \quad (5.59)$$

iii) Specific heat storage capacity

Sensible thermal storage stores sensible thermal energy only by temperature difference. Its storing capacity is dependent on thermal heat capacity (ρ.cp) of the storage material.

$$Q = mc_p\Delta T = \rho V c_p \Delta T \quad (5.60)$$

Where, cp is the specific heat of the material, ΔT is the temperature difference, V is the total volume of the storage material, and ρ is the density of the storage material.

iv) Storage efficiency

Storage efficiency is the ratio of energy output to energy input. It represents the heat losses to the surroundings.

$$\eta = \frac{E_{dis}}{E_{char}} \quad (5.61)$$

Where, E_{dis} discharged energy, E_{char} charging energy

5.4.3. Governing equation

The governing equation for thermal storage assisted solar air heater is the same as that of the conventional one, with an exception of integrating the storage effect on the absorber plate and adding one another equation for the storage. This is stated mathematical as given below:

The absorber plate

$$I\tau_c\alpha_p = \mathrm{U}_b(T_p - T_s) + h_{rPC}(T_p - T_c) + h_1(T_p - T_f) \quad (5.62)$$

$$T_p = \frac{I\tau_c\alpha_p}{\mathrm{U}_b+h_{rPC}+h_1} + \frac{\mathrm{U}_bT_s}{\mathrm{U}_b+h_{rPC}+h_1} + \frac{h_{rPC}T_c}{\mathrm{U}_b+h_{rPC}+h_1} + \frac{h_1T_f}{\mathrm{U}_b+h_{rPC}+h_1} \quad (5.63)$$

$$T_p = a_1I\tau_c\alpha_p + a_2T_s + a_3T_c + a_4T_f \quad (5.64)$$

Where,

$$a_{1s} = \frac{1}{\mathrm{U}_b+h_{rPC}+h_1} \quad (5.65)$$

$$a_{2s} = \frac{\mathrm{U}_b}{\mathrm{U}_b+h_{rPC}+h_1} \quad (5.66)$$

$$a_{3s} = \frac{h_{rPC}}{\mathrm{U}_b+h_{rPC}+h_1} \quad (5.67)$$

$$a_{4s} = \frac{h_1}{\mathrm{U}_b+h_{rPC}+h_1} \quad (5.68)$$

The steady state modeling of the storage material will give the vertical distribution of temperature at steady state. As the analysis is performed for an hour interval, the Governing equation is given by:

$$Amount\ of\ heat\ stored\ =\ Heat\ transferd\ by\ the\ steady\ state\ conduction * \Delta t$$
$$in\ the\ storage$$

Where, Δt is the approximated steady state assumption, i.e one hour, so that the all heat transfer process is at steady state within the range of one hour. Mathematically it can be expressed as:

$$\Delta m C_p \Delta T = \left[U_{ps}\left(T_p - T_s\right) - U_{sb}(T_s - T_b)\right] * \Delta t \qquad (5.69)$$

Where, T_s is temperature of the storage Gypsum, Δm element mass, ΔT is the temperature change of the element, T_p, T_s, T_b represent the absorber plate, storage and insulator temperature, respectively. To determine the temperature distribution inside the storage, forward Finite difference approach is used, the bed is discretized into 20 elements axially by assuming a constant temperature through the length (inlet to outlet). Equation 5.69 can be resolved as:

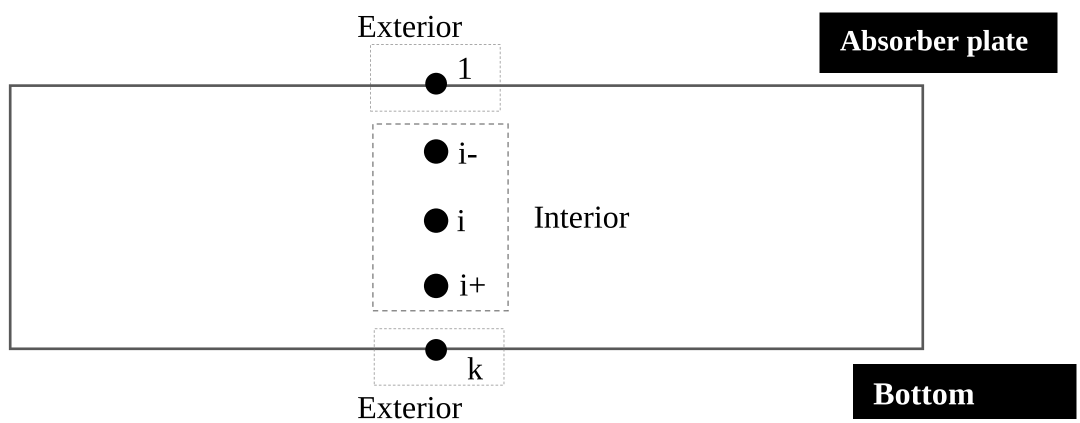

Figure 5.7: Finite difference analysis of sensible thermal storage

For **exterior nodes** near the absorber plate (N = 1) and near the bottom cover (N =k), where k=1, 2, 3,…20 respectively:

$$\Delta m C_p (T_{s1}^{t} - T_{s1}^{t-1}) = [U_{ps}\left(T_p^{t} - T_{s1}^{t-1}\right) - U_s(T_{s2}^{t-1} - T_{s1}^{t-1})] * \Delta t \qquad (5.70)$$

$$\Delta m C_p (T_{sN}^{t} - T_{sN}^{t-1}) = [U_s(T_{sN-1}^{t-1} - T_{sN}^{t-1}) - U_{sb}(T_a - T_{sN}^{t-1})] * \Delta t \qquad (5.71)$$

For interior nodes:

$$\Delta m C_p (T_{si}^{t} - T_{si}^{t-1}) = [U_s(T_{si-1}^{t} - T_{si}^{t-1}) - U_s(T_{si}^{t-1} - T_{si+1}^{t-1})] * \Delta t \qquad (5.72)$$

Those equations for near absorber plate, exterior and interior will are reduced to, respectively:

$$T_{s0}^{t} = aa * [\left(T_{p}^{t} - T_{s0}^{t-1}\right) - (T_{s1}^{t-1} - T_{s0}^{t-1})] * \Delta t + T_{s0}^{t-1} \quad \ldots\ldots(5.73)$$

$$T_{sN}^{t} = aa * [(T_{sN-1}^{t-1} - T_{sN}^{t-1}) - (T_{si} - T_{sN}^{t-1})] * \Delta t + T_{sN}^{t-1} \quad \ldots\ldots(5.74)$$

$$T_{si}^{t} = aa * [(T_{si-1}^{t} - T_{si}^{t-1}) - (T_{si}^{t-1} - T_{si+1}^{t-1})] * \Delta t + T_{si}^{t-1} \quad \ldots\ldots(5.75)$$

Where, $aa = \frac{U_s \Delta t}{\Delta m C_p}$, t is time, i represent the nodal element and k is the total number of nodes. Neglecting the contact resistance between the plate and the storage and between the storage and insulator the value of the coefficient (aa) can be applied for any of the three cases.

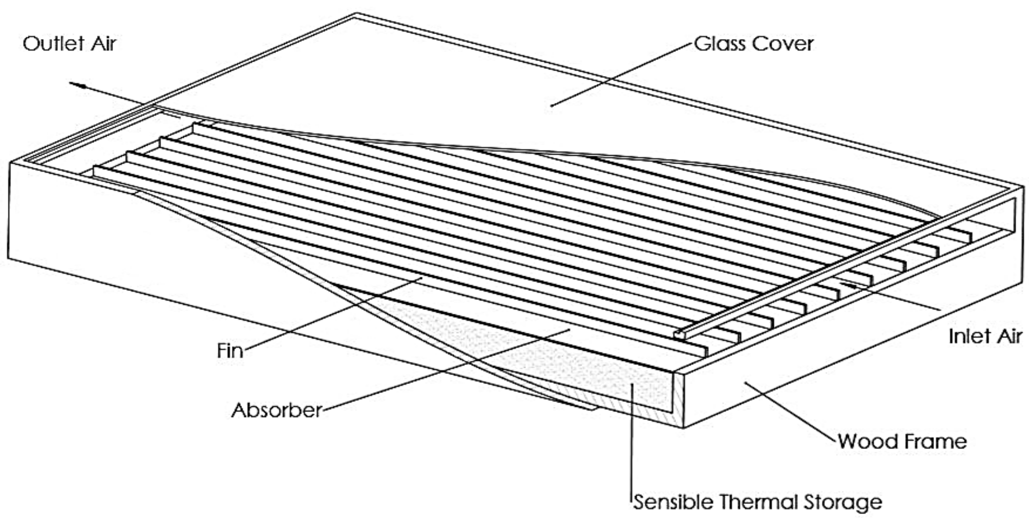

Figure 5.8: Fin and thermal storage integrated solar air heater

Modeling and thermal Analysis of solar air heater with finned absorber integrated with sensible thermal storage and reflector is calculated by combining the previous modeling in to one. A python code is developed for all cases in Appendix E. The code integrates a *Coolprop* module to take a temperature dependent thermo-physical property of the working fluid.

5.5. Numerical performance result of SAH

In this section, results obtained from the solar air heater (SAH) models are discussed in detail. Validation of the model is done by comparing the numerical result obtained with experimental results. Air heater daily and monthly energetic performance for varying weather conditions is described. The effect of longitudinally finned absorber, reflector and gypsum thermal storage on the efficiency of the solar air heater is discussed both numerically and experimentally. Lastly, the results on the application of the solar air heater for crop drying and poultry farm space heating are discussed briefly.

5.5.1. Air temperature variation at the outlet of SAH

The heat transfer fluid outlet temperature variation throughout the day for different seasons are calculated iteratively using Python program for each variation of solar radiation incidence on the solar air heater for the conventional and the modified one is given on the successive figure below. The heat transfer coefficients and fluid properties are considered temperature dependent.

5.5.1.1. Air temperature variation at the outlet of the conventional SAH

As shown in the Figure 5.9, at the initial hours until morning, the outlet temperature from the air heater is the same as the ambient temperature of the day, and then it starts rising the heat transfer

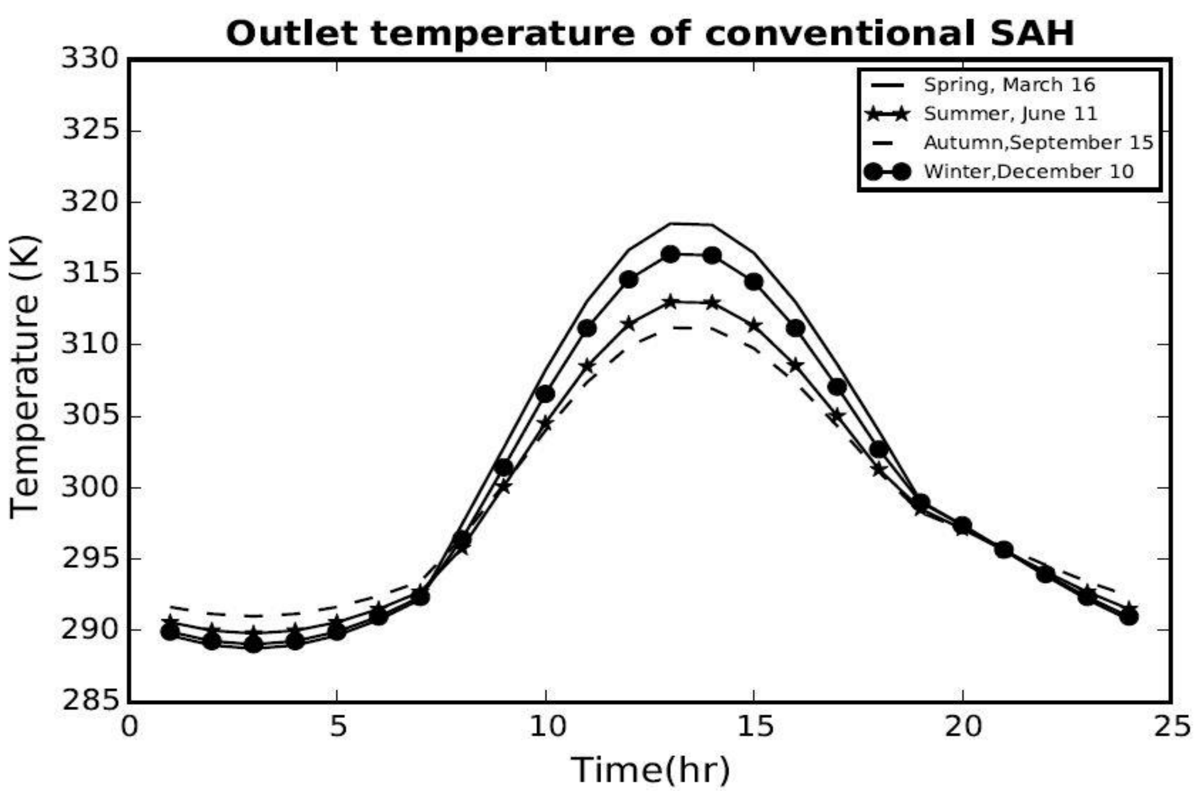

Figure 5.9: Outlet temperature of the conventional solar air heater for the representative day of each season of first month

fluid temperature until sunsets. Evidently, winter and spring season experience maximum solar irradiation in the middle of the day (at noon) on a normal surface. These high available solar resources cause higher useful heat transfer to the solar air heater which raises the hot outlet air temperature. It is important to note that there is also a temperature variation in each month of the seasons.

5.5.1.2. Air temperature variation at the outlet of the reflector integrated SAH

From figure 5.10, one can clearly see that the temperature profile of the hot outlet air is the same as the conventional one with an increase in magnitude. This is because of the top and the sides' reflector effect on the solar air heater.

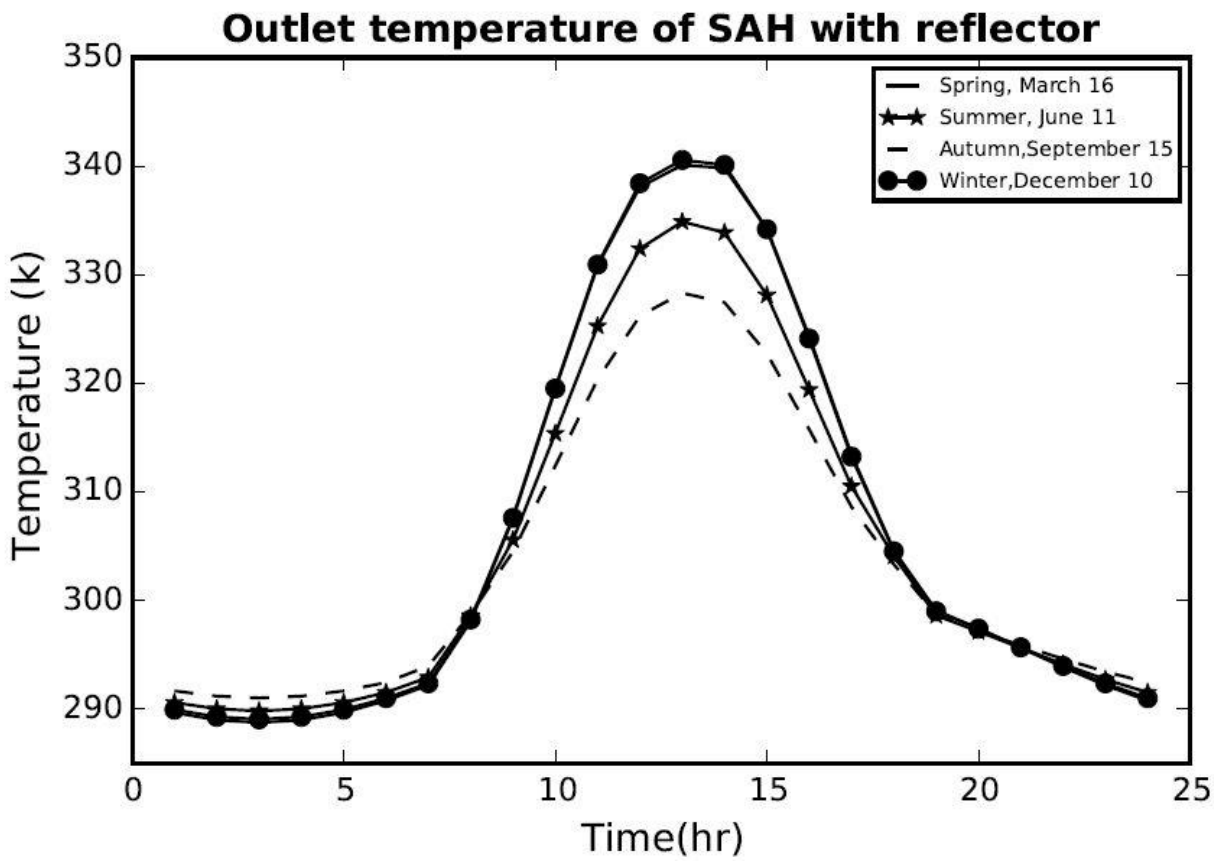

Figure 5.10: Outlet temperature of the solar air heater with reflector for the representative day of each season of first month

5.5.1.3. Air temperature variation at the outlet of the thermal storage integrated SAH

As shown in the Figure 5.11, at the initial hours of the day, the outlet air in the solar air heater-Gypsum thermal energy storage (TES) system heated until morning by discharging from the thermal storage during off times for solar irradiation. Then, it starts as the sun rises and starts rising the heat transfer fluid temperature until the sunsets and discharging from the thermal energy storage continues.

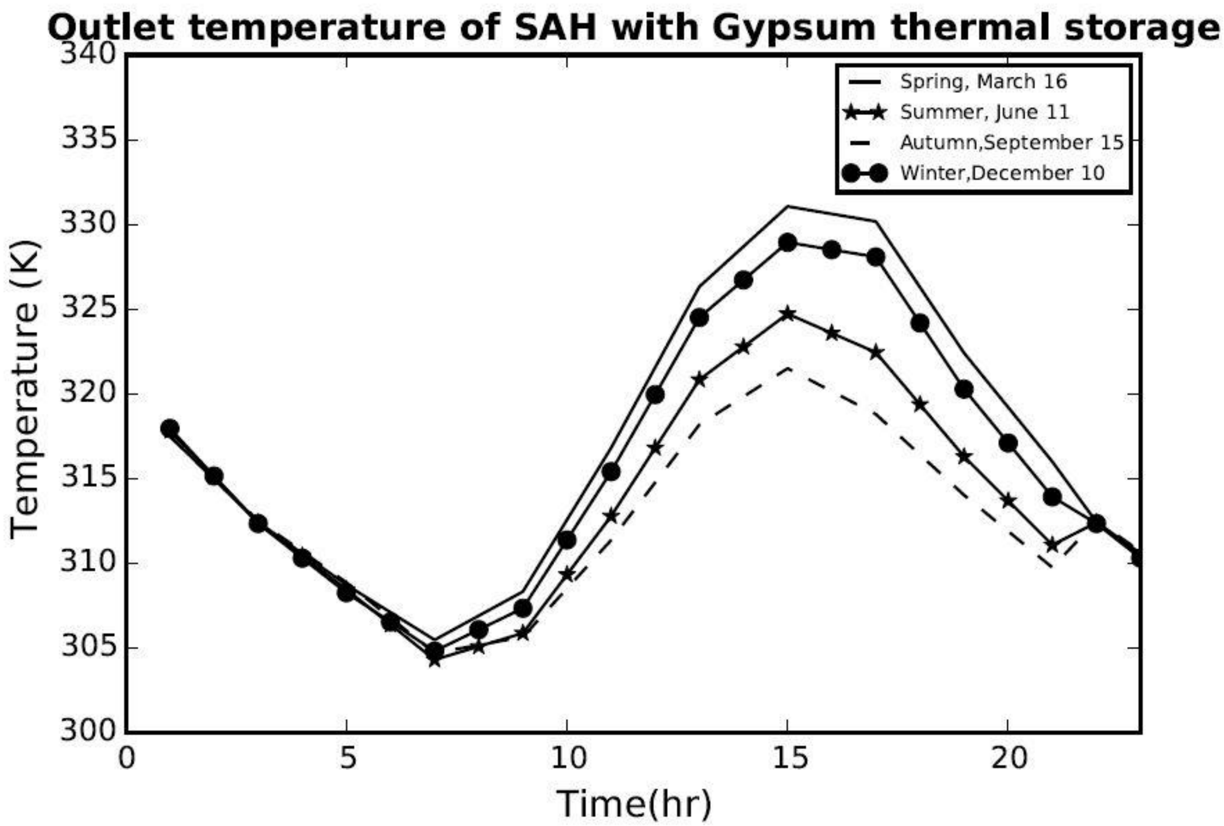

Figure 5.11: Outlet temperature of the solar air heater with Gypsum thermal storage for the representative day of each season of first month

5.5.1.4. Air temperature variation at the outlet of SAH with finned absorber

From figure 5.12, one can clearly see that the temperature profile of the hot air is the same as the conventional one with a little increase in magnitude. This is because of the fin integrated on the absorber.

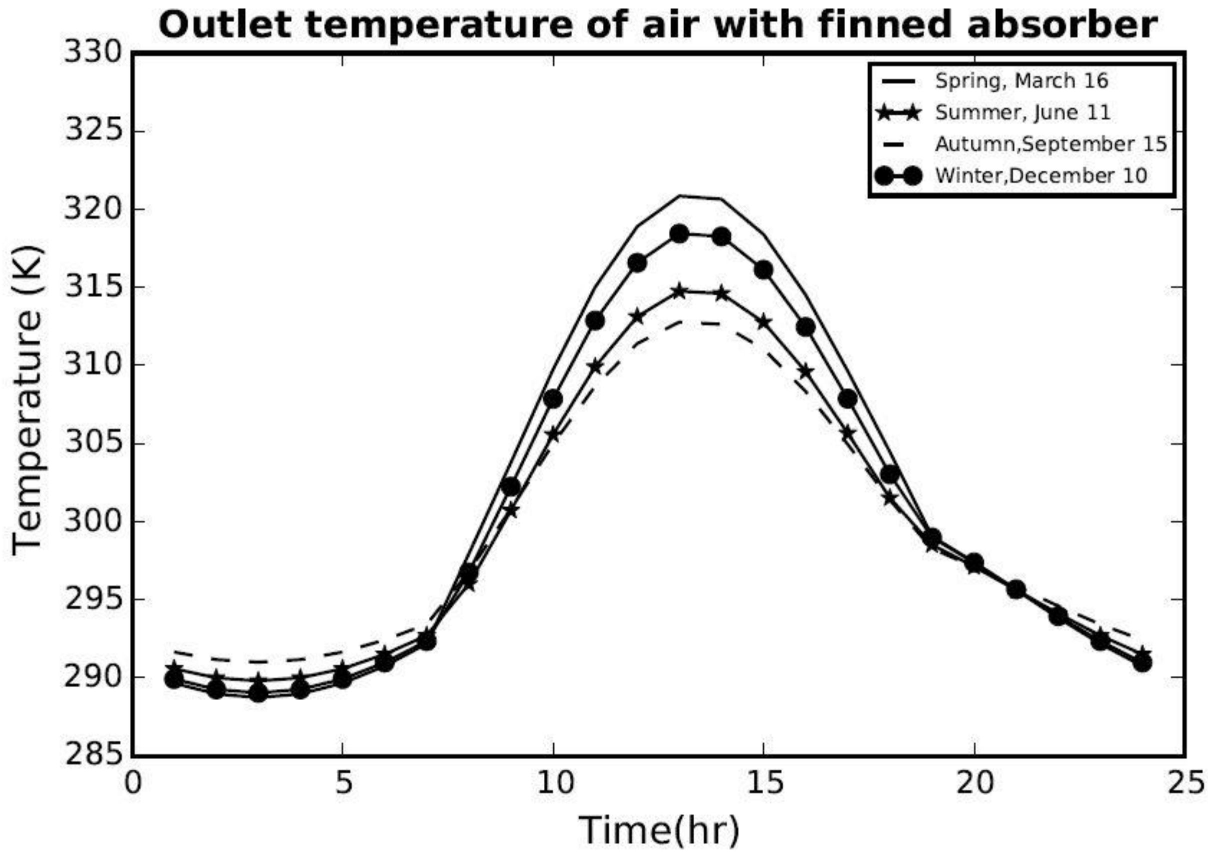

Figure 5.12: Outlet temperature of the solar air heater with finned absorber for the representative day of each season of first month

5.5.1.5. Air temperature variation at the outlet of SAH with the combined enhancement techniques

The air outlet temperature for the combined effect of the three enhancement techniques is shown in Figure 5.13. The graph shows that both the temperature and sustainability of the solar air heater is increased for this case. The thermal storage gives an increase in the working time of the air heater while the reflector and finned absorber give a higher temperature output to the system.

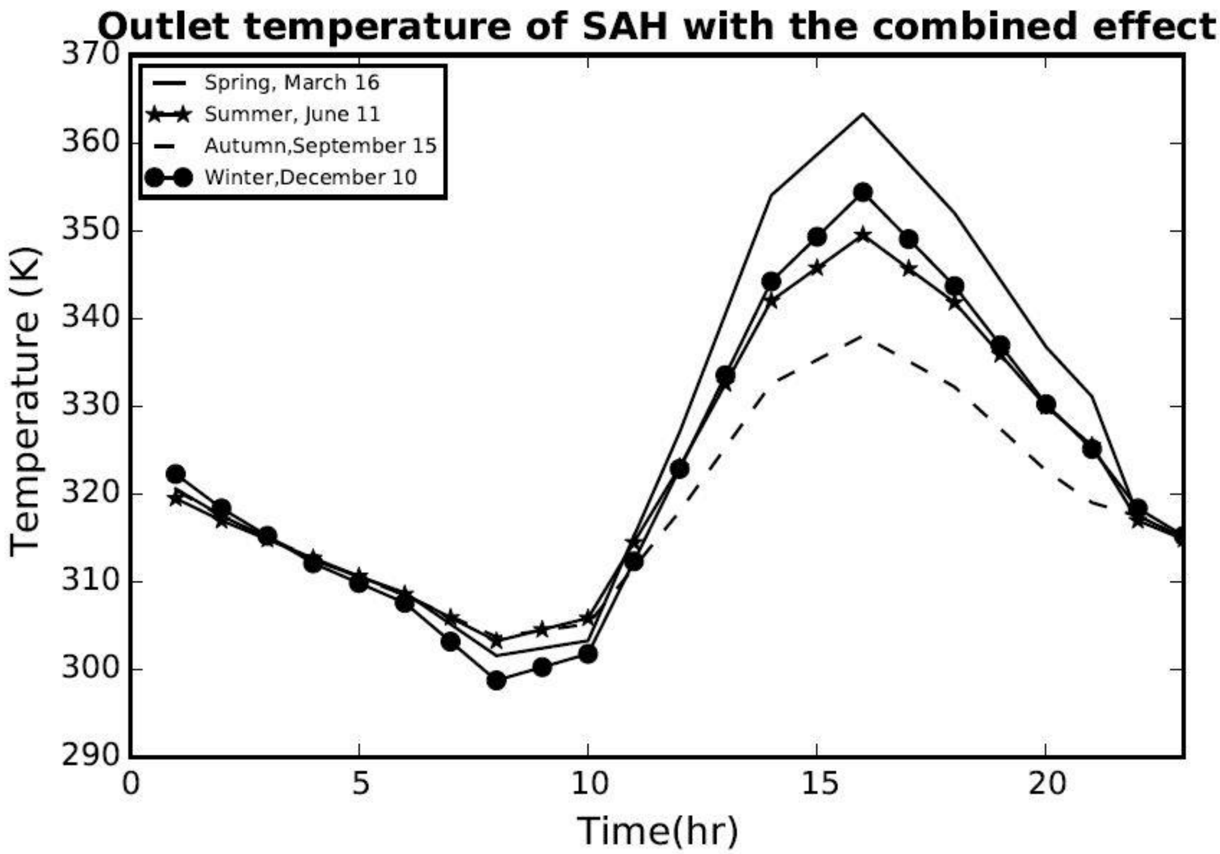

Figure 5.13: Outlet temperature of the solar air heater with three enhancement technics for the representative day of each season of first month

5.5.2. Air temperature variation through the SAH section

Working fluid inlet to outlet temperature for the whole case of analysis is shown in Figure 5.14. The graph shows the air temperature for the air heater for the case of January 17 at noon time. It is clearly depicted that as enhancing effect is integrated to the system the outlet temperature is increased with a large visible change shown for the reflector case. Combining all those cases gives us a comprised better effect to the system.

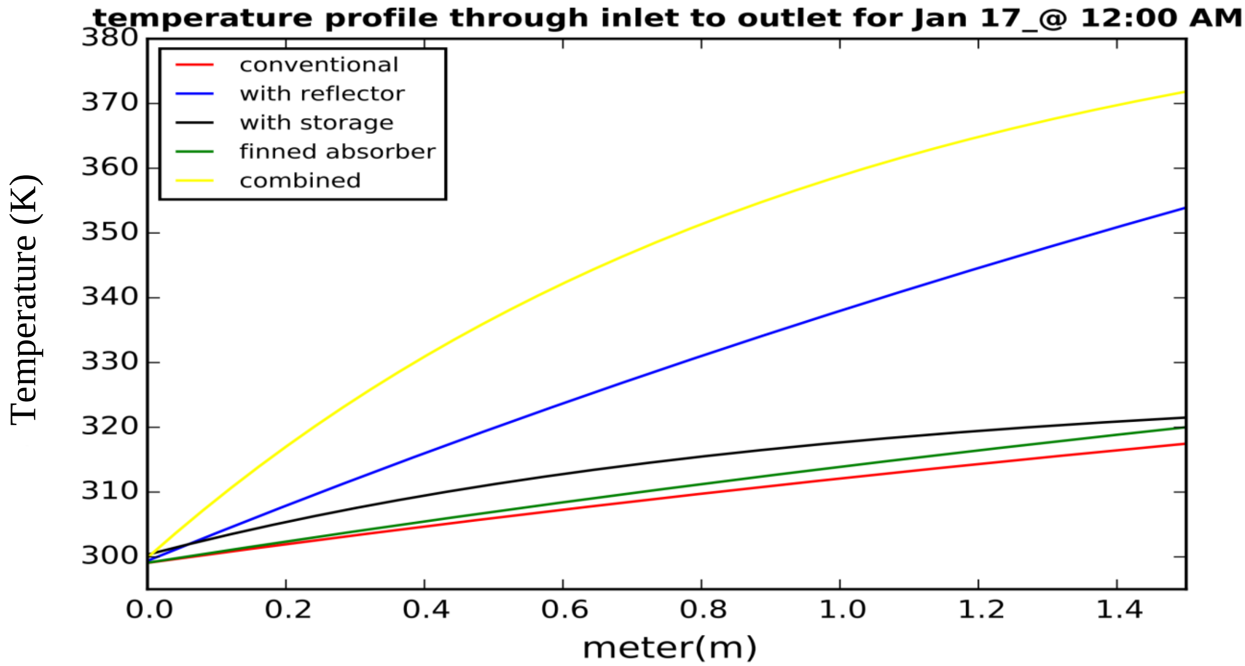

Figure 5.14: Inlet to outlet temperature profile of the working fluid through the solar air heater section for January 17 at 12:00 AM

5.5.3. Temperature variation of absorber

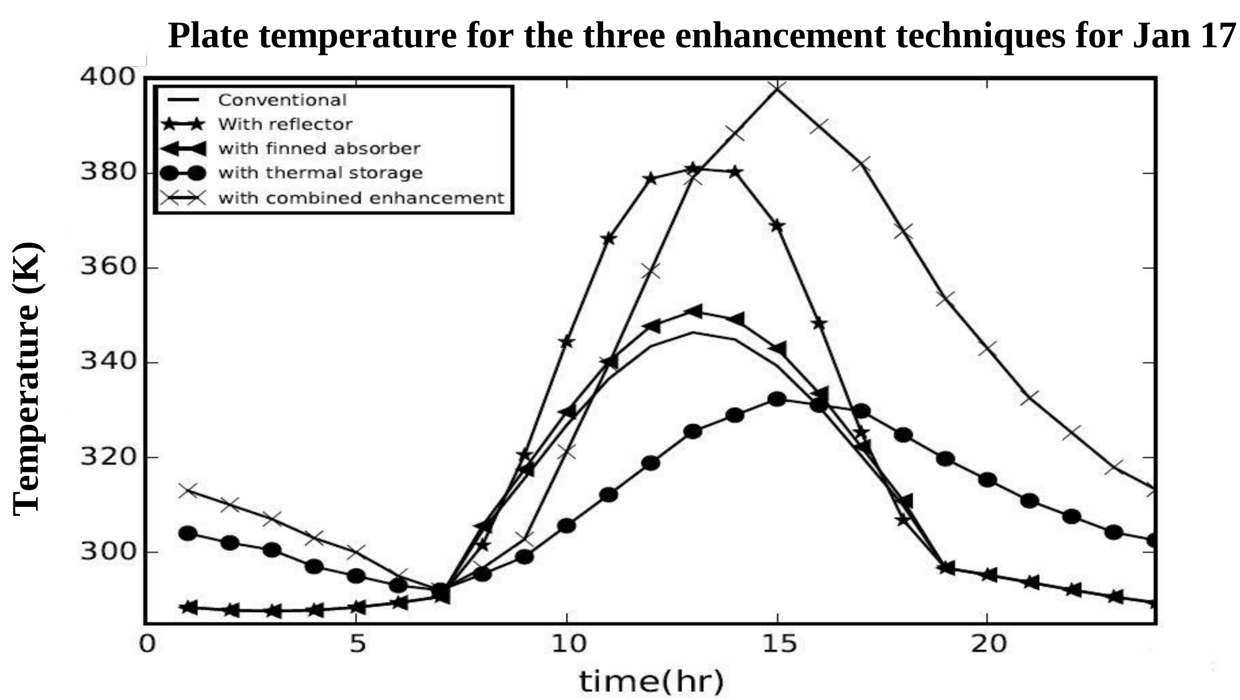

Figure 5.15: plate temperature of the solar air heater with those enhancement technics for January 17

5.5.4. Temperature variation of gypsum thermal storage

The gypsum thermal storage integrated SAH is analyzed by discretizing the element to 20 elements. Figure 5.16 shows the temperature variation of the thermal storage at node 0 (@ the absorber), 5, 10, 15 and 20. The graph clearly shows the charging and discharging characteristics of each node throughout the day for January 17.

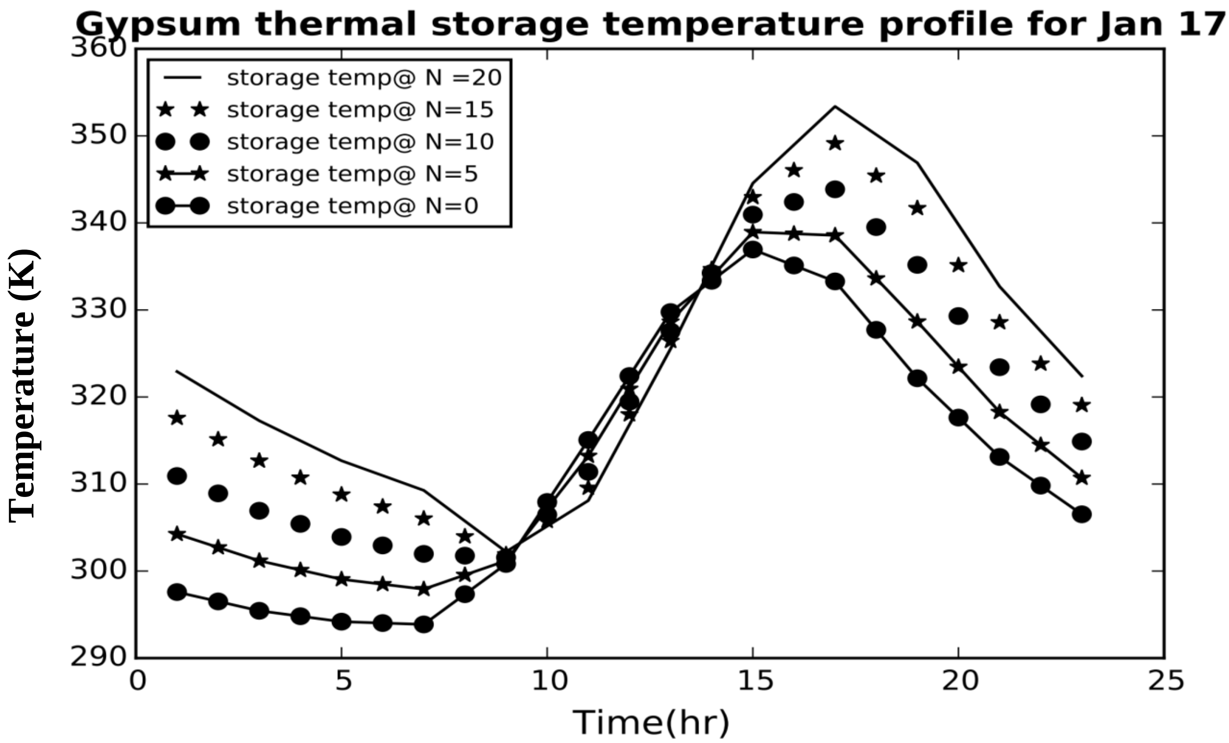

Figure 5.16: Temperature profile of the Gypsum integrated solar air heater at each axial nodes for January 17

The charging and discharging temperature profile of Gypsum integrated SHA is shown in Figure 5.17. The graph clearly shows that during the morning time and early noon time, the storage is in a charging mode i.e., at the time of 10:00 AM, 12:00 AM and 2:00 PM. Then after the Gypsum storage is shifted to discharging mode i.e., at the time of 4: 00 PM and 6: 00 PM. evidently, it can be seen that the working time of the solar air heater is increased with enhanced efficiency.

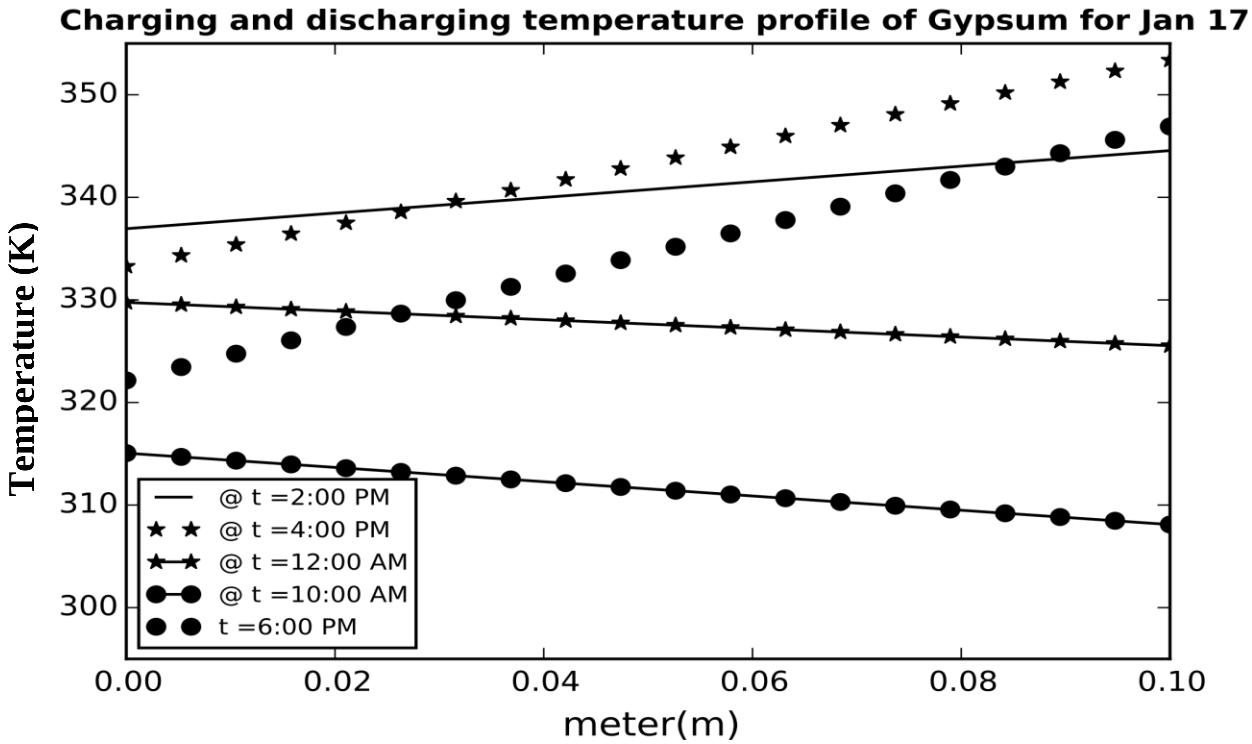

Figure 5.17: Charging and discharging temperature profile of the Gypsum integrated solar air heater at each axial nodes for January 17

5.5.5. Useful energy collected and efficiency of the air heater

5.5.5.1. Instantaneous useful energy collected

Instantaneous useful heat gained by SAH for each hour interval from sunrise to sunset is calculated from the result found from outlet fluid temperature variation of the solar air heater, by multiplying the temperature rise of the air to its mass flow rate, and specific heat capacity. Below, the hourly average useful energy gains of the solar air heater for conventional and the enhanced one.

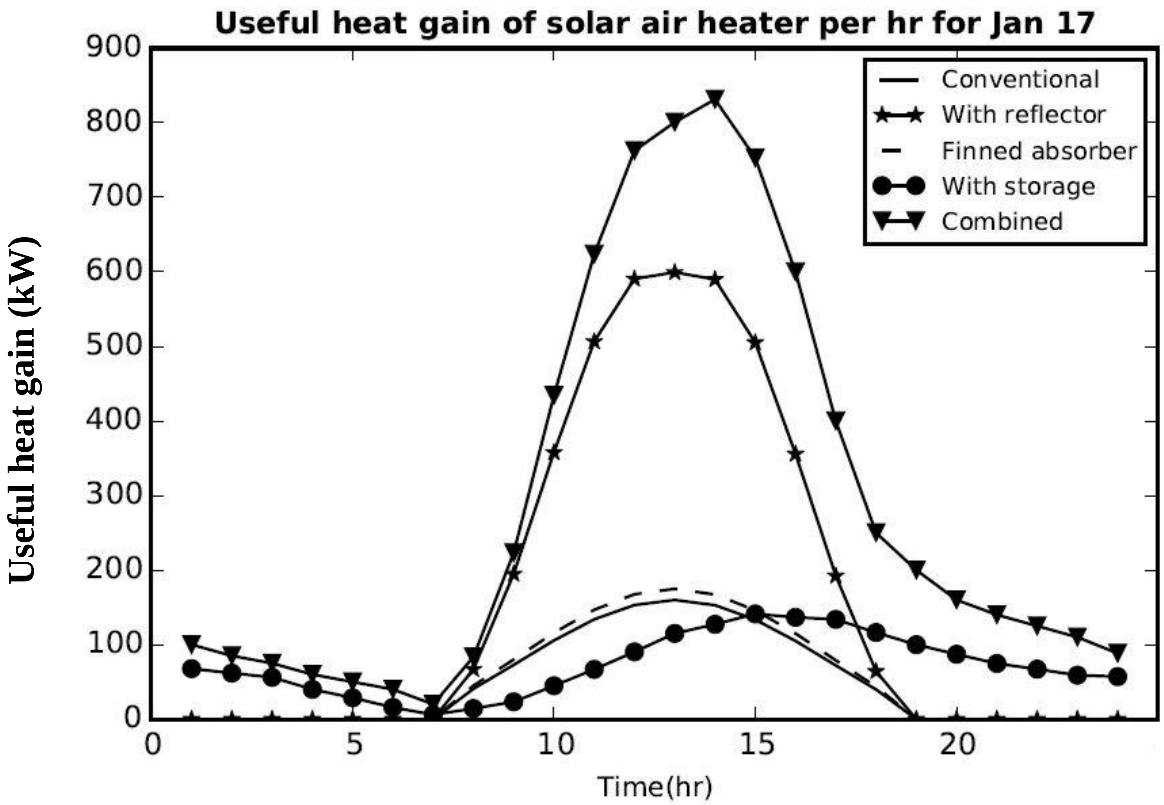

Figure 5.18: Useful hourly heat gain of the solar air heater with the three enhancement technics for January 17

5.5.5.2. Daily average useful energy collected by solar air heater (SAH)

The total amount of energy that can be collected by the solar air heater throughout the day is analyzed for each representative day of the months. The daily average useful energy collected by each SAH cases is depicted in the following graphs.

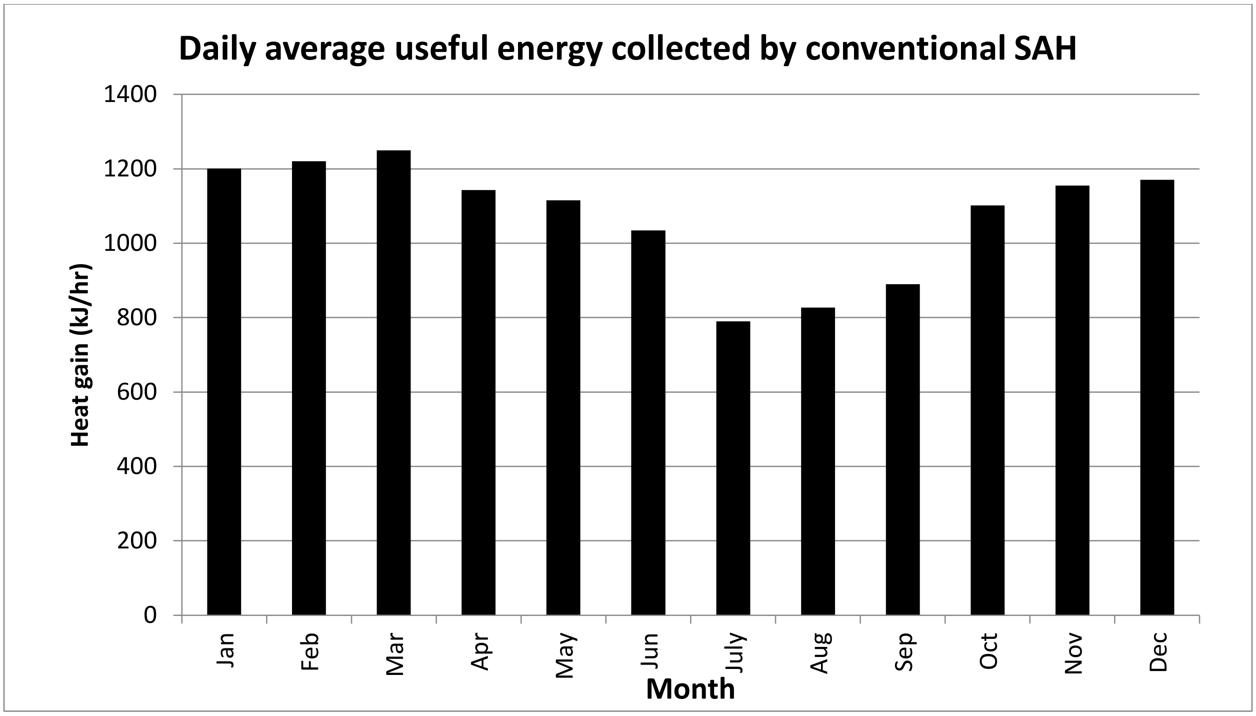

(a) Convectional SAH

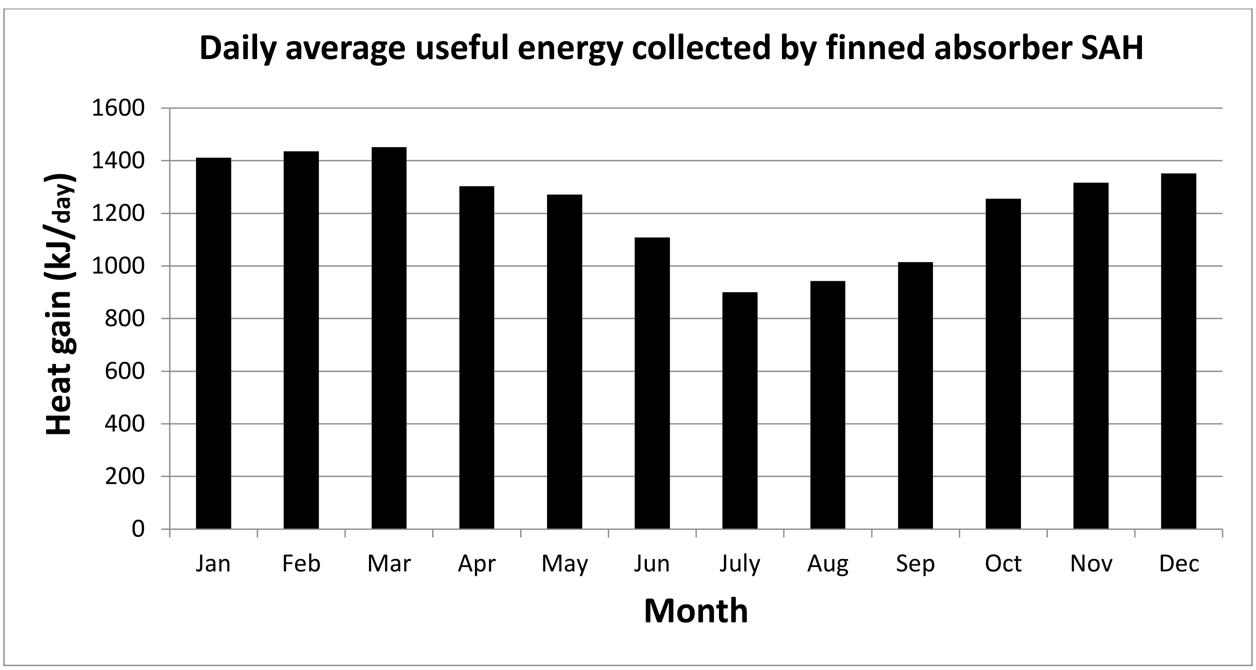

(b) Finned absorber SAH

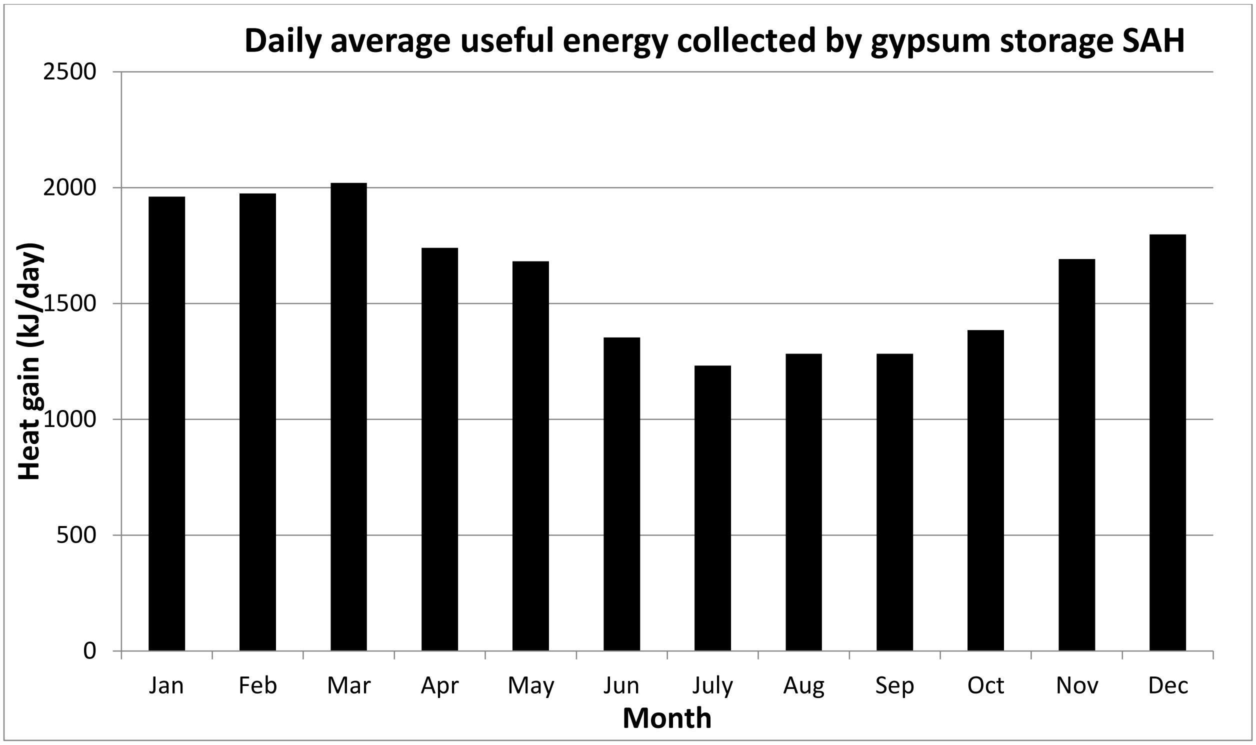

(c) Gypsum integrated SAH

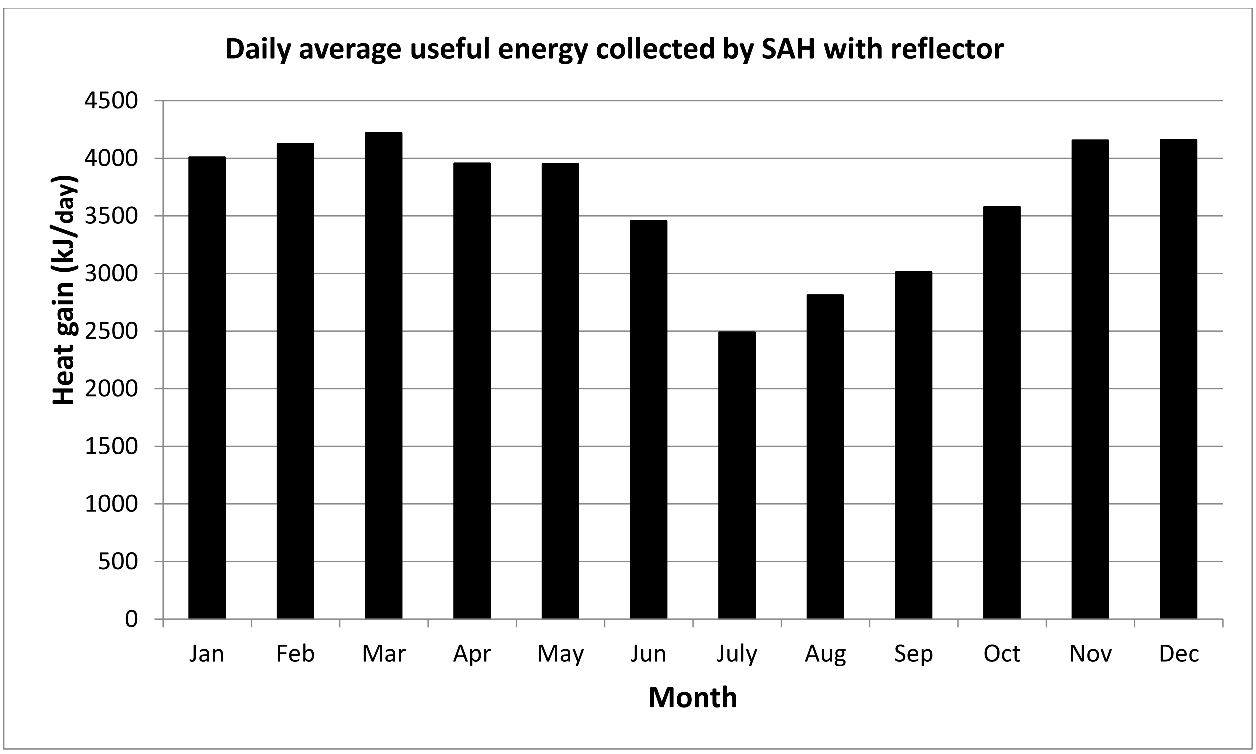

(d) SAH with reflector

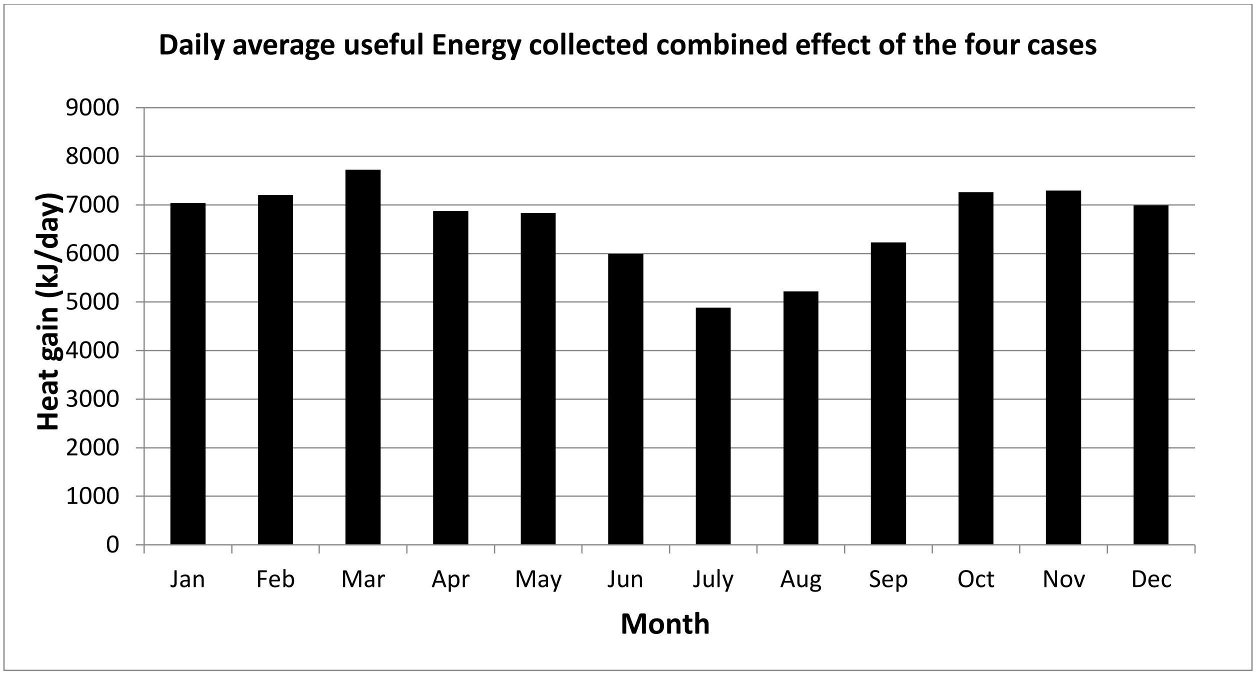

(e) Combined enhanced SAH

Figure 5.19: Monthly average daily average useful energy collected by the solar air heater for each case

From the results of Figure 5.19, the maximum total amount of energy that can be collected per day by the SAH for the case of conventional, finned absorber, Gypsum thermal storage, reflector and combining effect is 1249.991 kJ/day, 1451.881 kJ/day, 2020.621 kJ/day, 4217.50 kJ/day and 7721.589 kJ/day in the month of March, respectively. While the minimum amount of energy collected is 790.039 kJ/day, 943.115 kJ/day, 1231.490 kJ/day, 2486.887 kJ/day and 4883.041 kJ/day for the month of July, respectively. This shows, the average daily solar intensity on March is higher compared to the other months of the year and the solar intensity reaches the lowest value on July.

5.5.6. Thermal efficiency of the solar air heater

The thermal efficiency of the SAH is calculated based on the heat gain, solar intensity and aperture area of the collector.

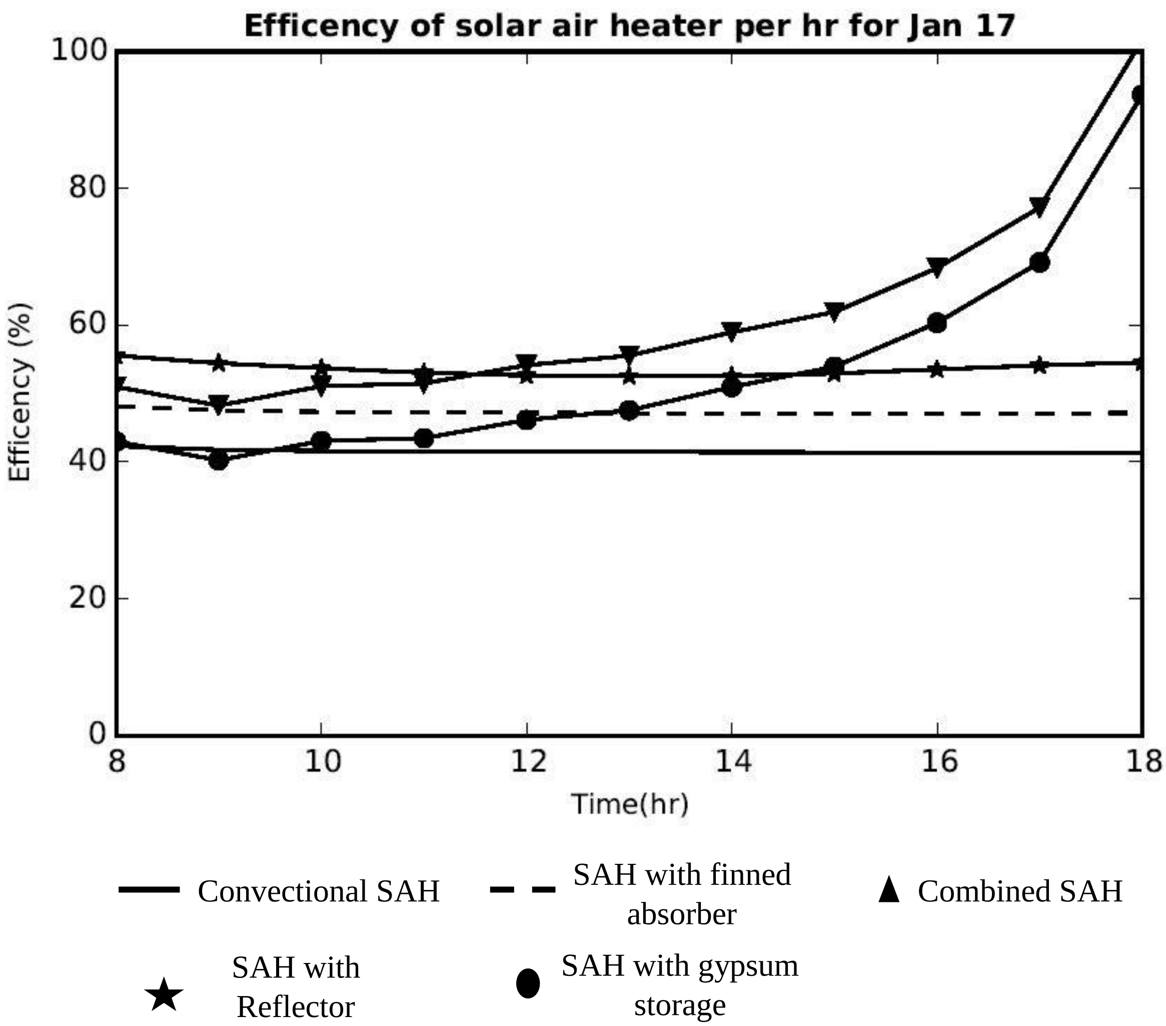

Figure 5.20: Instantaneous efficiency variation of solar air heater in each case for January 17

It can be noticed that the thermal efficiency of the collector is relatively uniform throughout the day for the three cases i.e. conventional, reflector and finned absorber, with a little lowering in the middle. This is due to the fact that thermal loss to the environment is getting higher as the sun radiation incident to SAH increase. But for the Gypsum storage, one can clearly dictate that the efficiency of the system increased as the time approach to the sunset. This is due to the fact that the stored energy is discharged to the working fluid to sustain the operation of the system without a significant input form the external.

5.5.7. Validation

The result of numerical simulation for SAH is validated against the experimental work as shown in Figure 5.21. These results are compared for the conventional and combined enhancement technics. From the graph one can clearly dictate that the numerical and experimental works are comparable. Taking the outlet temperature data is started at 3:00 AM and lasted at 5:00 PM, this is considered to nullify the effect of unsteady result caused by warming up the setup, if the setup is not warmed well the incident radiation will be taken by the component of the SAH.

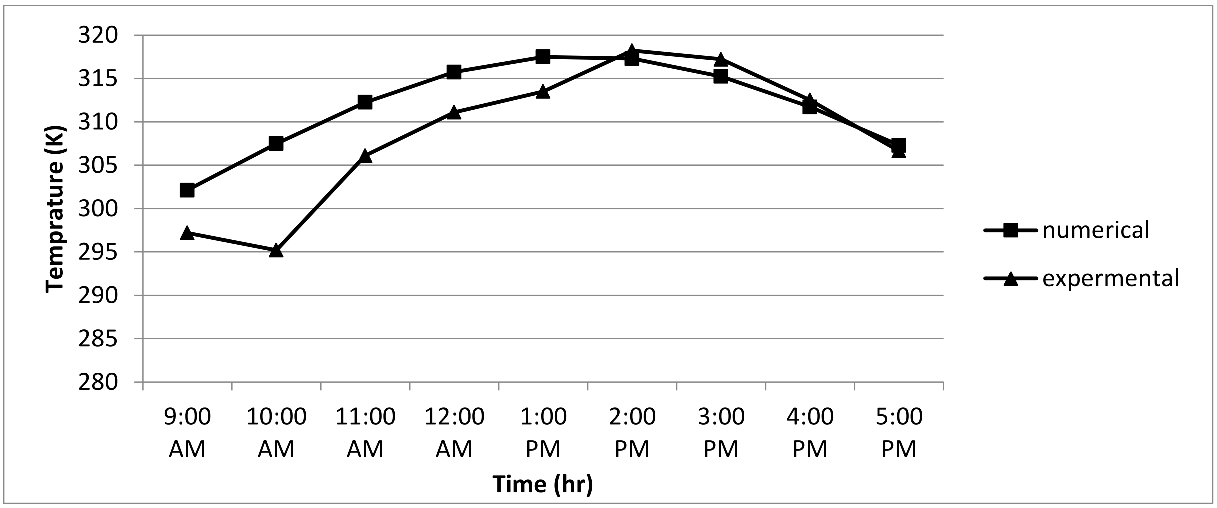

(a) Conventional SAH

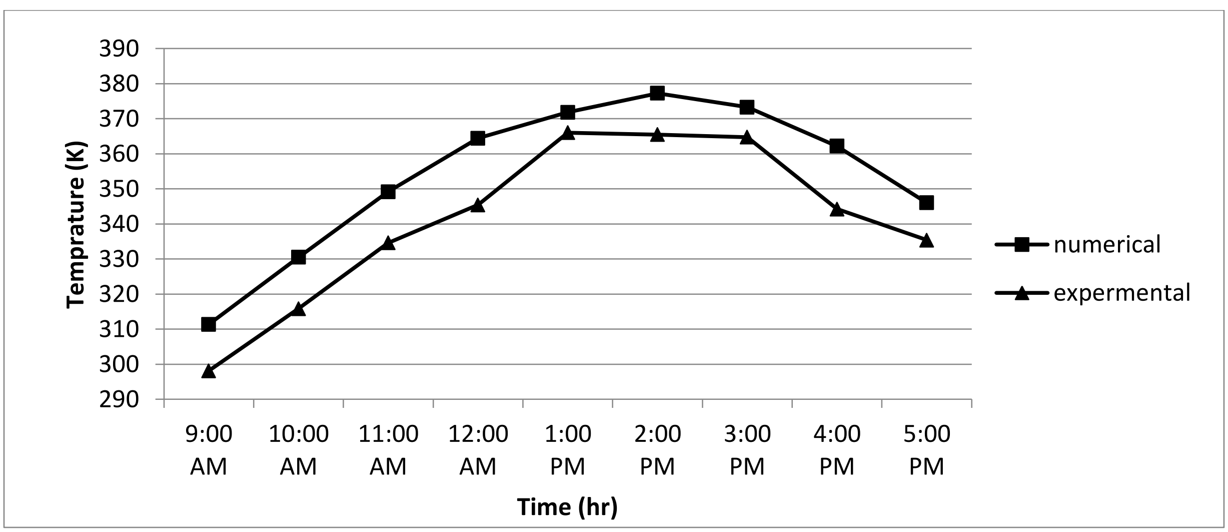

(b) Combined effect SAH

Figure 5.21: Comparisons of numerical results with experimental data

Figure 5.21, shows both the experimental and numerical results are comparable with some fluctuation on the experimental one. This may be due to the unpredicted condition of the day and some measuring errors.

5.6. Poultry farm space heating

Poultry includes all domestic birds kept for the purpose of human food production (meat and eggs) such as chickens, turkeys, ducks, geese, ostrich, guinea fowl, doves and pigeons. Poultry farming is the form of animal husbandry which raises domesticated birds such as chickens, ducks, turkeys and geese to produce meat or eggs for food. Thus poultry production is synonymous with chicken production under the present Ethiopian conditions (Solomon, 2007).

In Ethiopia chickens are the most widespread and almost every rural family owns chickens, which provide a valuable source of family protein and income (Tadelle *et al*., 1996). The total chicken population in the country is estimated to be 56.5 million with native chicken representing 96.9%, hybrid chicken 0.54% and exotic breeds 2.56% (CSA, 2014). However, the economic contribution of the sector is not still proportional to the huge chicken numbers, attributed to the presence of many productions, reproduction and infrastructural constraints (Aberra, 2000; Halima, 2007)

One and the major suggested solution to increase the production and productivity of chicken is utilization of chicken production system which is modern, market oriented and compatible with the existing situation of the farming system. Therefore, by minimizing the production constraints through use of selected and productive poultry breed as well as improvement of the production system like providing temperature controlled environment and housing it is possible to supply chicken products for the market demand over the household consumptions.

5.6.1. Brooding process

Brooding can simply defined as "Application of heat to the birds at early part of their life". Brooding is the care of young chicks by provision of optimum environment. The temperature by external heat source provided until the chicks not become able to regulate its body temperature efficiently. The temperature is most important factor during brooding. The metabolic thermoregulatory capacity of chicken develops when feathering starts at 2-3 weeks of age to replace "down". Low body temperature delays the maturation of above-mentioned three systems and makes chick more susceptible to different infections. Chicks at earlier part of life cannot efficiently regulate its body temperature because: Lose heat more quickly due to: Higher metabolic body size, Higher body temperature than adult bird and Lack of feathers.

The main objective in brooding chicks is to efficiently and economically provide a comfortable, healthy environment for growing birds. Temperature, air quality, humidity and light are critical factors to consider. Failure to provide the adequate environment during the brooding period will reduce profitability, resulting in reduced growth and development, poorer feed conversion, and increased disease, condemnation and mortality.

One of the goals during brooding is to maintain chicks within their comfort zone, which is where they are not using energy to gain or lose heat to maintain body temperature. When birds are kept in environmental temperatures above or below their comfort zone, more energy must be expended to maintain body temperature. This extra energy will ultimately be supplied by the feed consumed. Therefore, the energy from the feed will be used to maintain body temperature instead of growth and development resulting in poorer feed conversion. Thus, the environmental temperature plays a major role in determining the cost of producing a pound of meat or a started pullet.

Research has shown that chicks that are subjected to cold temperature have impaired immune and digestive systems. As a result, cold stressed chicks have reduced growth and increased susceptibility to diseases. Cold stressed chicks will exhibit higher incidence of ascites, a metabolic disorder that results in reduced performance, increased mortality and increased condemnations at the processing plant.

5.6.2. Ventilation in brooding process

Ventilation is needed to regulate temperature and remove carbon dioxide, ammonia, other gases, moisture, dust and odors. Fresh air must be introduced uniformly, mixed well with house air, and circulated properly throughout the house. Ventilation is one of the most important principles of raising broiler chickens in farms, which is the only key to reduce the respiratory problems of the bird and to reach the highest productivity and the highest conversion rate. Ventilation is an important factor that controls the productive performance of birds. Poor ventilation leads to low weight and food conversion rate, as well as respiratory diseases that increase the mortality rate, reduce the immunity of birds and make them susceptible to bacterial and viral diseases and eventually develop respiratory disease Chronic Respiratory Disease.

Effect of good ventilation on the chicks;

- No respiratory problems.
- Increase the appetite of the bird.
- Disappearance of the smell of ammonia in the house and reduce the problems of the eye.
- In the end, the efficiency of the conversion rate rises and we get high weights

5.6.3. Application of solar air heater for brooding Broiler of local poultry farm space heating

In this section the enhanced solar air heater is applied to one of local poultry farm found in Adama city. The farm brood 1000 broiler chickens and supply to the local market that can feed breed the chicken until they are ready for consumption. The farm uses 8 light bulbs of 250 W each to heat the house and control the temperature of the brooding for 24 hrs which consume large amount of electrical energy. The other major problem in this farm is the problem of ventilation. As mention the previous section ventilation is one of the crucial parameter for brooding.

In this section the solution for this major problems are designed and introduced. The electrical consumption of the light bulbs that set for heating the houses will be reduced by half by using solar air heaters in substitute of the light bulbs for day times while solving ventilation problems by introducing hot fresh air to the house. The application begins with calculating the heating load of the selected local poultry farm.

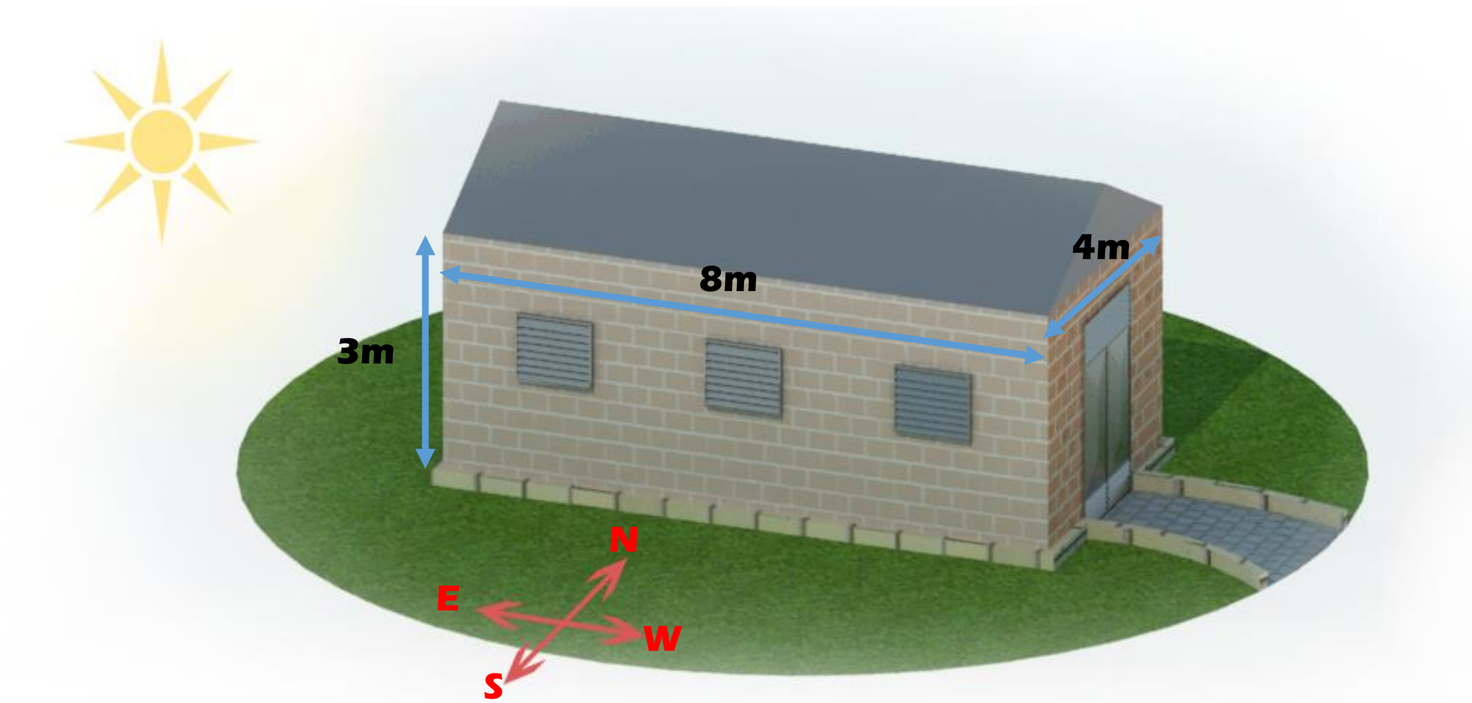

Figure 5.22: Specification of the selected poultry farm

Specification of the selected poultry farm

The type of poultry farm selected is local type and has the following specification

Table 5.2: Poultry farm specification

No.	Parameter	Description
Chicken detail		
1	Chicken types	Broiler(meat)
2	Number of chickens	1000
House Detail		
3	Location	Adama, Ethiopia
4	Orientation	South faced
5	Dimension	8mx4mx4m
6	Type of window	Perforated metal
7	Number of window	4
8	Type of door	Perforated metal
9	Number of door	1
Installations and appliance detail		
13	Lighting wattage in watt	60
14	No of lighting	4
15	Appliance	No

5.6.4. Heating load estimation of the local poultry farm

The factors that contribute to the space heating requirements are:

- Characteristics of the house, that is, transmission and ventilation heat losses (allowing for heat t recovery) and thermal capacity.
- Characteristics of the heating system, particularly the control system and the heating system's ability to respond to changes in heating requirements.
- Internal temperature, that is, the temperature level required by the users and variations in the temperature level in different parts of the house and at different times of the day.
- Internal heat gains other than from the heating system, which is, from occupants, cooking and hot water, lighting and electrical appliances.
- Solar gains.
- External weather conditions, principally temperature.

$q_h + q_i + q_s = H(T_i - T_o)$…………………………………………………………………(5.78)

Where, $H = \left(\sum AU + C_p\dot{V}\right)$ q_h output from heating system q_i internal heat gains q_s solar gains AU transmission heat loss per degree $C_p\dot{V}$ ventilation heat loss per degree T_i interna1 temperature T_o external temperature and although all the terms vary with time, the equation may be applied to mean values over 24-hour period. The mean daily output required from the heating system to achieve a mean internal temperature, T_i is

$q_h = H(T_i - {(q_i + q_s)}/{H} - T_o)$…………………………………………………………..…(5.79)

This can be reduced as:

$Q_h = H(T_b - T_o)$…………………………………………………………………………...…(5.80)

Where, $T_b = T_i - {(q_i + q_s)}/{H}$ it's called base temperature. To obtain the space heating requirement, this equation is integrated over the period under consideration. In this integral, there are two cases to consider:

Case: 1 $T_b > T_o$

In this case the internal and solar gains are insufficient to attain the required internal temperature T. and heating is required.

Case: 1 $T_b < T_o$

In this case the internal and solar gains exceed the heat losses. In practice either T. or the ventilation part of H must increase, since Equation 1 must always be satisfied; but n6 output is required by the heating system. Thus the integral may be obtained by a summation of (Tb - To) over days for which case (I) applies, with nothing included for other days when case (II) applies. The integral is the accumulated temperature difference, ATD[T_b]. The heating requirement is, therefore:

$Q_h = \int q_h dt = H \times ATD[T_b]$………………………………………………………….….(5.81)

The principal factor causing variations in T_b is the solar gain term, q_s. Separate values of q_s, and therefore T_b, can be obtained for each month, and Equation 5.81 used with ATD[T_b] as the accumulated temperature difference for that month. Summation of Q_h for each month then gives the annual heating requirement.

Transmission loss

Transmission loss q_{tran}, (W), is the sum of heat losses from the conditioned space through the external walls, roof, ceiling, floor, and glass. In the case of this poultry farm house, because light is not allowed to enter through the window to control the light requirement of the brooding process the transmission thought window is ignored.

Roofs and walls

For winter: In winter the heat loss is simple transmission based on the inside and outside temperature, and U-value of composite structure;

$$q_{tr-winter} = UA(T_i - T_o) \quad (5.82)$$

For summer: In summer the solar radiation affects the outside surface of wall and roof. The absorbed radiation increases the temperature of the outside surface to a value that is greater than outside air temperature. This outside surface temperature is called Sol-air temperature. It depends on the properties of wall and roof structure, outside surface material and color, and solar radiation intensity component perpendicular to the outside surface. The solar radiation amount depends on the orientation of the surface, solar altitude angle, and solar azimuth angle. An approximate equation for the sol-air temperature (T_s) of the outside surface of a given wall or roof is:

$$T_s = T_o + \frac{\alpha(I_d + I_s)}{H_{so}} \quad (5.83)$$

$$q_{tr-sum} = UA(T_i - T_s) \quad (5.84)$$

Ventilation heat loss

As soon as the volume flow rate of ventilation, (m^3/hr), is determined, the sensible heat loss from Ventilation Q_{vent}, W, can be calculated as:

$$q_{vent} = \dot{V}\rho_a C_{pa}(T_i - T_o) \quad (5.85)$$

Where, ρ_a density of outdoor air, (kg/m^3).

Internal heat gains

In the case of the farm considered the only internal heat gain comes from the lighting used to give light for the brooding broilers. The Heat Gain from Lighting can be expressed as:

$$q_{light} = WF_{ul}F_{sa} \qquad (5.86)$$

Where, q_l is heat gain, W is total light wattage F_{ul} is lighting use factor F_{sa} is lighting special allowance factor.

5.6.5. Solar space heating system

The main aim of this section is to introduce and implement the new solar air heating system to the selected poultry farm. The proposed solar air heating system will reduce the expense of electrical energy used to heat the house during the day times. More than reducing the cost of electric power consumed it reduces the mortality rate of the chickens due to lack of fresh air introduced to the space.

Description of components of solar space heating system

- Enhanced solar air heater: The enhanced solar collector is used to heat the ambient air that supplied to the conditioned space
- Solar powered fan: solar powered fan is used to suck air through the solar heater while forcing to the conditioned space.
- Fabric duct air distribution system: special fabric duct with openings is used to evenly distribute the heated air though out the house.
- Thermostat: the thermostat is a component that used to detect the temperature of the house and maintain the desired temperature by starting and cutting off the fan.
- Auxiliary heating system: the auxiliary heating system is used to supply heat energy at the time when the sun is down.

The working principle of the proposed solar space heating system

The proposed solar space heating heats the ambient air and deliver the compartment to heat the space and create favorable environment for brooding chickens. This process begins when the thermostat detects and response the temperature of the house is below the desired temperature. The response of the thermostat triggers the fan motor that supplies hot air to the house. The fan inlet is attached to the solar air heater outlet though insulated pipe and the outlet of the fan is fixed to the opening the wall of the house. When the fan starts to suck the air, its flows though the heated surface of the solar air heater and get heated and then the heated air is distributed by the fabric duct that is attached to the out let of the fan and extended until the opposite wall. Since the opposite side of the duct is closed, the forced air through the duct will blow out the duct through the opening provided along the length of the fabric duct. The holes are arranged in a way that allows the air to be distributed evenly throughout the compartment. The supply of the heated air will raise the temperature of the room and the temperature of the room will attain the desired brooding temperature. At the time the temperature drops the thermostat will start the fan and the fan supply hot air to maintain the desired temperature. During night time, rainy days and cloudy days the auxiliary heating system will take the part of the solar space heating system.

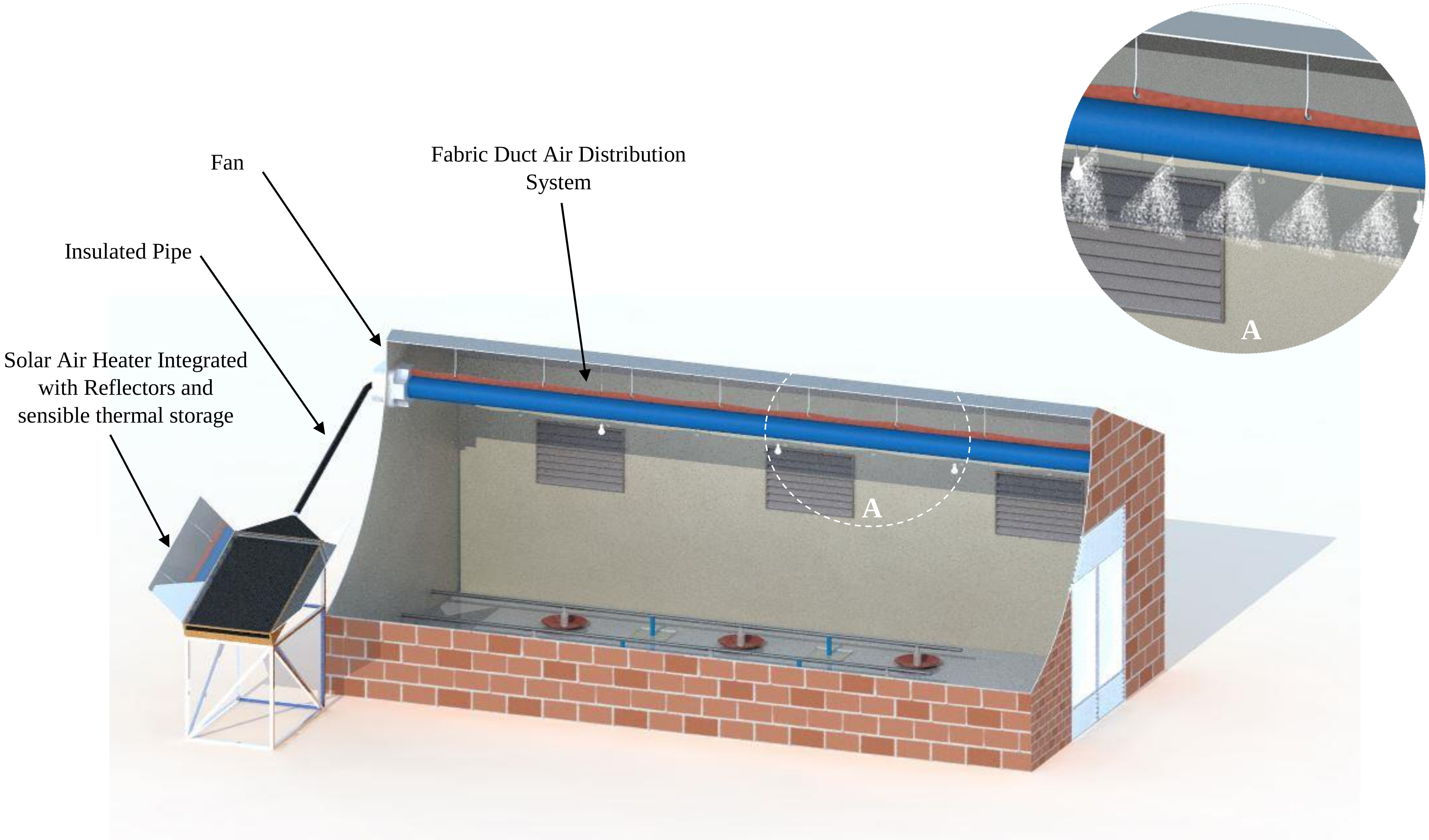

Figure 5.23: Proposed poultry farm solar space heating design

5.6.6. Performance result of enhanced solar air heater for poultry farm space heating

The flow rate of the solar air heater is determined from the ventilation rate recommended for the poultry farm which is listed in Appendix C. From this data the output temperature of the fluid from enhanced solar air heater is provided as follows on Figure 5.24 at different flow rate.

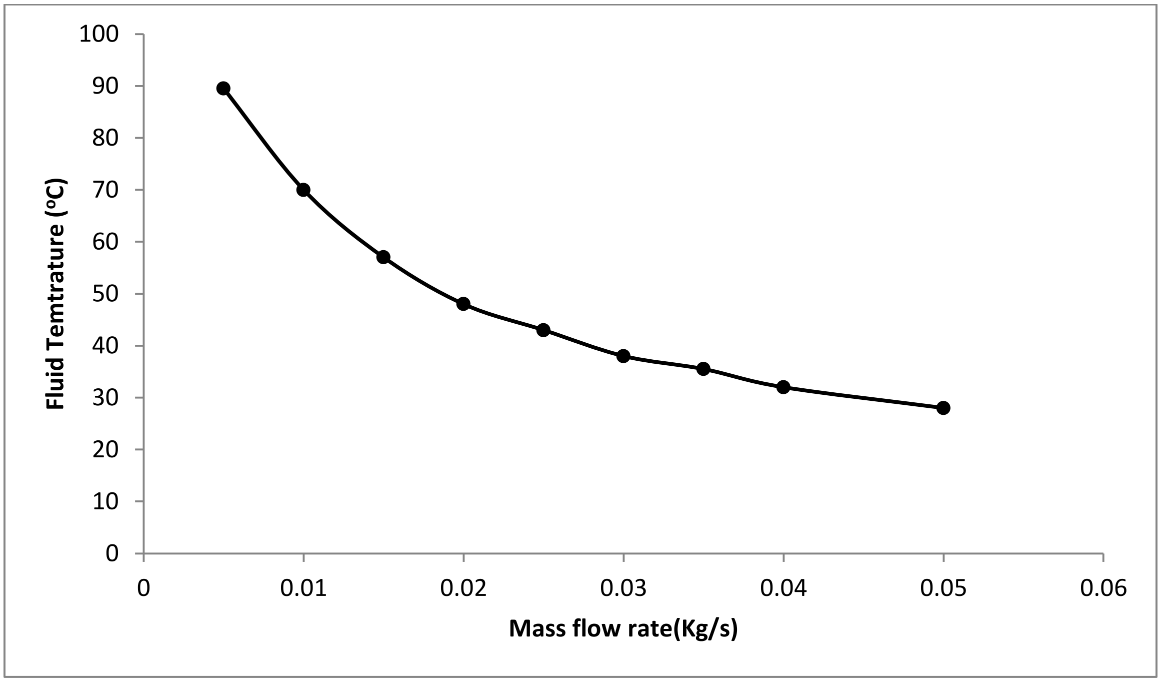

Figure 5.24: Enhanced solar air heater Fluid temperature verse mass flow rate

The annual heating load needed for the selected poultry farm is estimated as shown on the Figure 5.25. The peak heating load appears in the summer seasons whereas the minimum heating load is appeared in winter season.

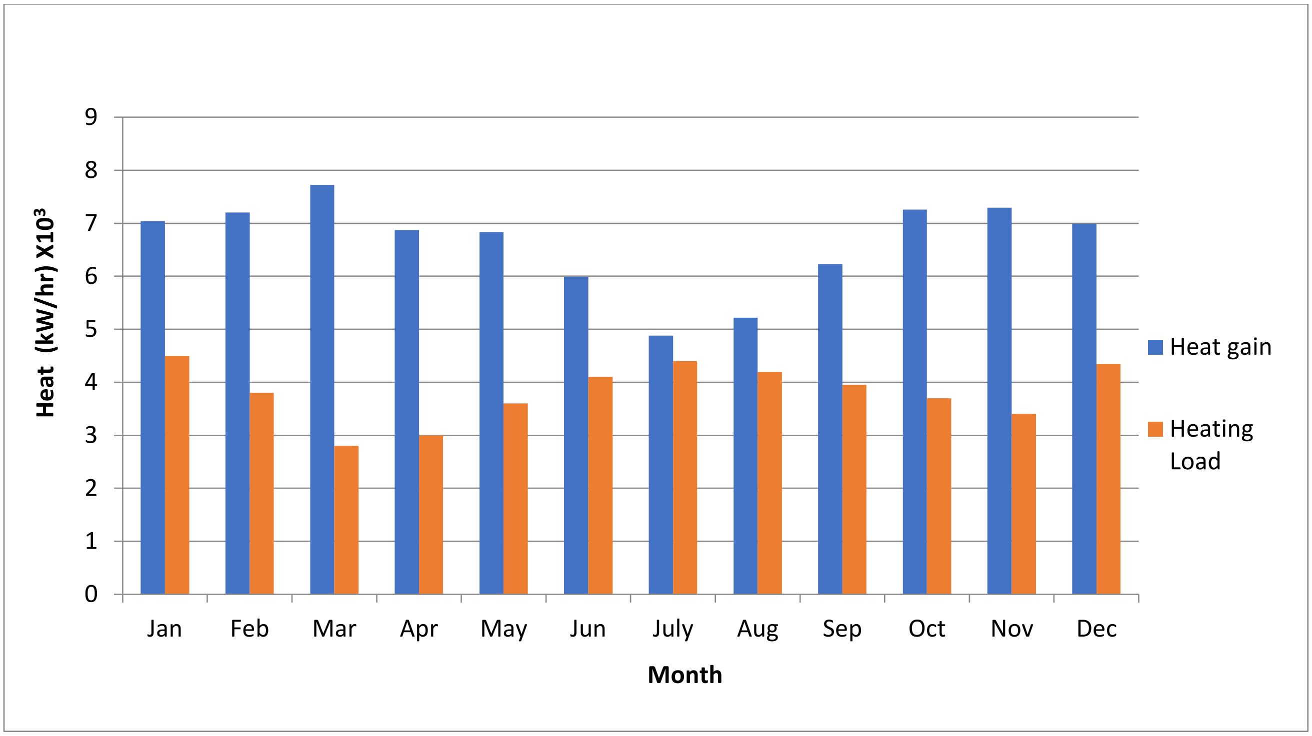

Figure 5.25: Poultry farm heating load and Enhanced Solar air heater heat gain

The maximum ventilation rate required for the brooding is 0.5 kg/s and maximum heating load of 4532 kW/hr. to meet the ventilation requirement 5 units of enhanced solar air heater has to be employed. The annual heating load and useful energy harvested from the solar air heater at the required mass flow rate is shown. As shown on the Figure 5.25 the designed solar air heater meets the heating load demand for the poultry farm throughout the year. Therefore, this enhanced solar air heater can be used as space heating and ventilation system by substituting the electric heating of the poultry farm for brooding of chickens.

CHAPTER 6: CONCLUSION AND RECOMMENDATION

6.1. Conclusion

In this study the numerical and experimental performance investigation of enhanced solar air heater integrated with finned absorber, sensible thermal storage and reflector has been carried out. A mathematical model is developed for both conventional and enhanced solar air heater, and the numerical results were validated by an experiment conducted on each solar air heater. The response of the system has been investigated by varying enhancement techniques to the system.

From the results, it can be clearly dictated that the integration of finned absorber increases heat transfer surface area of the absorber plate which increase the outlet temperature of the fluid. Therefore the efficiency of the solar air heater elevated. The numerical and experimental average efficiency is found to be 40.3 and 38 % for conventional, 42 and 40.2 % for finned absorber plate, respectively. Whereas, the pressure drop across the finned absorber solar air increase relative to the convectional solar air heater.

The second type of the solar air heater configuration is solar air heater integrated with gypsum sensible thermal storage. The result shows that the solar air heater with gypsum thermal storage increase the efficiency of the system compared to the convectional type by increasing the working time. The time extension and low thermal conductivity properly of the gypsum improve the system average efficiency. The third type is solar collector integrated with top, left and right side reflector. The integration of reflector increases the amount of radiation fall on the collector by a factor of 2-3 compared to the convectional type. However, it is clear that from the result, integrating reflector only does not increase the efficiency of the system significantly since the radiation loss of the absorber plate increase due to high temperature of plate is achieved because of concentrated radiation.

Moreover, as can be understood from the effect of enhancement techniques and their result, the combination of these will reduce the drawbacks and gives the significant performance enhancement. The study shows that the highest average efficiency is achieved by combined enhanced solar air heater which is 68 and 71.3 % for experimental and numerical one, with optimum mass flow rate of 0.003 kg/s. respectively. This is because of the combined effect of increase in heat transfer area; storage and heat lose reduction effect of the gypsum storage and increase in the amount of radiation fall on the absorber due to the integration of reflectors.

The root mean square error between the experimental data and numerical predicted data is analyses and for all analysis conducted the maximum error is found to be $\pm$9.6 ^{o}C. This value implies that the error between the mean of the experimental solar air heater outlet air temperature and the mean of the simulated solar air heater outlet air temperature indicates a good quality but with some visible loss due to the loss of sun-collector alignment because of the manual tracking and measurement error.

Lastly, the application of solar air heaters in drying injera, Tomato and banana is investigated experimentally whereas enhanced solar air heater is implemented to local poultry farm located at Adama City. From the experiment conducted in drying the products, the dryer integrated with enhanced solar air heater gives higher drying efficiency in all three products. In addition to this the demand of space heating and ventilation is accomplished by employing five arrays of enhanced solar air heaters for the poultry farm selected.

6.2. Recommendations

Using solar air heaters for drying products and space heating application is better alternative rather than using electricity and other convectional energy sources. The system allows the adaptation for the application of dryer and space heating. Farmers and poultry farms can apply this enhanced solar air heater as dryer and space heating, respectively. However for the case of space heating application the integration of auxiliary energy source has to be employed to compensate energy demand during cloudy days and low solar radiation. In addition, to get efficient enhancement the reflectors has to be adjusted according to the sun position. Therefore its recommended to manipulate the angle of reflectors according the scaled points on manual tracking system to work the manipulation of the reflectors.

6.3. Future work

- The numerical analysis in this thesis is entirety done on the base of one dimensional heat transfer. A two dimensional study can set as a future work to go.
- Variable plate and glass temperature profile can be used through the air heater collector as a future work to get a better accuracy.

- Transient analysis can be developed as a future work of study.
- Manual tracking is used in this work with a little loss of sun- collector alignment. One can use an automatic tracking system to get better accurate experimental results.

REFERENCES

Abera, M. (2000). Comparative studies on performance and physiological responses of Ethiopian indigenous (Angete Melata) chickens and their f1 crosses to long term heat exposure. PhD dissertation, Martin-Luther University, Germany.

Aboul, E., Sebaii,E., Ramadan, M. and Gohary E.(2000).Parametric study of a solar air heater with and without thermal storage for solar drying applications. *Renewable Energy*, 21(3-4): 505 -522.

Adzimah, K.S, and Seckley, E. (2009). Improvement on the Design of a Solar Cabinet Drier. *American Journal of Engineering and Applied Science,* 2(1): 217-288.

Alta. D., Bilgili, E., Ertekin, C. and Yaldiz, O. (2010). Experimental investigation of three different solar air heaters: energy and exergy analyses. *Applied Energy*87:2953–73.

Alvarez, G., Lira, C., Arce, J. and Heras, M. Thermal performance of an air solar collector with an absorber plate made of recyclable aluminum cans. *Solar Energy*, 77(1):107-113.

Aman, D. (1986).Collector, collector-reflector systems an analytical and practical study. *International Journal of Engineering and Technical Research,*26(1):33-39.

Amma, A. (2014). Effect of different drying methods on the functional and physicochemical properties of the flour of selected yam cultivators in Ghana. *Kwame Nkrumah University of Science and Technology*, Kumasi Ghana.

Baccoli, R.,Mastino1, C.,Innamorati R., Serra, L.,Curreli, S.,Ghiani, E.,Ricciu, R. and M. Marini.(2015). A mathematical model of a solar collector augmented by a flat plate above reflector: Optimum inclination of collector and reflector. *Energy Procedia*,81: 205 – 214.

Balcomb, J. D.(1992).Passive Solar Buildings. Massachusetts Institute of Technology. ISBN, **1**:34-73.

Billy, A. (2010). Effect of absorber plate material on flat plate collector efficiency, University of Malaysia Pahang.

Bolaji, B. (2005). Performance evaluation of a simple solar dryer. *Annual Engineering Conference Proceedings*, 6(1) :8-13.

Bolaji, B. (2005). Performance Evaluation of a Simple Solar Dryer.*6th Annual Engineering Conference Proceedings*, FUT Minna.8-13.

Bukola, O. and Ayoola P. (2008). Performance Evaluation of a Mixed-mode Solar Dryer. Technical Report, *AU J.T*, **11**(4):225-231.

Caouris, Y. (2011). Solar thermal systems: components and applications. *Comprehensive Renewable Energy*,2.

Daniels, D., Lowndes, D., Mathew,H., Reynolds,J. and R.Gray (1975).Enhanced solar energy collection using reflector-solar thermal collector combinations. *International Journal of Engineering and Technical Research,*17(5): 277-283.

Deepak, k. And Prasanta, K. Reducing postharvest losses during storage of grain crops to strengthen food security in developing countries.*US National Library of Medicine National Institutes of Health*6(1): 9-15.

Drew, F. (2011). Development and Evaluation of a Natural Convection Solar Dryer for Mango in Rural Haitian Communities. *Agricultural and Biological Engineering, University of Florida*.

Drew, F. S. (2011). Development and Evaluation of a Natural Convection Solar Dryer for Mango in Rural Haitian Communities. (Unpublished) M.Sc. Thesis, Agricultural and Biological Engineering, University of Florida.

Ekechukwu, O. and Norton, B. (1999). Review of solar-energy drying systems II, *An overview of solar drying technology*, **40**:615–655.

Eze, J. and Agbo, K. (2011).Comparative studies of sun and solar drying of peeled and unpeeled ginger. *American Journal of Scientific and Industrial Research*, 2(2): 136-143.

Fikre, A. (2000). Base line data on chicken population, productivity, husbandry, feeding and constraints. Ambo, Ethiopia.

Forson, F., Nazha, A., Akuffo, F. and Rajakaruna, H. (2007). Design of Mixed mode Natural Convection Solar Crop Dryers: Application of Principles and rule of thumb. *Renewable Energy,* **32**: 1-14.

Garg, H. and Sharma, V. (1984). Performance of integrated rock bed solar air heater, *science direct*.**3**:15–20.

Garg, H., Mullick, A. and Bhargava, K. (2019).Solar thermal energy storage, *Spring Nature* ,2(19):82-153.

Getu, H. (2018). Seasonal solar thermal energy storage, Thermal Energy Battery with Nano-enhanced PCM.*Mohsen Sheikholeslami Kandelousi*.

Gizem, M. (2012).An experimental study on enhancement of heat transfer in a solar air heater collector by using porous medium.

Hagge, J. and Junkhan,G. (1975).Experimental study of a method of mechanical augmentation of convective heat transfer in air, Tech. Rep. HTL3, ISU-ERI-Ames-74158 Iowa State University, Amsterdam, Netherlands.

Halima, HM. (2007). Phonotypic and genetic characterization of indigenous chicken populations in Northwest Ethiopia.

Hans, H. and Lucie, P. (2018). The benefits and risks of solar-powered irrigation - a global overview. *Food and Agriculture Organization of the United Nations*.

Hazem, E. and Tayler, A. (2011). Evaluation of renewable energy alternatives for high way maintenance facility.The Ohio Department of Transportation, Office of State wide Planning and Research.

Himanshu, T., Avinash, K. and Satvasheel, P. (2018).*Application of solar energy*. Satvasheel power editor.

https://www.livestocking.net/standard-broiler-feed-chart-growth-weight
http://www.scielo.br/scielo.php?script=sci_arttext&pid=S1516-635X2013000100002

Indrajit, A., Bansal, N. and Garg, H. (1985). An experimental study on a finned type and nonporous type solar air heater with a solar simulator. *Energy Conversion and Management* 25(2):135–8.

Ioan, S. and Calin, S. (2018).A comprehensive review of thermal energy storage.*Sustainability*,10(1).

Jain, D and Jain, R (2004). Performance evaluation of an inclined multi-pass solar air heater with in-built thermal storage on deep-bed drying application. *Journal of Food Engineering*,65:497 -509.

Kabeel, A. and Mearik, K. (1998). Shape optimization for absorber plates of solar air collectors, *Renewable Energy*,13(1):121-131.

Kalogirou, A. (2004). Solar thermal collectors and applications. Progress in Energy and Combustion Science 30(1): 231–295.

Leon, A. M., Kumar, S. and Bhattachaya, S.C. (2002). A Comprehensive Procedure for Performance Evaluation of Solar Food Dryers, *Renewable and Sustainable Energy Reviews*. 6:367-393.

Maheshwari, B., Rajendra, K. and Gharai, s. (2011). Performance study of solar air heater having absorber plate with half-perforated baffles. *International Scholarly Research Notices*, 1(13).

Misha, S., Mat, S., Ruslan, M.H., Sopian, K. and Salleh, E. (2013). Review on the application of tray dryer system for agricultural products. *World Applied Science Journal*, 22 (3): 424-433.

Mohanraj, M. and Chandrasekar, P. (2009). Performance of a solar drier with and without heat storage material for copra drying. Global Energy Issues, 31(2): 305 – 314.

Mohanraj, M. and Chandrasekar, P. (2009). Performance of Forced Convection Solar Drier Integrated with Gravel as Heat Storage material for Chilli Drying. *Journal of Engineering Science and technology*, 4 (3):305-314.

Naphon, P. (2005).On the performance and entropy generation on double pass solar air heater with Fins. *Renew Energy*,30:1345-57.

Naphon, P. and Kongtragool, B. (2003).Theoretical study on heat transfer characteristics and performance of the flat-plate solar air heaters, *International Communications in Heat and Mass Transfer*, 30(8): 1125-1136.

Neelkanth, G., Bhavish, G., Sheeraz, R. and Jigyasa, M. (2010). Solar air heater. *Journal of Engineering Research and Applications*, 6(5): 48-51.

Nigussie, M. and Teklay, T. (2017). Improving efficiency of flat plate collector integrated with reflectors. *International Journal of Engineering and Technical Research*, 7(2): 2454-4698.

Pawar,R., Takwale, M. and Bhinde, V. (1994). Evaluation of the performance of the solar air heater. *Energy Conversion and Management*;35(8):699–708.

Pradhapraj, M., Velmurugan, V. and Sivarathinamoorthy, H. (2010). Review on porous and nonporous flat plate air collector with mirror enclosure, *International Journal of Engineering Science and Technology*, **2**(9): 4013-4019.

Prashant, S., Dhiraj, V. and Satvasheel, P. (2018). Review on Integration of Solar Air Heaters with Thermal Energy Storage. *Indian Institute of Technology*, 2(4): 978-981.

Rajkumar, P. (2007). Comparative performance of solar cabinet, vacuum assisted solar and open sun drying methods. *Journal of energy*, 1(21).

Ramadhani, B., Rwaichi, J. and Karoli, N. (2014). Effect of Glass Thickness on Performance of Flat Plate Solar Collectors for Fruits Drying. *Journal of Energy*, 2: 17-88.

Ramadhani, B., Rwaichi, J. and Karoli, N. (2014).Effect of glass thickness on performance of flat plate solar collectors for fruits drying. *Journal of energy*, 1(8).

Ravish, K. and Ajeet, K. (2017).A review on solar air heater technology. *International Journal of Mechanical Engineering and Technology*, 8(7):1122–1131.

Sean, A. (2013). Construction and Performance Testing of a Solar Food Dryer for Use in Developing Countries. *All Theses and Dissertations.* Brigham Young University, Provo.

Sengar, S., Mohod, A.G. and Khandetod, Y. (2012). Experimental Evaluation of Solar Dryer for Kokam Fruit. *Global Journal of Science Frontier Research Agriculture and Biology*. 12(3): 83-89.

Shyam, K., Balaji, N. and Mahesh, B. (2016). Experimental analysis of heat transfer and losses in solar absorber plate. *IJSART,* 2(5): 2395-1052.

Siddique, M., Khaled, R., Abdulhafiz, N. and Boukhary, A. (2010). Recent advances in heat transfer enhancements: a review report. International Journal of Chemical Engineering,1(28).

Sreekumar, A. (2010). Techno-economic analysis of a roof-integrated solar air heating system for drying fruit and vegetables. *Energy Conversion and Managemen*t ,51:2230–8.

Thakar, M. and Prajapati, D. (2020). Performance evaluation of solar air collector in sensible heat storage by forced convection with cherry powder. *International Journal of Current Engineering and Technology,* 1(1): 2347 – 5161.

Tonui K.S., Mutai, E., Mutuli, D., Mbuge O. and Too K. (2014).Design and Evaluation of Solar Grain Dryer with a Back-up Heater. *Research Journal of Applied Science, Engineering and Technology*.**7** (15): 3036-3043.

Tyagi, V., Panwar, N., Rahim, N. and Richa, K. (2012). Review on solar air heating system with and without thermal energy storage system. *Renewable and Sustainable Energy Reviews* 16:2289–2303.

Vivek, S., Ajay, S. and Ashish, V. (2017).A Review on experimental analysis of double pass solar air heater with baffled absorber plate. *International Journal of Trend in Scientific Research and Development*, 1(6):2456-6470.

Wazed, M,,Nukman, Y. and Islam, M. (2010). Design and fabrication of a cost effective solar air heater for bangladesh. *Applied Energy,* 87(6): 6–3030.

Womac, A., Tompkins, F. and Busk, K. (1985). Evaluation of solar air heaters for crop drying. *Energy Agricultural* 4:147–57.

Zhao, D., Li, Y., Dai, Y. and Wang, R.(2011).Optimal study of a solar air heating system with pebble bed energy storage. *Energy Conversion and Management*. 52(6):2392–400.

APPENDIX

ANNEX A: Initial and final moisture contents and maximum allowable drying temperatures (Brooker et al., 1974)

Crop		Moisture Content		Maximum Allowable Temperature (^{o}C)
		Initial (% wet basis)	Final(% wet basis) safe storage	
Grain	Paddy, raw	22-24	11	50
	Paddy	30-35	13	50
	Parboiled	35	15	60
	Maize	20	16	45
	Wheat	24	14	50
	Corn	24	11	50
	Rice	20-22	9-10	40-60
	Pulses	20-22	7-9	40-60
	Oil seeds	80	5	65
Vegetables	Green peas	80	6	65
	cauliflower	70	5	65
	Carrots	70	5	75
	Green beans	80	4	75
	Onion	80	4	55
	Garlic	80	4	55
	Cabbage	75	7	55
	Sweet potato	75	13	75
	Potatoes	80	5	75
	Chilies	80	24	65
Fruit	Apple	85	18	65
	Apricot	80	15-20	70
	Grapes	80	15	70
	Bananas	80	7	65
	Guavas	80	20	65
	Okra	80	10	65
	Pineapple	96	10	60
	Tomatoes	95	6	60

ANNEX B: Broiler Weight Per Week (https://www.livestocking.net/standard-broiler-feed-chart-growth-weight)

Age	Male in Kg	Female in Kg
1st Week	0.175	0.171
2nd Week	0.443	0.414
3rd week	0.886	0.779
4th week	1.421	1.246
5th week	2.062	1.775

ANNEX C: Ventilation rate for brooding

(http://www.scielo.br/scielo.php?script=sci_arttext&pid=S1516-635X2013000100002)

Age	Ventilation Rate m^3/Kgh	Temp. ^oC
1st Week	0.5	45
2nd Week	1.0	40
3rd week	1.2	35
4th week	1.8	30
5th week	2.5	25

ANNEX D: Common Sensible thermal storage Materials
(https://www.engineeringtoolbox.com/sensible-heat-storage-d_1217.html)

Material	Density ρ (kg/m3)	Thermal Conductivity	Specific Heat cp (J/kgoC)
Aluminum	2700	36	0.87
Brick	1969	0.47	0.9
Concrete	2305	1.7	0.75
Fireclay	2200	1.4	0.89
Granite	2400	3	0.79
Gypsum	1602	0.17	1.09

ANNEX E: Side Reflectors Inclination Angle Variation

For n_L=0.5 and n_R=0.5

Month		**8:00A.M**	**3:00A.M**	**4:00A.M**	**5:00A.M**	**12:00P.M**	**1:00P.M**	**2:00P.M**	**3:00P.M**	**4:00P.M**
January	λ_L	86.8	78.2	70.3	64.1	61.5	25.2	19.0	11.2	2.6
	λ_R	2.6	11.2	19.0	25.2	27.8	64.1	70.3	78.2	86.8
February	λ_L	85.9	76.7	68.1	60.8	57.4	28.6	21.3	12.6	3.4
	λ_R	3.4	12.6	21.3	28.6	31.9	60.8	68.1	76.7	85.9
March	λ_L	85.4	75.9	66.7	58.6	54.4	30.8	22.6	13.4	3.9
	λ_R	3.9	13.4	22.6	30.8	34.9	58.6	66.7	75.9	85.4
April	λ_L	85.7	76.4	67.6	60.0	56.4	29.3	21.7	12.9	3.6
	λ_R	3.6	12.9	21.7	29.3	32.9	60.0	67.6	76.4	85.7
May	λ_L	86.6	77.8	69.8	63.3	60.6	26.0	19.5	11.5	2.8
	λ_R	2.8	11.5	19.5	26.0	28.7	63.3	69.8	77.8	86.6
June	λ_L	87.1	78.7	71.1	65.3	62.9	24.1	18.2	10.6	2.2
	λ_R	2.2	10.6	18.2	24.1	26.5	65.3	71.1	78.7	87.1
July	λ_L	86.8	78.2	70.4	64.2	61.7	25.1	18.9	11.1	2.5
	λ_R	2.5	11.1	18.9	25.1	27.7	64.2	70.4	78.2	86.8
August	λ_L	85.9	76.8	68.2	60.9	57.6	28.4	21.2	12.5	3.4
	λ_R	3.4	12.5	21.2	28.4	31.7	60.9	68.2	76.8	85.9
September	λ_L	85.4	75.9	66.7	58.5	54.4	30.8	22.6	13.4	3.9
	λ_R	3.9	13.4	22.6	30.8	35.0	58.5	66.7	75.9	85.4
October	λ_L	85.7	76.5	67.6	60.0	56.5	29.3	21.7	12.9	3.6
	λ_R	3.6	12.9	21.7	29.3	32.8	60.0	67.6	76.5	85.7
November	λ_L	86.6	77.9	69.9	63.5	60.8	25.8	19.4	11.4	2.7
	λ_R	2.7	11.4	19.4	25.8	28.5	63.5	69.9	77.9	86.6
December	λ_L	87.1	78.7	71.1	65.3	62.9	24.1	18.2	10.6	2.2
	λ_R	2.2	10.6	18.2	24.1	26.5	65.3	71.1	78.7	87.1

ANNEX F: Top Reflector Inclination Angle Variation

For n_T=0.5 at noon time

Month	Monthly Optimum Inclination Angle of Top reflector
January	-5.5
February	-9.6
March	-12.6
April	-10.6
May	-6.4
June	-4.1
July	-5.4
August	-9.4
September	-12.6
November	-10.5
October	-6.2
December	-4.1

ANNEX G: Python programing code for numerical analysis of solar air heater

```
# -*- coding: utf-8 -*-

"""

Created on Fri Feb 07 15:30:36 2020

This code is developed to solve the radiation data analysis for each day and months of the year, that feed to the next codes on the solar dryer analysis. The row data for the sunshine, temperature and wind speed is taken from the National Metrology Agency, Adama branch of Ethiopia.

@author: Yisak Tola

"""

from scipy import *

from numpy import *

from pylab import *

from CoolProp.HumidAirProp import HAPropsSI

import CoolProp as CP

import matplotlib.pyplot as plt

from mpl_toolkits.axes_grid1 import host_subplot

import matplotlib.pyplot as plt

a = 8.5263#latitude of Adama

Isc = 1367# solar constant

A=array([[0.0]*(12)]*(12))

A[0][:] = [17 ,47 ,75 ,105 ,135 ,162 ,198 ,228 ,258 ,288 ,318 ,344]
           #representative day of each months
```

```
A[1][:] = 23.45*sin((360*(284+A[0][:])/365)*pi/180)#declination angle

A[2][:] = [10.0, 9.567, 10.533 ,8.8 ,8.8667 ,7.533 ,5.566 ,6.0 ,7.5
,9.666 ,10.633 ,10.2667]              #sun shine hours

A[3][:]= np.arccos(-tan(a*pi/180)*tan((A[1][:])*pi/180))*180/pi#sunset
hour angle

A[4][:] = 2*A[3][:]/15          # number of daylight hours

A[5][:] = -0.110 + 0.235*cos(a*pi/180) +
0.323*(np.divide(A[2][:],A[4][:]))#regression parameter

A[6][:] = 1.449 - 0.533*cos(a*pi/180) -
0.694*(np.divide(A[2][:],A[4][:]))#regression parameter

A[7][:] = 0.409 + 0.5016*sin((A[3][:] - 60)*pi/180)#regression
parameter

A[8][:] = 0.6609 - 0.4767*sin((A[3][:] - 60)*pi/180)#regression
paramete

ho1 = 1 + 0.033*cos((360*A[0][:]/365)*pi/180)

ho21 =cos(a*pi/180)*cos(A[1][:]*pi/180)

ho22 = sin(A[3][:]*pi/180)

ho2 =  np.multiply(ho21,ho22)

ho31 = sin(a*pi/180)*(pi*A[3][:]/180)

ho32 = sin(A[1][:]*pi/180)

ho3 = np.multiply(ho31,ho32)

A[9][:] = np.multiply((24*3600*(Isc/pi)*ho1),(ho2 +
ho3))/3600000#daily extraterresterial radiation on a horizontal
surface
```

```
A[10][:] = np.multiply(A[9][:],(A[5][:]
+np.multiply(A[6][:],(np.divide(A[2][:],A[4][:])))))#mont

A[11][:] = np.multiply(A[10][:],(0.931 -
0.814*(np.divide(A[2][:],A[4][:]))))# monthly

x = array([[0.0]*24]*12)

y = array([[0.0]*24]*12)

w =array([0.0]*24)

for t in range (1,25):

    if t == 1:

        w[t-1] = -180

    else:

        w[t-1]=w[t-2]+15

for i in range (1,13):

##Monthly average hourly global radiation on a horizontal surface

    for j in range (1,25):


         I =A[10][i-1]* pi/24*(A[7][i-1] + A[8][i-1]*cos(w[j-
1]*pi/180))*(cos(w[j-1]*pi/180) - cos(A[3][i-1]*pi/180))/(sin(A[3][i-
1]*pi/180) - pi/180*A[3][i-1]*cos(A[3][i-1]*pi/180));

         if I > 0:

             x[i-1][j-1] = I

##Monthly average hourly diffuse radiation on a horizontal surface

         else:
```

```
            x[i-1][j-1] = 0

    for j in range(1,24):

        Id =(A[11][i-1]* (pi)/24)*(cos(w[j-1]*pi/180) - cos(A[3][i-1]*pi/180))/(sin(A[3][i-1]*pi/180) - pi/180*A[3][i-1]*cos(A[3][i-1]*pi/180));

        if Id>0:

            y[i-1][j-1] = Id;



        else:

            y[i-1][j-1] = 0;

z = x-y   #Monthly average beam radiation on a horizontal surface

##Hourly temperature variation analysis

Tmax = array([26.6, 29.37, 29.667, 29.03, 31.663, 31.233, 26.966, 27.566, 28.3, 29.166, 27.0, 27.1])          # Maximum temperature of the day

Tmin = array([14.433, 15.6, 16.4667, 17.633, 17.566, 19.2, 17.133, 17.866, 16.666, 15.9, 15.133, 12.333])      # Minimum temperature of the day

def hourly_temp(t):

    T = Tmax - ((Tmax-Tmin)/2)*(1 - sin((pi*t-9*pi)/12))

    return T

T = array([[0.0]*(12)]*24)

for i in range (1,25):

    T[i-1][:] = hourly_temp(i)
```

```
T = np.transpose(T)

T = 273.14 + T

## Atmospheric temperature for March, 16 @Tmax = 29.7 and @Tmin =
16.466

## Solar radiation on an inclined surface

B=array([[0.0]*24]*12)

b = 23     #Inclination angle

p = 0.2    #Ground reflectivity

for i in range (1,13):

    for j in range (1,25):

         teta = cos(A[1][i-1]*pi/180)*cos(w[j-
1]*pi/180)*(cos(a*pi/180)*cos(b*pi/180) +sin(a*pi/180)*sin(b*pi/180))
+ sin(A[1][i-1])*(sin(a*pi/180)*cos(b*pi/180) -
cos(a*pi/180)*sin(b*pi/180))

         teta_z = cos(A[1][i-1]*pi/180)*cos(w[j-
1]*pi/180)*cos(a*pi/180) + sin(a*pi/180)*sin(A[1][i-1]*pi/180)

         Rb = teta/teta_z

         It =z[i-1][j-1]* Rb +y[i-1][j-1] * ((1+cos(b*pi/180))/2)
+x[i-1][j-1]*p*((1-cos(b*pi/180))/2)

         if It > 0:

             B[i-1][j-1] = It

## Monthly average hourly diffuse radiation on a horizontal surface

         else:

             B[i-1][j-1] = 0
```

```
B = 1000*B

# Reflected radiation analysis

gama_top=array([[0.0]*24]*12)

gama_left=array([[0.0]*24]*12)

gama_right=array([[0.0]*24]*12)

z_right=array([0,0,0,0,0,0,90.0,75.0,60.0,45.0,31.0,17.0,8.0,-17.0,-
31.0,-45.0,-60.0,-75.0,-90.0,0,0,0,0,0,0])

z_right=abs(z_right)

atit=z_right-90.0

for i in range (1,13):

    for j in range (1,25):

        teta_z = np.arccos(cos(A[1][i-1]*pi/180)*cos(a*pi/180) +
sin(a*pi/180)*sin(A[1][i-1]*pi/180))*180/pi

        atit_angle=90.0-z_right[j-1]

        for ww in range (1000):

            xx = -50+0.1*ww

            top =0.5*sin((teta_z+xx)*pi/180)-sin((67.0-teta_z-
2*xx)*pi/180)

            if top < 0.05:

                gama_top[i-1][j-1] = xx

        for ww in range (1000):

            yy =ww*(90.0/1000.0)
```

```
            left=0.5*sin((157.0-atit_angle-yy)*pi/180.0)-
sin((atit_angle+2*yy-157.0)*pi/180.0)
            if left < 0.001:
                gama_left[i-1][j-1] = yy
                break
        for ww in range (1000):
            yy =ww*(90.0/1000.0)
            right=0.5*sin((atit_angle+23-2*yy)*pi/180.0)-sin((2*yy-
atit_angle-23)*pi/180.0)
            if right < 0.001:
                gama_right[i-1][j-1] = yy
                break
gama_right= 90-gama_left
gama_left[i-1][j-1] =44.7-0.667*z_right[j-1]
##Radiation on reflection surface
I_top=array([[0.0]*24]*12)
I_left=array([[0.0]*24]*12)
I_right=array([[0.0]*24]*12)
P_ref =0.9
for i in range (1,13):
    for j in range (1,25):
        x_top            = 2*gama_top[i-1][j-1]+atit[j-1]-b
```

```
        II_top           =z[i-1][j-1]*cos((gama_top[i-1][j-1]+atit[j-
1])*pi/180)
        I_top[i-1][j-1]  =P_ref*II_top*sin(x_top*pi/180)
        d_left           =atit[j-1]+b-gama_left[i-1][j-1]
        x_left           =2*gama_left[i-1][j-1]-(atit[j-1]+b)
        II_left          =z[i-1][j-1]*sin(d_left*pi/180)
        I_left[i-1][j-1] =P_ref*II_left*sin(x_left*pi/180)
        d_right          =180-(atit[j-1]+b-gama_right[i-1][j-1])
        x_right          =2*gama_right[i-1][j-1]+(atit[j-1]+b)-180
        II_right         =z[i-1][j-1]*sin(d_right*pi/180)
        I_right[i-1][j-1]=P_ref*II_right*sin(x_right*pi/180)
I_top=abs(I_top)
I_left=abs(I_left)
I_right=abs(I_right)
xan=linspace(1,24,24)
fig = plt.figure(1)
plt.figure(figsize=(8,5))
plt.subplots_adjust(right=0.85)
plt.subplots_adjust(top=0.85)
plt.subplot(2,2,1)
plt.plot(xan,I_left[8][:],label='Left',color ='black')
plt.plot(xan,I_top[8][:],'v',label='Top',color ='black')
plt.plot(xan,I_right[8][:],'s',label='Right',color ='black')
```

```
plt.ylabel('Radiation(kwh/m$^{2}$/hr')
plt.title('autumn,september 15 ',color ='black', fontweight = 'bold')
legend(loc='left',prop={'size':9})
plt.subplot(2,2,2)
plt.plot(xan,I_left[10][:],label='Left',color ='black')
plt.plot(xan,I_top[10][:],'v',label='Top',color ='black')
plt.plot(xan,I_right[10][:],'s',label='Right',color ='black')
plt.title('Winter,December 10', fontweight = 'bold')
legend(loc='left',prop={'size':9})
plt.subplot(2,2,3)
plt.plot(xan,I_left[2][:],label='Left',color ='black')
plt.plot(xan,I_top[2][:],'v',label='Top',color ='black')
plt.plot(xan,I_right[2][:],'s',label='Right',color ='black')
plt.ylabel('Radiation(kwh/m$^{2}$/hr')
plt.xlabel('Time(hr)')
plt.title('spring, march 16', fontweight = 'bold')
legend(loc='left',prop={'size':9})
plt.subplot(2,2,4)
plt.plot(xan,I_left[5][:],label='Left',color ='black')
plt.plot(xan,I_top[5][:],'v',label='Top',color ='black')
plt.plot(xan,I_right[5][:],'s',label='Right',color ='black')
plt.title('Summer, June 11',color ='black', fontweight = 'bold')
```

```
plt.xlabel('Time(hr)')

plt.xlim([0,24])

legend(loc='left',prop={'size':9})


# -*- coding: utf-8 -*-

"""

Created on Fri Feb 07 15:30:36 2020

This code is developed to determine the steady state analysis of the comprehensive enhanced solar air heater. The daily Temperature extraction form the collector is determined for representative day of each month. The code needs a radiation data to call from the previous code. a two dimensional array is created to fill the data for each hour output. The specification for the collector as per the data is used to evaluate the result. And, a module called Coolprop library is used to take thermo-physical property for each time variation of the air.

@author: Yisak Tola

"""

from scipy import *

from numpy import *

from pylab import *

from CoolProp.HumidAirProp import HAPropsSI

import CoolProp as CP

import matplotlib.pyplot as plt

from mpl_toolkits.axes_grid1 import host_subplot
```

```
import matplotlib.pyplot as plt

w=array([6,4.667,4.2,3.933,4.066,2.866,5.4,3.733,3.1334,4.6667,3.3334,
4.3334])        #Wind speed

m = 0.003       #Mass flow rate in the duct

wid = 1.0       #Width of glass

t = 0.07        #Air gap thickness

L = 1.5         #Length of glass

dx =0.01        #Discretized element

Mon = 12        #Month of the year

HR  = 24        #Hour of the day

N   = L/dx                  #Number of nodes

N = int(N)                  #Number of nodes

ks  = 1.5                   #Thermal conductivity of storage

kin = 0.113                 #Thermal conductivity of insulation

t_in = 0.025                #Thickness of insulation

Tr_glas = 0.91              #glass transmisivity

e_abso = 0.1                #Absorber emissivity

e_glass = 0.06              #glass absorptivity

a_abso = 0.94               #absorber absorptivity

sigma = 5.67*10**(-8)       #Stefan Boltzmann constant

beta =23.5                  #inclination angle

Nu = 7.54                   #Nulset number of the duct

Ap = 1.5                    #Absorber area
```

```
Ag = 1.5                   #Cover area

Dh = 2*t*wid/(t+wid)       #Hydraulic diameter

Tg = array([[26.5+273.14]*HR]*Mon)    # array for glass temperature

Tp = array([[26.0+273.14]*HR]*Mon)    # array for absorber temperature

Tw = array([[25+273.14]*N]*(HR*Mon))# array for working fluid
temperature

Ts = array([[27+273.14]*NN]*HR)  # array for thermal storage

for x in range (Mon):

    for y in range (HR):

        for z in range(N):

            density
=PropsSI('D','P',101325,'T',Tw[y+Mon*x][z],'Air.mix')#calling coolprop
for density of air

            enthalpy
=HAPropsSI('H','T',Tw[y+Mon*x][z],'P',101325,'R',0.72)#calling
coolprop for enthalpy of air

            Visco
=HAPropsSI('M','T',Tw[y+Mon*x][z],'P',101325,'R',0.10)#calling
coolprop for daynamic viscosity of air

            k_cond
=HAPropsSI('K','T',Tw[y+Mon*x][z],'P',101325,'R',0.10)#calling
coolprop for thermal conductivity of air

            cp
=HAPropsSI('cp','T',Tw[y+Mon*x][z],'P',101325,'R',0.10)

            hc2=Nu*k_cond/Dh  #convective heat transfer in the duct
```

```
            hc1=5.7 + 3.8*w[x]#convection loss to the environment form
the glass

            hr1=Tr_glas*sigma*((Tg[x][y])**2 + (T[x][y])**2)*(Tg[x][y]
+T[x][y])                 #radiation between the glass and ambient

            hr2=(sigma*((Tp[x][y])**2+(Tg[x][y])**2
)*(Tp[x][y]+Tg[x][y]))/(1/e_abso +(Ap/Ag) *((1/e_glass) -1))
#radiation between glass and plate

            Ub=kin/t_in

            Ut=hc1+hr1

            A1,A2,A3,A4
=(Ut/(Ut+hr2+hc2)),(Ut/(Ut+hr2+hc2)),(hr2/(Ut+hr2+hc2)),(hc2/(Ut+hr2+h
c2))

            A5,A6,A7,A8
=(1/(Ub+hr2+hc2)),(Ub/(Ub+hr2+hc2)),(hr2/(Ub+hr2+hc2)),(hc2/(Ub+hr2+hc
2))

            A9,A10,a   =dx*hc2/(m*cp),dx*hc2/(m*cp),wid*dx/(m*cp)

            A11        =A9+A10+1

            if B[x][y]==0:

                Tg[x][y]=T[x][y]

                Tp[x][y]=T[x][y]

                Tw[y+HR*x][z]=T[x][y]

            else:

                Tg[x][y]=A1*e_glass*B[x][y] + A2*T[x][y] + A3*Tp[x][y]
+ A4*(Tw[y+HR*x][z]+Tw[y+HR*x][0])/2.0
```

```
                Tp[x][y]=b*A5*Tr_glas*a_abso*B[x][y] + A6*T[x][y] +
A7*Tg[x][y] + A8*(Tw[y+HR*x][z]+Tw[y+HR*x][0])/2.0
                if z==0:
                    Tw[y+HR*x][z] =a*A9*Tg[x][y] + a*A10*Tp[x][y] +
T[x][y]*(1-2*a*A9)
                else:
                    Tw[y+HR*x][z] =a*A9*Tg[x][y] + a*A10*Tp[x][y] +
Tw[y+HR*x][z-1]*(1-2*a*A9)
    q =3600.0*Us*(Tp[y]-Tb[y-1])
    Tav = q/(MM*Cp)+Tav
    Tb[y]= 2*Tav-Tp[y]
    for W in range(NN):
        C2           =Tp[y]
        C1           =(Tb[y]-Tp[y])/t
        Ts[y][W]     =C1*(W/(NN*1.0))+ C2
for x in range (11):
        Ts[2*x+1][:]=(Ts[2*x][:]+Ts[2*x+2][:])/2.0
for x in range (11):
        Tp[2*x+1]=(Tp[2*x]+Tp[2*x+2])/2.0
Tw   =np.transpose (Tw)
Zan  =linspace(1,24,24)
fig  =plt.figure(2)
```

```
plt.plot(zan,Tw[N-1][0:24],color           ='black',label='fluid temp@
N')

plt.plot(zan,Tw[N-15][0:24],'*',color ='black',label='fluid temp@ N-
15')

plt.plot(zan,Tw[N-30][0:24],'s',color ='black',label='fluid temp@ N-
30')

plt.plot(zan,Tw[N-50][0:24],'v',color ='black',label='fluid temp@ N-
50')

plt.plot(zan,Tw[N-60][0:24],'^',color ='black',label='fluid temp@ N-
60')

plt.title ('air temperature at each node for Jan 17', fontsize = 12,
fontweight = 'bold')

plt.ylim([285,400])

plt.xlabel('meter(m)', fontsize = 12)

plt.ylabel('Temperature ($^{o}$C)', fontsize = 12)

legend(loc='best',prop={'size':10})

show ()
```